NUCLEAR MAGNETIC RESONANCE STUDIES OF GROWTH HORMONE RELEASING FACTOR ANALOGS

by

Michael Paul Lamb

A Dissertation Submitted to the Faculty of the

DEPARTMENT OF PHARMACEUTICAL SCIENCES

In Partial Fulfillment of the Requirements
For the Degree of

DOCTOR OF PHILOSOPHY

In the Graduate College

THE UNIVERSITY OF ARIZONA

1 9 9 6

INFORMATION TO USERS

This manuscript has been reproduced from the microfilm master. UMI films the text directly from the original or copy submitted. Thus, some thesis and dissertation copies are in typewriter face, while others may be from any type of computer printer.

The quality of this reproduction is dependent upon the quality of the copy submitted. Broken or indistinct print, colored or poor quality illustrations and photographs, print bleedthrough, substandard margins, and improper alignment can adversely affect reproduction.

In the unlikely event that the author did not send UMI a complete manuscript and there are missing pages, these will be noted. Also, if unauthorized copyright material had to be removed, a note will indicate the deletion.

Oversize materials (e.g., maps, drawings, charts) are reproduced by sectioning the original, beginning at the upper left-hand corner and continuing from left to right in equal sections with small overlaps. Each original is also photographed in one exposure and is included in reduced form at the back of the book.

Photographs included in the original manuscript have been reproduced xerographically in this copy. Higher quality 6" x 9" black and white photographic prints are available for any photographs or illustrations appearing in this copy for an additional charge. Contact UMI directly to order.

UMI

A Bell & Howell Information Company
300 North Zeeb Road, Ann Arbor MI 48106-1346 USA
313/761-4700 800/521-0600

NUCLEAR MAGNETIC RESONANCE STUDIES OF GROWTH HORMONE RELEASING FACTOR ANALOGS

by

Michael Paul Lamb

A Dissertation Submitted to the Faculty of the

DEPARTMENT OF PHARMACEUTICAL SCIENCES

In Partial Fulfillment of the Requirements
For the Degree of

DOCTOR OF PHILOSOPHY

In the Graduate College

THE UNIVERSITY OF ARIZONA

1 9 9 6

THE UNIVERSITY OF ARIZONA ®
GRADUATE COLLEGE

As members of the Final Examination Committee, we certify that we have read the dissertation prepared by Michael Paul Lamb

entitled Nuclear Magnetic Resonance Studies of Growth Hormone Releasing Factor Analogs.

and recommend that it be accepted as fulfilling the dissertation requirement for the Degree of Doctor of Philosophy

Neil MacKenzie.	Date 4/11/96
William A Pomers	Date 4/11/96
William R. Montfort	Date 4/11/96
Arnold Martin	Date 4/11/96

Final approval and acceptance of this dissertation is contingent upon the candidate's submission of the final copy of the dissertation to the Graduate College.

I hereby certify that I have read this dissertation prepared under my direction and recommend that it be accepted as fulfilling the dissertation requirement.

Neil MacKenzie	4/11/96
Dissertation Director	Date

STATEMENT BY AUTHOR

This dissertation has been submitted in partial fulfillment of requirements for an advanced degree at The University of Arizona and is deposited in the University Library to be made available to borrowers under rules of the Library.

Brief quotations from this dissertation are allowable without special permission, provided that accurate acknowledgment of source is made. Requests for permission for extended quotation from or reproduction of this manuscript in whole or in part may be granted by the head of the major department or the Dean of the Graduate College when in his or her judgment the proposed use of the material is in the interests of scholarship. In all other instances, however, permission must be obtained from the author.

SIGNED: 

ACKNOWLEDGMENTS

I would like to thank the following people for their assistance and support: Dr. Neil MacKenzie, Dr. Gregory Needham, Dr. Arnold Martin, Dr. William Remers, Dr. William Montfort, Dr. Dezheng Zhao, Dr. I. Glenn Sipes, Mr. Constantin Job, and Dr. Sue Roberts. I would also like to thank Eli Lilly and Company for their generous financial support of this project.

TABLE OF CONTENTS

LIST OF FIGURES

LIST OF TABLES

ABSTRACT

The solution structures of three potent growth hormone releasing factor (GRF) analogs corresponding to GRF(1-29), GRF(1-44), and GRF(1-76) were investigated by nuclear magnetic resonance (NMR) and circular dichroism (CD) spectroscopies. The analogs contained a deletion of Tyr^1 and acylation of Ala^2 with a para-methyl hippuric acid. In addition, eight amino acid substitutions were made in the GRF(1-76)OH analog versus human GRF. The substitutions were retained in the respective shorter analogs. Each of the three peptides (pmh29, pmh44, and pmh76, for simplicity) was studied in aqueous solutions of trifluoroethanol (TFE), while pmh76 was additionally studied in an aqueous buffer. Complete sequential assignment was made for pmh29 in 45% TFE. Nuclear Overhauser effect (NOE) data, chemical shift data, and CD spectra defined pmh29 as nearly completely helical. Long-range NOEs in the NOESY spectra of pmh29 revealed the presence of tertiary structure. Split proton resonances and a wide span of long-range NOE interactions suggested a conformationally heterogeneous tertiary structure. Distance geometry and simulated annealing were performed using NOE data to calculate the two predominant tertiary structures. The calculated structures for pmh29 were in accordance with a consensus of previously proposed bioactive conformational characteristics. Complete sequential assignment was accomplished for pmh44 in 45% TFE. The pmh44 molecule was nearly completely helical as determined by NOE data, chemical shift data, and CD spectroscopy. Long-range NOEs provided evidence of tertiary structure in the pmh44 molecule. The coincidence of chemical shifts and long-range NOEs in pmh44 and pmh29 pointed to a similar structure for both molecules, with the 15 C-terminal residues of pmh44 forming a linear helical extension. Severe signal overlap impaired the assignment of pmh76 in 30% TFE and aqueous buffer. Chemical shift correlation between the three analogs in TFE suggested a similar conformation in

the corresponding regions of the pmh76 peptide, with the C-terminal extension forming a linear helix. These studies provide the first evidence of a global tertiary fold in any GRF analog or member of the secretin family. The potency of these analogs is likely due to a combination of metabolic stability and the adoption of preferred secondary and tertiary structures.

INTRODUCTION

Growth hormone releasing factor (GRF) is an amidated 44-residue hypothalamic peptide that acts in conjunction with its inhibitory counterpart somatostatin (SS) to effect the pulsatile release of growth hormone from the anterior pituitary (Ling et al., 1985). GRF was first obtained from two human pancreatic tumors by two separate groups (Guillemin et al., 1982; Rivier et al., 1982). Guillemin et al. found primarily GRF(1-44)NH_2 with some GRF(1-40)OH and GRF(1-37)OH fragments present. Rivier et al., however, found only the GRF(1-40)OH to be present. Isolation and recombinant cloning of a cDNA encoding human GRF showed that GRF is translated as a 76-residue polypeptide, and residues 45-76 are cleaved prior to expression (Mayo et al., 1983). Studies performed both *in vitro* and *in vivo* of C-terminally deleted analogs have revealed that GRF(1-29) is the shortest analog to retain near full bioactivity (Rivier et al., 1982; Grossman et al., 1984; Lance et al., 1984; Ling et al., 1984).

It has been shown that GRF can stimulate the release of growth hormone in growth hormone and GRF deficient persons, and therefore has implications as a therapeutic agent for the treatment of dwarfism in children (Grossman et al., 1984; Rochiccioli et al., 1987; Vance, 1990). Additionally, species-specific GRF can increase milk production (Mehigh et al., 1993) in dairy cows and increase growth in livestock with a concomitant increase in the muscle to fat ratio (Campbell et al., 1995). The therapeutic and commercial implications of human and livestock GRF have prompted intensive study of GRF and several analogs. The goal of these studies has been to elucidate the bioactive conformation of the molecule and the pathways of metabolic inactivation in an attempt to obtain a long-acting, potent analog of GRF.

Metabolic inactivation of GRF is thought to occur by several pathways, namely deamidation of Asp^8; Ala^2- Asp^3 cleavage by dipeptidylpeptidase IV (DPP-IV); trypsin-

like cleavage between Arg^{11}-Lys^{12}, Lys^{12}-Val^{13}, Arg^{20}-Lys^{21}, and/or Lys^{21}- Leu^{22}; and nonenzymatic oxidation of Met^{27} (Rivier et al., 1984; Frohman et al., 1986; Frohman et al., 1989; Friedman et al., 1991). Analogs containing [desNH_2Tyr^1] and/or [D-Ala^2] have shown resistance to DPP-IV, while addition of an Ala^{15} substitution, to give the [desNH_2-Tyr^1, D-Ala^2, Ala^{15}] trisubstituted analog, confers resistance to trypsin-like degradation (Frohman et al., 1989). These degradation resistant analogs have exhibited increased affinities and activities *in vitro* and *in vivo* (Lance et al., 1984; Campbell et al., 1995). Fragments of GRF(1-29) designed to mimic DPP-IV and trypsin-like degradation products, on the other hand, have shown low binding affinity and intrinsic activity (Campbell et al., 1991).

Stabilization of a preferred bioactive conformation may also lead to analogs with increased potencies. The solution structures of GRF(1-29) and several analogs have been solved in aqueous and less polar solvent systems by the use of circular dichroism and nuclear magnetic resonance spectroscopy (Clore et al., 1986; Theriault et al., 1988; Madison et al., 1989; Campbell et al., 1991; Fry et al., 1992; Stevenson et al., 1993). Results of these studies have concluded that in aqueous systems the peptide is largely unstructured, whereas, in less polar systems, such as trifluoroethanol (TFE) and methanol, the peptide assumes a mainly amphiphilic helical conformation. Stabilization of the helix or enhancement of its amphiphilic character increases receptor binding affinity resulting in increased potency. Substitution of an alanine residue for Gly^{15} augments the amphiphilic character of GRF(1-29) while concomitantly increasing the rigidity of the helix via increased intramolecular interactions (Madison et al., 1989; Campbell et al., 1991). The resulting analog shows an increase in total helicity by 2 residues in aqueous solution (residues 9-15 and 21-26 with Ala^{15} vs. residues 9-14 and 24-28 with Gly^{15}) and has a ~ 4-fold increase in binding affinity and ~ 5-fold increase in

potency versus GRF(1-29) *in vitro*. A Gly^{15}-Sar substitution destabilizes the helix and results in a >1000-fold decrease in affinity and potency (Campbell et al., 1991).

Cyclized GRF analogs have been used to explore the relationship between helical stability and bioactivity (Friedman et al., 1991; Fry et al., 1992). Cyclic analogs that destabilize the helix, $cyclo^{3,12}$ and $cyclo^{11,16}$, showed decreased *in vitro* activity versus the natural product, while a cyclic analogs that stabilizes the helix, $cyclo^{8,12}$, showed comparable *in vitro* activity to that of the natural product. Rigidification of the central portion of the helix via a $cyclo^{16,20}$ modification, however, results in a significant decrease in activity (Fry et al., 1992).

GRF is a member of the secretin family of peptide hormones which includes secretin (Bodanszky et al., 1966), glucagon (Bromer et al., 1957), vasoactive intestinal peptide (VIP) (Said & Mutt, 1970, 1972), pituitary adenylate cyclase-activating polypeptide (PACAP) (Miyata et al., 1989), helodermin (Vandermeers et al., 1987), and peptide histidine isoleucine (PHI) (Tatemoto & Mutt, 1981). The solution structures of most members of this family, save for PHI and helodermin, have been previously determined in aqueous solutions of less polar solvents (Table 1). The lack of conformational

Table 1: Previously determined structures for members of the secretin family.

Peptide	Solvent	Structure	Reference
Glucagon	micelles	2 regions of helix (10-14 & 17-29)	Braun et al., 1983
Secretin	40% TFE	2 regions of helix (7-13 & 17-25); partial turn in 14-16	Gronenborn et al., 1983
PACAP 27	30% TFE	helix from 9-26 with disruption in 20 and 21	Wray et al., 1993
PACAP 38	30% TFE	helix from 9-26 with disruption in 20 and 21; helix from 28-34	Wray et al., 1993
PACAP 27	25% MeOH	2 regions of helix (12-20 & 22-25)	Inooka et al., 1992
VIP	40% TFE	2 regions of helix (7-15 & 19-27); undefined region in 16-18	Theriault et al., 1991
VIP'	25% MeOH	2 regions of helix (9-17 & 23-28)	Fry et al., 1989
VIP'	50% MeOH	helix from 8-26	Fry et al., 1989
Nle^{27}- GRF(1-29)NH_2	30% TFE	2 regions of helix (6-13 & 16-29); bend around 14 and 15	Clore et al., 1986
Ala^{15}-GRF(1-29)NH_2	75% MeOH	single long helix with a kink around 16	Fry et al., 1992
GRF(1-32)NH_2	40% MeOH	2 regions of helix (7-15 & 21-27)	Stevenson et al., 1992
GRF(1-32)NH_2	80% MeOH	2 regions of helix (3-15 & 21-28)	Stevenson et al.., 1992
Asp^{8}-GRF(1-32)NH_2	80% MeOH	2 regions of helix (4-15 & 19-27)	Stevenson et al., 1992
GRF(1-29)NH_2	40% TFE	single long helix (2-29)	Theriault et al., 1988

stability of this family of peptides in water and the consequent low solubility necessitate the addition of less polar solvents or micelles for NMR study.

The conformation of glucagon in dodecylphosphocholine micelles was studied by ^1H NMR spectroscopy (Braun et al., 1983). Results of this investigation showed glucagon to contain two helical regions residing in residues 10-14 and 17-29. Extended conformations were observed in residues 5-10 and 14-17, while the four N-terminal residues did not assume a stable structure. A lack of long-range NOEs indicated that the peptide did not adopt a globular tertiary structure in this micellar environment.

Secretin assumed a stable conformation in an aqueous solution of 40% trifluoroethanol as determined by CD and two-dimensional ^1H NMR spectroscopies (Gronenborn et al., 1987). The CD results indicated that secretin exhibits 60-70% helical content in this environment. The ^1H NMR results characterize the structure as consisting of two helices (residues 7-13 and 17-25) connected by a partial turn (residues 14-16) and flanked at the N- (residues 1-6) and C-termini (residues 26 and 27) by irregular or unstructured regions. Additionally, restrained molecular dynamics calculations based on NOE data showed secretin to exist as a non-globular peptide (Clore et al., 1988).

The structures of two naturally occurring PACAP peptides PACAP38 (an amidated 38 residue peptide) and PACAP27 (the amidated 27 residue N-terminal portion) have been characterized in a solution of 50% aqueous trifluoroethanol by CD spectroscopy and a combination 2D ^1H NMR spectroscopy with distance geometry and refined molecular dynamics and energy minimization calculations (Wray et al., 1993). CD experiments revealed that at TFE concentrations greater than 30% both peptides assumed stable conformations with helicities of 54% (PACAP38) and 68% (PACAP27). The structure of PACAP27 calculated from 2D ^1H NMR experiments was comprised of a disordered N-terminal region (residues 1-8) followed by an α-helix from residues 9-26 with a

disruption at residues 20 and 21. The homologous residues of PACAP38 assumed the same structure followed by a short α-helix from residues 28-34 in the C-terminal extension.

Another study investigated the structure of PACAP27 in an aqueous solution of 25% methanol with CD and ^{1}H NMR spectroscopies (Inooka et al., 1992). In this solvent system the peptide formed two regions (residues 9-20 and 22-25) of stable structure. Residues 9-12 formed a β turn-like conformation followed by an α-helical region (residues 12-14) and a looser helical region (residues 15-20), while a single α-helical turn was formed in residues 22-24. These results corroborated CD spectroscopy experiments that showed the peptide to contain 22% helix. These findings were similar to those of Wray et al.(1993) but differed primarily by the proposed β turn-like conformation in residues 9-12. It was suggested by Wray et al. (1993) that limited NOE data, limited distance geometry calculations, lack of refinement, and possible misinterpretation of the qualitative NOE data may have led Inooka et al. (1992) to a suspect conformation.

The conformations of VIP (Theriault et al., 1991) and a potent analog Ac-[Lys^{12}, Lys^4,Nle^{17}, Val^{26},Thr^{28}]VIP (VIP') (Fry et al., 1989) have been determined in aqueous solutions of TFE and methanol, respectively, by CD and 2D ^{1}H NMR spectroscopies. ^{1}H NMR spectroscopy was used to characterize the secondary structure of VIP in an aqueous solution containing 40% TFE. Results of this study showed VIP to consist of two helical regions (residues 7-15 and 19-27) connected by an undefined region (residues 16-18), with the N-terminal region being unordered. This structure most resembled the structure of VIP' in 25% methanol (see below). CD spectroscopy experiments of VIP' showed an increase in helical content concomitant with increasing methanol concentration from 0% to 25% and 25% to 50%. Structures were calculated, using molecular dynamics and energy minimizations of NOE-derived distance constraints, for the peptide in both 25%

and 50% methanol. In 25% methanol VIP' consisted of two helical regions (residues 9-17 and 23-28), with the remaining portions of the peptide lacking stable structure, while in 50% methanol VIP' formed a well-defined α-helix in residues 8-26 and a type III β-turn in residues 5-8, with the remaining residues lacking an ordered structure.

A characteristic secondary structure for members of the secretin family emerged and was identified (Gronenborn et al., 1987; Wray et al., 1993, 1994). This characteristic structure consisted of a disordered N-terminal region of 6-8 residues followed by a helical region of 19 ± 2 residues which may contain a break of 2-4 residues in the middle. It was proposed that the active portion of the peptide is the disordered region which adopts a specific conformation at the receptor (Wray et al., 1993). Furthermore, Wray et al. (1993) proposed that the helical portion may bind in the lipid portion of the membrane surrounding the receptor and that the small differences in helix structures and amino acid composition between members of the family imparted binding specificity.

The secondary structures of glucagon, secretin, PACAP, and VIP adhere well to the secretin family structural motif, but do the GRF peptides conform to these proposed structural requirements? CD and 2D ^{1}H NMR spectroscopy studies were performed on [Nle^{27}]-GRF(1-29)NH_2 in an aqueous solution of 30% TFE. CD results indicated that the peptide has a high (81%) helical content. ^{1}H NMR results showed the peptide to indeed consist of two helical regions (residues 6 to 13 and 16 to 29) connected by a two residue linker. The N-terminal region, however, was not disordered, but assumed a β-strand conformation (Clore et al., 1986). NOE data were then subjected to restrained molecular dynamics and distance geometry calculations which verified the secondary structure (including the N-terminal β-strand) and also suggested a possible tertiary structure where the peptide has a slight bend around the linker region between the two helices (residues 14 and 15) to give a banana-shaped structure (Brünger et al., 1987).

Studies of [Ala^{15}]-GRF(1-29)NH_2 and its cyclic (cyclo$^{8-12}$ and cyclo$^{21-25}$) and dicyclic (dicyclo$^{8-12;\ 21-25}$) analogs in an aqueous solution of 75% methanol revealed structures that agree with the proposed model of secretin family peptides (Fry et al., 1992). 2D ^{1}H NMR spectroscopy experiments followed by constrained molecular dynamics and energy minimization calculations concluded that all of the peptide analogs exist as a single long α-helix with a disordering of one to three residues at the N- and C-termini in this solvent system. The linear analog exhibited a tendency to form a kink near residues 16 and/or 25, similar to the tertiary structure of Brünger et al. (1987).

The conformation of a 32-residue GRF analog Leu^{27}-hGRF(1-32)NH_2 and its deamidation products Asp^{8}Leu^{27}-hGRF(1-32)NH_2 and isoAsp^{8}Leu^{27}-hGRF(1-32)NH_2 were investigated in aqueous solutions of 40% and 80% methanol by CD and NMR spectroscopies (Stevenson et al., 1993). At both concentrations of methanol the CD results indicated similar helical content for all three analogs. In 40% methanol, 2D ^{1}H NMR results characterized Leu^{27}-hGRF(1-32)NH_2 to be comprised of two helical regions (residues 7-15 and 21-27). The conformations of all three analogs were explored in 80% methanol using 2D ^{1}H NMR. The parent analog showed an increase in helicity upon increasing the MeOH concentration, extending the N-terminal helix to Asp^3 and the C-terminal helix to Ser^{28}. The deamidation products also existed in conformations containing two helices. The Asp^8 analog had an N-terminal helix from residues 4-15 and a C-terminal helix from residues 19-27, while the isoAsp^8 analog had a much shortened N-terminal helix (residues 11-15) and a similar C-terminal helix (residues 20-27). The isoAsp^8 residue adds a methylene group into the peptide backbone which apparently disrupted the ability of this analog to form a helix in the region of this addition. In addition, the isoAsp^8 residue acts like a D-amino acid extending the side chain into the

core of the helix. The parent analog and the Asp^8 analog, however, exhibited structures that are in agreement with the secretin motif.

Although the aforementioned studies described conformations of GRF(1-29) analogs that adhere rather closely to the proposed model of a disordered N-terminal region followed by a long helix, a study of GRF(1-29)NH_2 showed that the natural product assumes a single long helix beginning at Ala^2 and ending at the C-terminus in aqueous TFE (40%) (Theriault et al., 1988). 2D ^1H NMR experiments gave rise to a pattern of NOEs purported to be indicative of a completely helical peptide. Amide exchange data appeared to confirm these results and also suggested a possible hydrophobic core in residues 13 to 27, although a tertiary structure was not corroborated by the presence of long-range NOEs.

In contrast to the thorough characterization of the secondary structure of members of the secretin family, little information has been obtained regarding the tertiary structure of these peptides. Clore et al. (1988) performed restrained molecular dynamics calculations on secretin using short-range NOE data obtained for the peptide in an aqueous solution of 40% TFE. Results of this work showed secretin to be in an extended conformation with a "half-turn" in the region (residues 14-16) between the two helices. A similar conformation was calculated for Nle^{27}-hGRF(1-29)NH_2 in 30% TFE by distance geometry and molecular dynamics using short-range NOE data (Brünger et al., 1987). Although there was not a convergence to a single structure, all conformations were extended, "banana-shaped" entities with a loose bend around the region (residues 14 and 15) connecting the two helices. A study by Fry et al. (1992) elucidated a sharper kinked structure at residue 16 and/or 25 of Ala^{15}-GRF(1-29)NH_2 using molecular dynamics and energy minimization simulations. Although these studies reported disruptions in the linearity of the helical structure with a bend or kink in the peptide, no previous

investigations of members of the secretin family have identified the presence of any global tertiary structure.

It is the aim of this study to elucidate the solution structures of three very potent, acylated polypeptide analogs of GRF. In these analogs Tyr^1 has been deleted and Ala^2 has been acylated with a para-methylhippuryl group (Figure 1). In addition to the amino-terminal deletion and acylation, eight amino acid substitutions have been made in the GRF(1-76)OH analog: asparagine for Ser^9, arginine for Lys^{12}, threonine for Gly^{15}, arginine for Lys^{21}, leucine for Met^{27}, leucine for Met^{51}, arginine for Lys^{56}, and leucine for Met^{59} (Figure 1). The corresponding amino acid substitutions are retained in the shortened analogs. The three peptides are analogous to GRF(1-29)NH_2, GRF(1-44)OH, and GRF(1-76)OH. Herein, an investigation into the solution structures of these analogs (which we will call pmh29, pmh44, and pmh76, for simplicity) by the combined use of circular dichroism and NMR spectroscopies is detailed. The results are then correlated to the increased potencies of the analogs.

Figure 1: Amino acid sequences of GRF analogs **pmh29, pmh44, and pmh76.** The pMeHipp represents the para-methylhippuryl group which has the structure indicated.

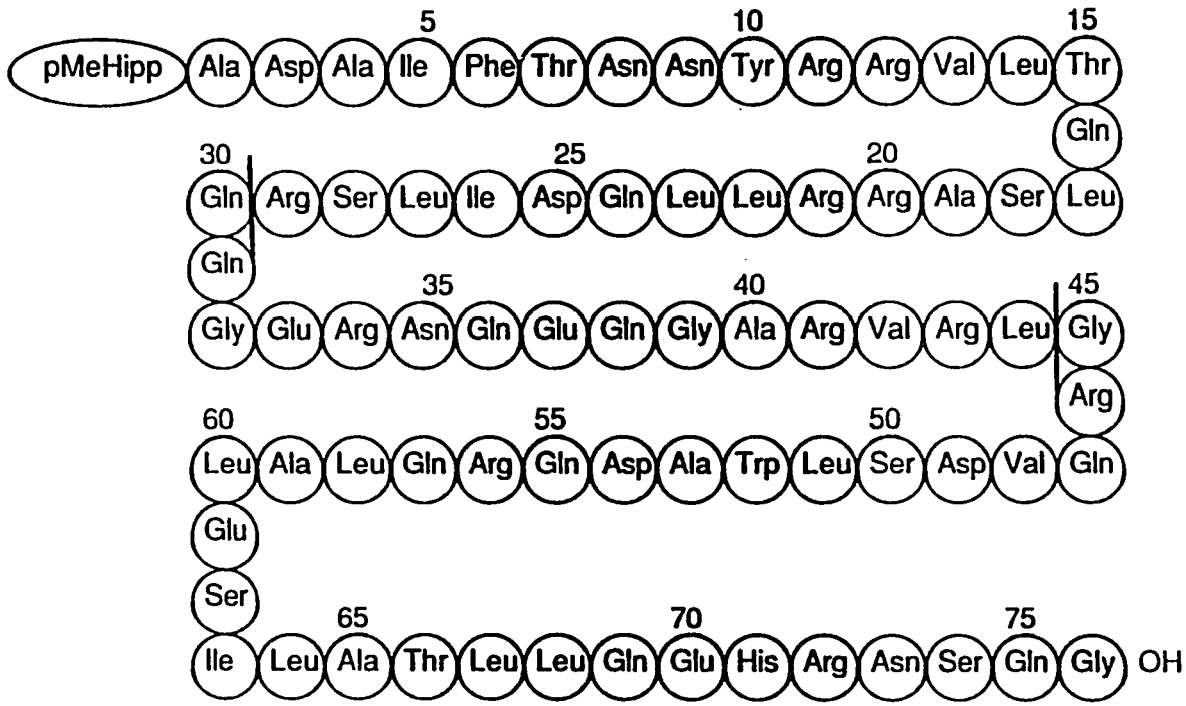

PMH29: MATERIALS AND METHODS

SAMPLE PREPARATION. The pmh-GRF(2-29)NH_2 was obtained from Eli Lilly and Company (Lot F35-AVO-155B) and used without further purification. NMR samples were prepared by dissolving approximately 3.4 mg of lyophilized peptide in 0.5 ml of 45% 2,2,2,-Trifluoroethanol-d_3 (MSD Isotopes)/ 45% H_2O/ 10% D_2O (99.9% atom enrichment, Cambridge Isotope Laboratories) to give a final concentration of about 2 mM at pH 3.30. CD samples were prepared (G. F. Needham, Eli Lilly and Company) by appropriate dilution from stock solutions of TFE, water, and peptide in water (pH 3.9) following the method of Brems et al. (1985). All stock solutions were filtered through a 0.45 μm filter before mixing. Samples were made to constant volume and constant peptide concentration (0.15 mg/ml).

CD SPECTROSCOPY. Far UV Circular Dichroism (CD) spectra were collected (G. F. Needham, Eli Lilly and Company) at multiple TFE concentrations using an AVIV model 62 spectropolarimeter. Samples were collected at 0, 10, 20, 30, 40, and 50 percent TFE using a 1.0 nm bandwidth, a 0.25 nm stepsize, and an 8 second time constant in a 0.2 cm cell. All data were collected at 298 K. Results were reported as mean residue ellipticity ([Θ]) in degrees-cm^2-$dmol^{-1}$ (MRE) and were calculated with a mean residue weight of 116.

NMR SPECTROSCOPY. ^1H NMR spectra were recorded on a Bruker AM 500 spectrometer at 300 K with a spectral width of 5000 Hz. Spectra were referenced to an external sample of dioxane at 3.751 ppm downfield from 4,4-dimethyl-4-silapentane-1-sulfonate. TOCSY experiments (Bax & Davis 1985) were acquired with 32 transients, 900 complex points in the t_1 dimension, and 2048 points in the t_2 dimension. Phase-sensitive NOESY experiments (Jeener et al., 1979) were acquired with 64 transients, 900 complex points in t_1 dimension, and 2048 points in the t_2 dimension. All experiments

were performed with time proportional phase incrementation (Marion & Wüthrich, 1983), and were zero filled to 2K X 2K. A 60-degree shifted sine bell window function was applied to all experiments before transforming in both dimensions. NOESY experiments were recorded with mixing times of 150, 200, and 400 ms. TOCSY experiments were recorded with mixing times of 60, 100, and 140 ms. Additionally, two higher temperature (310 K and 320 K) 100 ms TOCSY experiments were performed using the aforementioned parameters for TOCSY experiments.

STRUCTURE CALCULATIONS. A total of 307 NOEs were observed 140 of which were interresidue NOEs. Structure calculations were performed on a Silicon Graphics Indigo workstation using softwares from Biosym Technologies, Inc. (INSIGHT II and NMRchitect). Long-range NOEs were divided into two groups to calculate two families of tertiary conformations (see discussion below). Both structures were calculated from a combination of distance geometry (DGII module) and simulated annealing. All NOEs were classified as strong (1.8-2.5 Å), medium (1.8-3.5 Å), or weak (1.8-2.5 Å) according to their relative intensities. A pseudoatom correction of 0.5 Å was added to the upper bound distance of equivalent protons present in the same group. The peptide was submitted to the distance geometry protocol in an extended conformation. The NOE distance bounds were smoothed using the triangle and group pairs tetrangle inequality strategies, and the smoothed bounds were embedded in 4D Cartesian space to give 20 structures for each family. The structures were optimized using simulated annealing schedule (maximum steps = 10,000; step size = 7×10^{-13}; temperature = 200 K) followed by conjugate gradient minimization (maximum iterations = 500; RMS gradient = 0.001). Each of the 40 distance geometry structures (20 per family) was subjected to further refinement by simulated annealing. The following simulated annealing schedule was employed: conjugate gradient energy minimization for 500 iterations; molecular

dynamics at 1000 K for 50 ps with a 1 fs time step doubling the force constants for distance restraints over the last 10 ps; cooling the system over 10 ps in 2 ps stages (1000 K → 650 K, 650 K → 475 K, 475 K → 385 K, 385 K → 340 K, 340 K → 300 K); energy minimization for 100 iterations using the steepest descent algorithm; conjugate gradient energy minimization for 500 iterations; steepest descent energy minimization for 100 iterations; and a final conjugate gradient energy minimization for 1500 iterations.

PMH29: RESULTS AND DISCUSSION

CD SPECTROSCOPY. Figure 2 shows the CD spectrum of pmh29 in varying amounts of TFE. In the absence of TFE, the peptide was in a random coil conformation. As the concentration of TFE was increased, minima appeared at 208 and 222 nm which were representative of a change from random coil to a helical structure. Increasing TFE concentration concomitantly increased the amount of helical content, although there was essentially no change in secondary structure at TFE concentrations above about 30%. At concentrations of TFE greater than 30%, it was estimated that the secondary structure of the peptide was nearly 100% helix (G. F. Needham, Eli Lilly and Company, personal communication).

NMR SPECTROSCOPY. SPIN SYSTEM ASSIGNMENT. TOCSY spectra were analyzed using standard assignment protocol for 2D spectra to assign proton spin systems to specific residue types (Wüthrich, 1986). Three spin systems containing only an αH and a high field βH crosspeak were observed in the NH-aliphatic region (Figure 3), and were attributed to the alanine residues. A single highfield αH-βH crosspeak in the aliphatic region of a TOCSY spectrum confirmed these assignments. Four spin systems had an αH and a low field βH crosspeak in the NH-aliphatic region. Two of these spin systems also had a highfield crosspeak, and were assigned to the threonine residues. The remaining two were identified as serine residues by the lack of a highfield peak. The threonine assignments were verified by the presence of αH-βH and αH-γH crosspeaks, as well as βH-γH crosspeaks in the aliphatic region. The sole valine residue was easily identified in the NH-aliphatic region (Figure 3) by the αH, βH, and two γH resonances. The arginine spin systems were readily assigned by observation of the εH protons which resonate near 6.9 ppm and show cross peaks to the αH, δH, βH, and γH protons for all five arginine

Figure 2: Circular dichroism spectrum of pmh29 in varying concentrations of aqueous trifluoroethanol at pH 3.9 and 298 K. Mean residue ellipticity (MRE) is in units degrees-cm^2-$dmol^{-1}$.

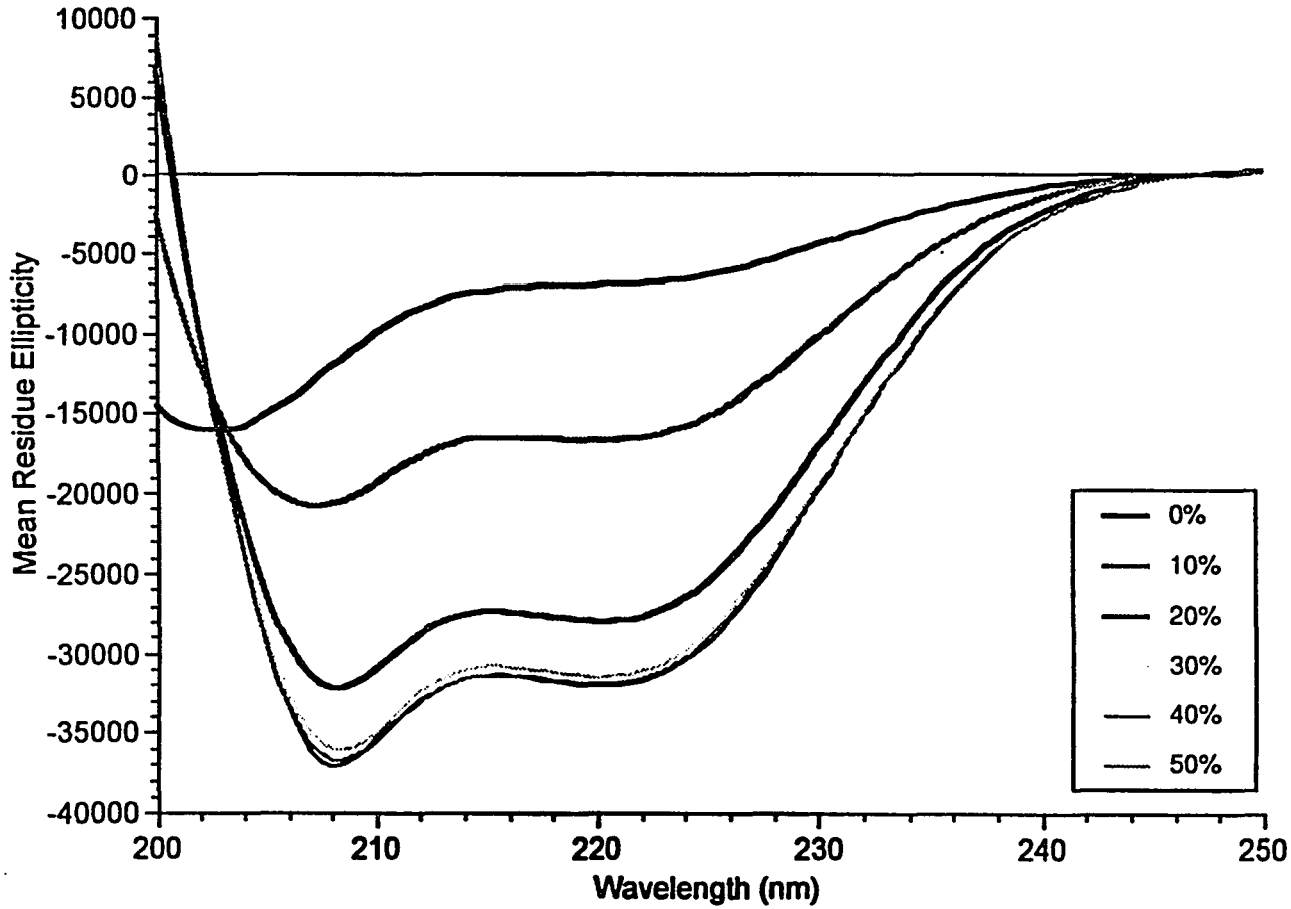

Figure 3: NH-aliphatic region of a 100 ms TOCSY spectrum for pmh29 in 45% d_3-trifluoroethanol, 45% H_2O, and 10% D_2O at 300 K. where the spin systems have been labeled at the αH resonance.

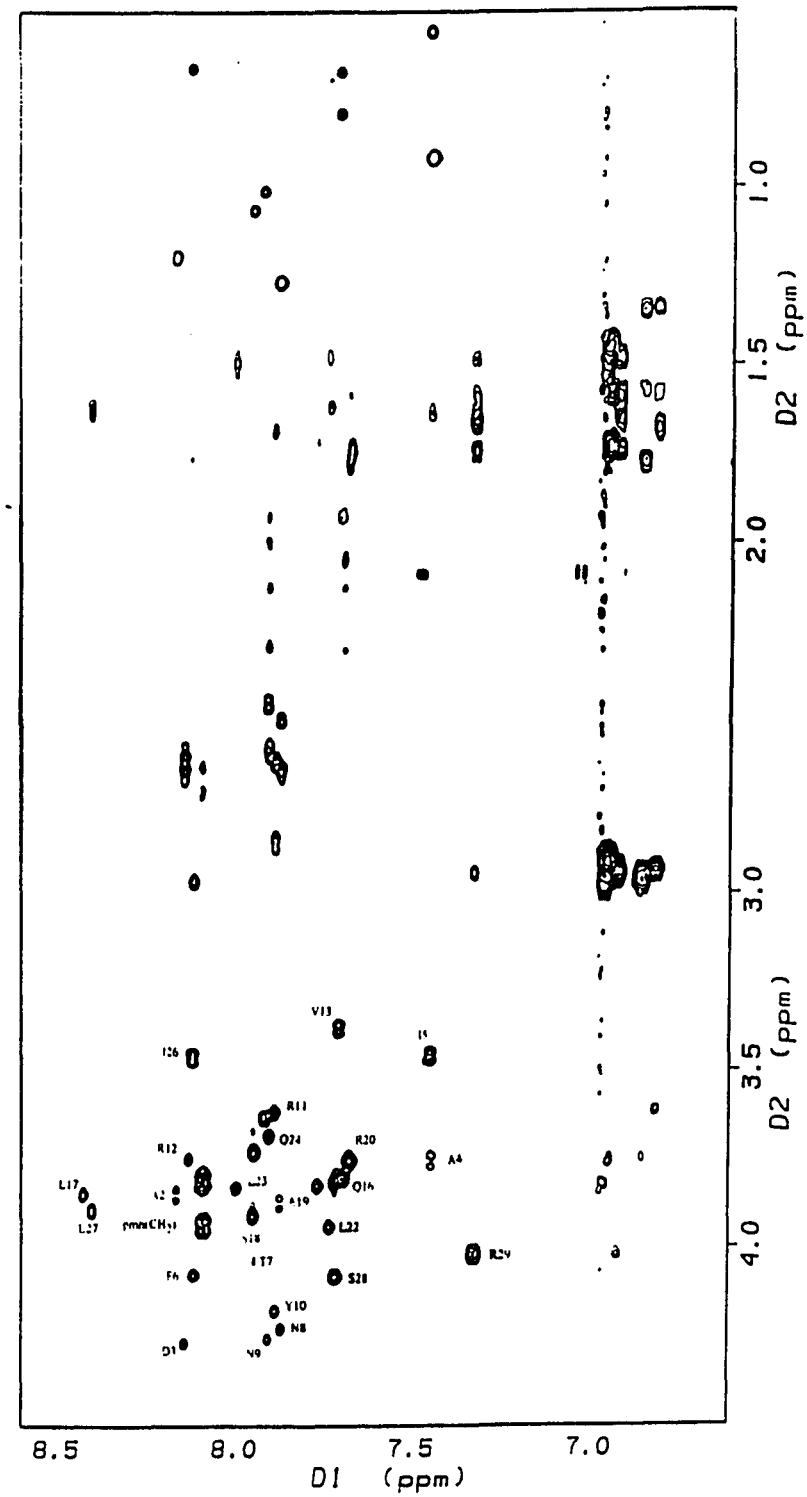

residues. Only two AM(PT)X spin systems were present in the spectra, and thus were assigned to the glutamine residues. A glycine-like doublet in the fingerprint region was readily attributed to a coupling between the NH and the methylene protons of the para-methylhippuryl group (see Figure 1), as there are no glycine residues in the sequence. The strong γCH_3 of the isoleucines in the NH-aliphatic region facilitated differentiation of these spin systems from those of leucine residues. The five remaining spin systems with crosspeaks in the very highfield portion of the spectrum (< 1.0 ppm) were then ascribed to the leucine residues. The 6 residual systems were all of the AMX type and were imputed to the 2 asparagine, 2 aspartate, 1 phenylalanine, and 1 tyrosine residues. Individual identification of these spin systems was only possible after analysis of NOESY spectra.

SEQUENCE-SPECIFIC ASSIGNMENTS. NOESY experiments were performed to obtain sequence-specific assignment of the spin systems identified in the TOCSY spectra. Sequential assignment was made by observation of NOE crosspeaks from the NH resonance of a given residue to the NH, αH, and/or βH of the proceeding residue in the sequence. Figure 4 indicates the NH-NH connectivities that were observed, while Figure 5 shows an expansion of the fingerprint region of the same 400 ms NOESY spectrum with labels marking the observable short-range connectivities. The NOESY spectra did not provide any long runs of sequential connectivities, therefore, most assignments were made by comparison of residue types showing a connectivity to residues that were adjacent in the sequence. Figure 6 is an expansion of the fingerprint region of the 100 ms TOCSY where 26 of 28 αH resonances have been assigned. The αH resonances of Leu^{14} and Asp^{25} are obscured by the overlap of the Arg^{12} αH and the para-methylhippuryl group methylene protons, respectively. Table 2 provides a complete list of the chemical shift assignments for all residues of pmh29.

Figure 4: The amide region of a 400 ms NOESY spectrum for pmh29 in 45% d_3-trifluoroethanol, 45% H_2O, and 10% D_2O at pH 3.45 and 300 K, where the NH-NH NOEs have been labeled

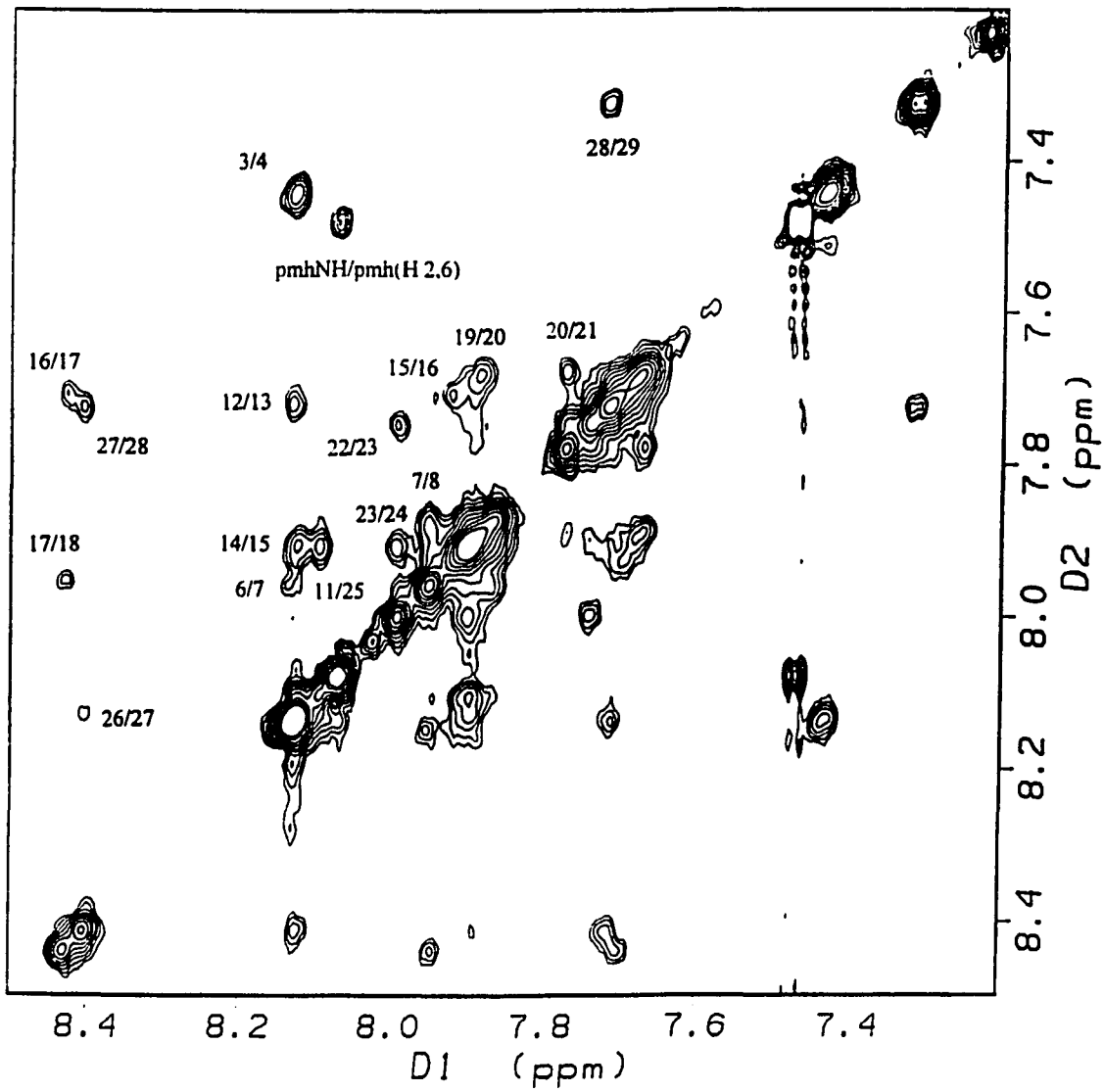

Figure 5: Expansion of the fingerprint region of a 400 ms NOESY spectrum for pmh29 in 45% d_3-trifluoroethanol, 45% H_2O, and 10% D_2O at pH 3.45 and 300 K, where the αH-NH and βH-NH NOEs have been labeled.

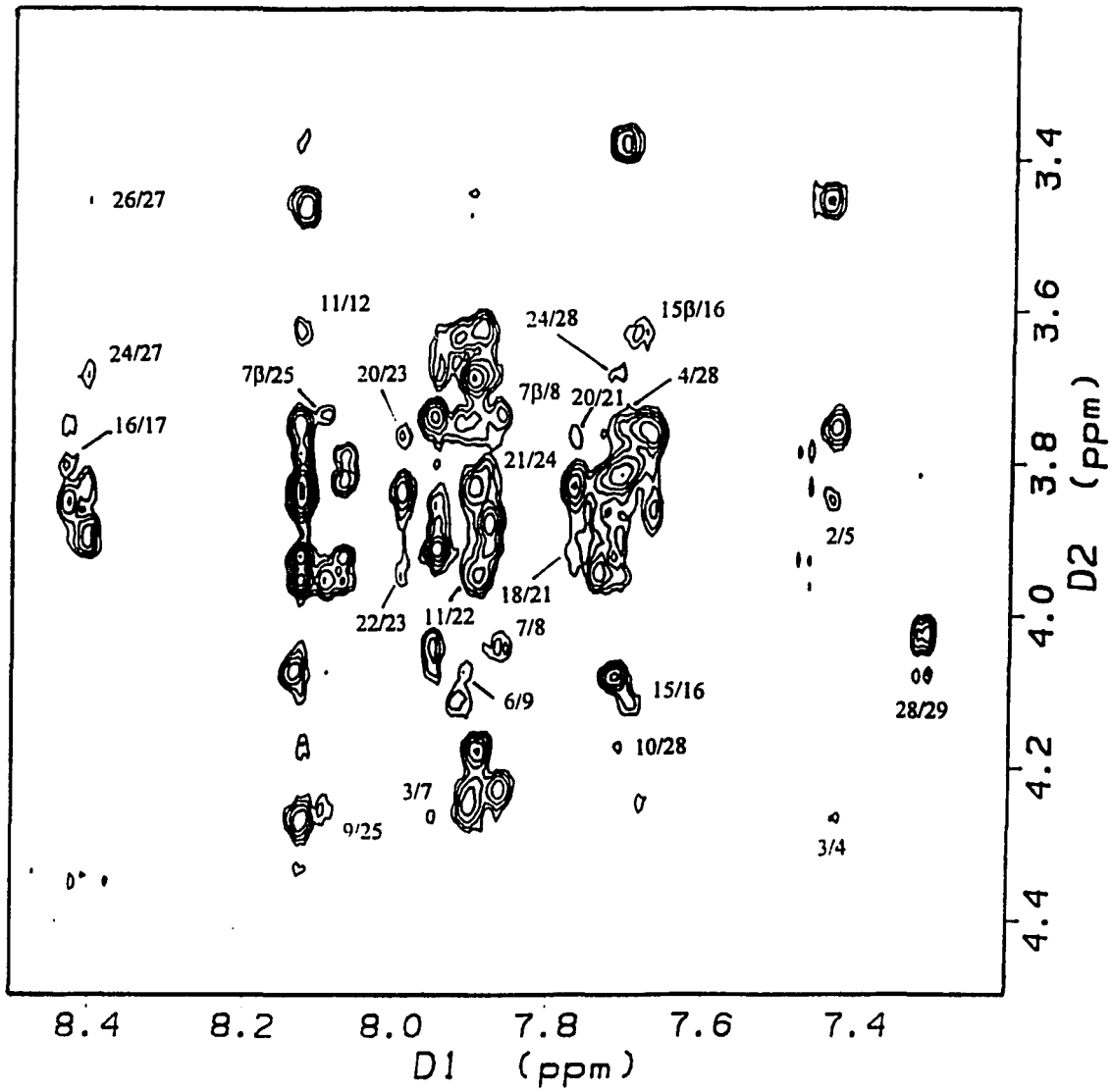

Figure 6: Expansion of the fingerprint region of a 100 ms TOCSY spectrum for pmh29 in 45% d_3-trifluoroethanol, 45% H_2O, and 10% D_2O at pH 3.45 and 300 K, where the sequence-specific assignments have been labeled.

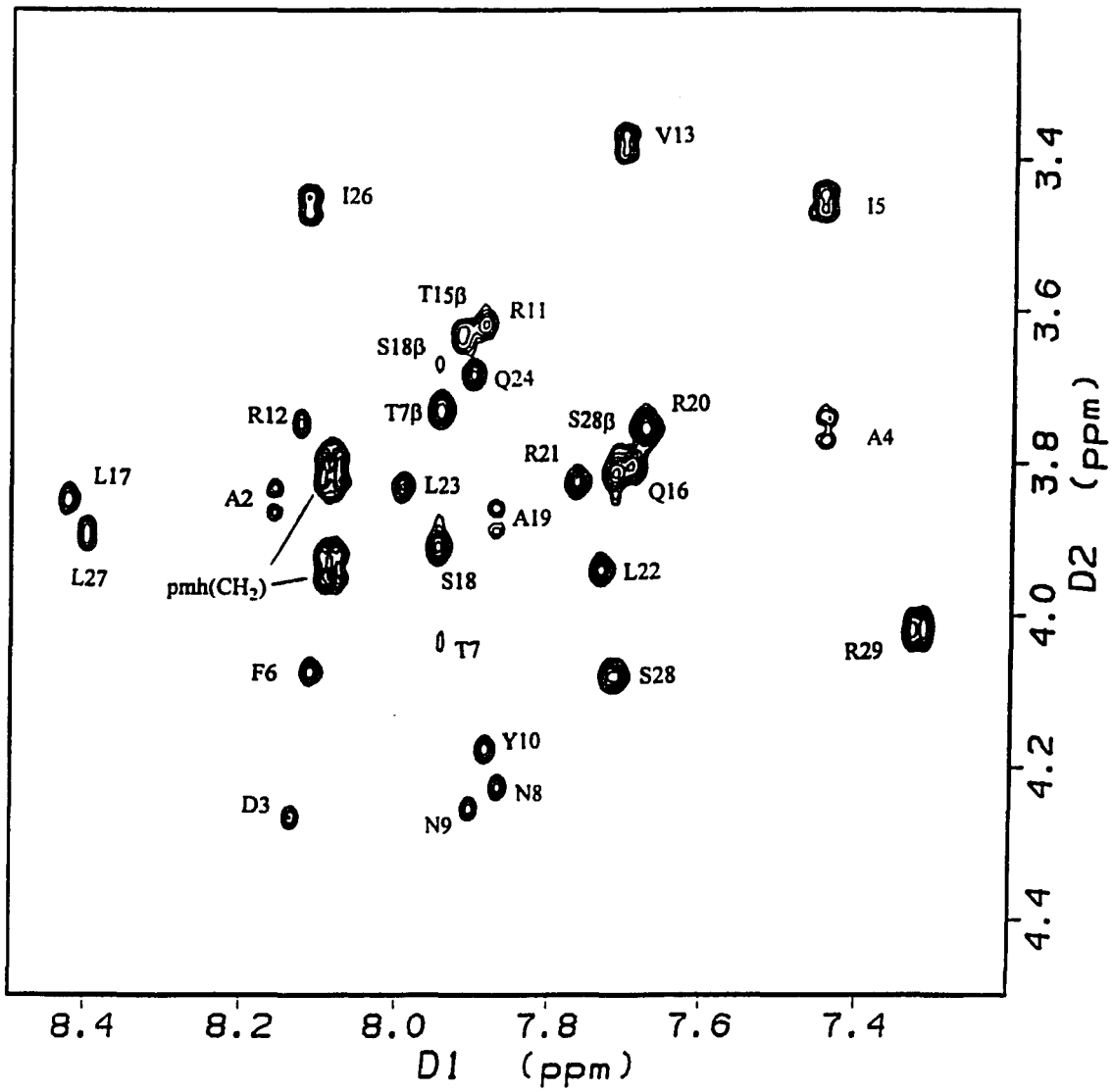

Table 2: ^{1}H Chemical Shifts for pmh29 in 45% TFE/45% H_2O/10% D_2O at pH 3.45 and 300 K.

Residue	NH	αH	βH	γH	δH	Others
pmh	8.09					CH_2 3.81, 3.94; (3,5)H 7.03; (2,6)H 7.48; (4)CH_3 2.09
Ala[2]	8.16	3.85	1.20			
Asp[3]	8.14	4.27	2.61, 2.64			
Ala[4]	7.45	3.76	0.92			
Ile[5]	7.45	3.46	1.63	1.31	0.88	γCH_3 0.56
Phe[6]	8.11	4.08	2.97			(2,6)H 6.88; (3,5)H 6.97
Thr[7]	7.94	4.04	3.73	1.07		
Asn[8]	7.87	4.23	2.52, 2.65			γNH_2 6.38, 7.32
Asn[9]	7.91	4.26	2.46, 2.60			γNH_2 6.31, 7.11
Tyr[10]	7.89	4.18	2.63, 2.85			(2,6)H 6.74; (3,5)H 6.52
Arg[11]	7.89	3.62	1.59, 1.68	1.34	2.94	εNH 6.82
Arg[12]	8.13	3.75	1.58, 1.78	1.35	2.97	εNH 6.85
Val[13]	7.71	3.38	1.93	0.67, 0.79		
Leu[14]	8.13		1.40	1.22	0.50, 0.53	
Thr[15]	7.92	4.11	3.63	1.01		
Gln[16]	7.70	3.80	1.92, 2.05	2.13, 2.30		
Leu[17]	8.42	3.85	1.61, 1.64	1.22	0.61	
Ser[18]	7.95	3.91	3.67			
Ala[19]	7.87	3.88	1.27			
Arg[20]	7.68	3.76	1.76	1.43, 1.59	2.91	εNH 6.95
Arg[21]	7.77	3.83	1.72, 1.78	1.48, 1.53	2.99	εNH 6.96
Leu[22]	7.74	3.94	1.62	1.48	0.66, 0.77	
Leu[23]	8.00	3.83	1.49		0.64	
Gln[24]	7.91	3.69	1.93, 2.00	2.12, 2.29		
Asp[25]	8.09	3.95	2.64, 2.73			
Ile[26]	8.12	3.46	1.78	1.57	0.58	γCH_3 0.66
Leu[27]	8.40	3.90	1.63	1.24	0.61	
Ser[28]	7.72	4.08	3.81			
Arg[29]	7.33	4.02	1.66, 1.75	1.48, 1.59	2.94	εNH 6.92; C(=O)NH_2 6.65, 7.01

SECONDARY STRUCTURE. NOE ANALYSIS. Table 3 details a quantitative analysis of the observed short- and medium-range NOE information obtained from NOESY spectra. A pattern of $d_{NN}(i,i+1)$, $d_{\beta N}(i,i+1)$, $d_{\alpha N}(i,i+3)$, and $d_{\alpha\beta}(i,i+3)$ NOEs emerges which are characteristic of α-helical structure. The presence of a medium intensity NOE between Ala[2]-αH and Ile[5]-NH and a weak intensity NOE between Asp[3]-αH and Thr[7]-NH implicates the helix initiation site as the N-terminus. A continuum of NOEs characteristic of helical structure (αH_i-NH_{i+3}; αH_i-NH_{i+4}; NH_i-NH_{i+2}; αH_i-βH_{i+3}) runs through the entire sequence ending at Arg[29] (Figure 7). The presence of a $d_{\alpha N}(i,i+4)$ NOE (Gln[24]-Ser[28]) and a $d_{\alpha N}(i,i+2)$ NOE (Leu[27]-Arg[29]) may suggest a distortion of the helix near the C-terminus. There is no break, however, in the observed helical NOE pattern which suggests that, in 45% TFE, pmh29 assumes an entirely helical secondary structure.

SECONDARY STRUCTURE. CSI ANALYSIS. The chemical shifts of Cα protons have been shown to be sensitive indicators of protein and peptide secondary structure (Pardi et al., 1983; Jiménez et al., 1987; Szilágyi & Jardetzky, 1989; Pastore & Saudek, 1990; Wishart et al., 1991). In α-helices αH chemical shifts are shifted upfield relative to random coil values, while in β-strands αH chemical shifts are shifted downfield relative to random coil values. Wishart et al. (1992) exploited this relationship to develop a simple empirical procedure for assigning polypeptide secondary structure solely from αH chemical shift data. This method, called the chemical shift index (CSI), compares experimentally observed αH chemical shifts with the random coil values (random coil values are those of Wüthrich (1986) with the exception of Ile and Val). Residues with an αH shifted upfield greater than 0.1 ppm from random coil values are assigned an index of "-1". Residues with an αH shifted downfield greater than 0.1 ppm from random coil values are assigned an index of "1". Residues whose αH chemical shifts are within a 0.1

Table 3: Quantitative summary of short- and medium-range NOE data for pmh29 in 45% TFE, 45% H_2O, and 10% D_2O at pH 3.45 and 300 K. Symbols correspond to NOE connectivity with O= weak, ◘= medium, and ●= strong intensity NOEs, respectively.

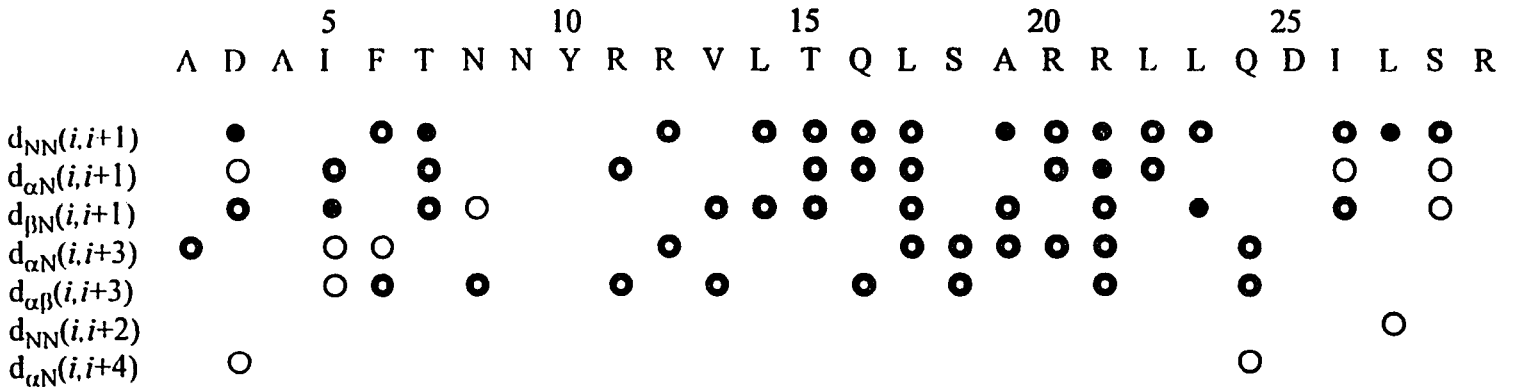

Figure 7: Amino acid sequence of pmh29 with observed medium-range NOEs indicated. Connections above the sequence indicate αH(*i*)-NH(*i*+3) NOEs. Connections below the sequence indicate αH(*i*)-βH(*i*+3) NOEs.

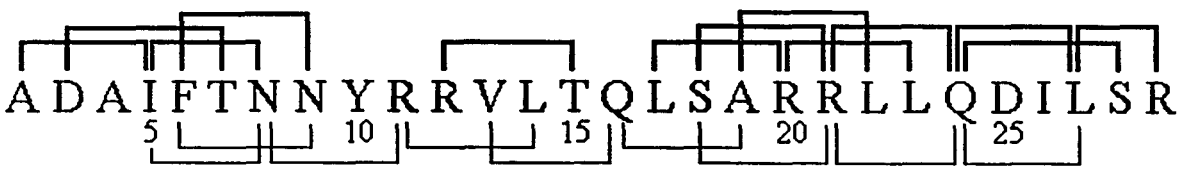

ppm range of random coil values are given a "0". Analysis of the polypeptide sequence and corresponding indices then provides the assignment of secondary structure. Groups of four or more "-1" indices without an intervening "1" are helical. Groups of three or more "1" indices without an intervening "-1" are β-strand. Finally, all other regions of the polypeptide sequence are deemed coil and include random coils, loops, turns and any other conformations that are neither α-helix nor β-strand.

The chemical shift index has been increasingly used as a qualitative tool to complement other methods of NMR secondary structure analysis such as NOE data, amide hydrogen exchange, and $^3J_{NH\alpha}$ coupling constants (Kloosterman et al., 1993; Rizo et al., 1993; Wray et al., 1993; Lee et al., 1994; Atkins et al., 1995; Craescu et al., 1995; Huang et al., 1995; Lu & Hall, 1995; Maciejewski & Zehfus, 1995; Mulhern et al., 1995). Several studies have also interpreted relative chemical shift changes in terms of a qualitative confirmation of secondary structure determined by other NMR methods, without specifically using the CSI analysis method (Li et al., 1992; Sipos et al., 1992; Mullen et al., 1993; Strickland et al., 1993; Hawkins et al., 1994; Jarvis et al., 1994; Thornton et al., 1994; Wray et al., 1994; Huq et al., 1995). In general, CSI analysis and similar techniques have provided accurate results that are consistent with the secondary structure characterized by other NMR methods and CD spectroscopy. The simplicity of the CSI technique makes it advantageous over amide hydrogen exchange and $^3J_{NH\alpha}$ coupling constants, especially in crowded spectra where overlap and ambiguities are common.

At the center of the αH CSI analysis are the random coil values of Wüthrich (1986). These random coil values were obtained at pH 7 and 308 K. The peptide structures used to derive the basis for structural assignment (greater or less than 0.1 ppm), however, were studied at various pH and temperature levels (Wishart et al., 1991, 1992). Is the method

then valid for peptides studied at temperatures and pHs different than those used to obtain random coil data? In addition, the random coil values obtained by Wüthrich (1986) were for a peptide of the sequence H-Gly-Gly-X-Ala-OH. Alanine has an inherent propensity to assume dihedral angles representative of helical structure (Chou & Fasman, 1978). Are the "random coil" values then truly random coil?

These questions were addressed by Merutka et al. (1995) who studied random coil chemical shifts at pH 5.0 and 308 K for the peptide series H-Gly-Gly-X-Gly-Gly-OH, and found only the αH shifts of aspartic acid, cysteine, and histidine to be appreciably different than those of Wüthrich (1986). The αH of the aspartic acid and cysteine residues showed an upfield shift of approximately 0.1 ppm, while the αH of histidine shifted downfield by the same magnitude. In addition, a discrepancy of approximately 0.05 ppm downfield was observed for the glutamic acid residue. The differences in the chemical shifts of the acidic residues and histidine were attributed to the change in pH and probable change in ionization state of their side chains. The sulfhydryl group of the cysteine sidechain was thought to be reduced, whereas it was suspected that Wüthrich (1986) had observed the chemical shift of a cysteine residue in a disulfide-bridged dimeric peptide, resulting in a different "random coil" value.

Wishart et al. (1995) also revisited the determination of random coil chemical shifts in an attempt to obtain more accurate results. The peptide series Ac-Gly-Gly-X-Ala-Gly-Gly-NH_2 was studied at pH 5 and 298 K. The peptides were dissolved, at lower concentrations than previous studies, in a buffer solution that contained 1 M urea to prevent any aggregation or residual structure formation. The chemical shift values obtained were commensurable with those of Wüthrich (1986) and Merutka et al. (1995). The residues that exhibited discrepancy from the values of the former study were primarily coincident with the latter: histidine, aspartic acid, glutamic acid, isoleucine, and

valine. Anomalies in histidine and the acidic residues were of the same magnitude and direction of Merutka et al. (1995), and were similarly ascribed to the two unit pH difference between the data sets. The chemical shifts for valine and isoleucine were upfield by approximately 0.05 ppm versus values of Wüthrich (1986). It was proposed that the lower concentrations used may have prevented hydrophobic aggregation to form a β-sheet-like structure. Values were obtained for both oxidized and reduced cysteine and were in agreement with Wüthrich (1986) and Merutka et al. (1995), respectively, confirming previous suggestions of disulfide bond formation in the former study.

The increasing use of TFE as a solvent in NMR investigations has raised the question of the accuracy of CSI analysis for non-aqueous solvent systems. Merutka et al. (1995) investigated the effect of TFE concentration (up to 50 mole percent) on the value of random coil chemical shifts. In general, the effect was found to be negligible with the largest effect shown to be a downfield shift of 0.04 ppm for arginine.

Variations in temperature also had a relatively small effect on αH random coil chemical shifts (Merutka et al., 1995). The H-Gly-Gly-X-Gly-Gly-OH peptide series was studied at 10 K intervals from 278 K to 318 K. The results showed an average downfield chemical shift of 0.02 ppm over the temperature range, with the largest change being 0.05 ppm for glutamic acid.

The CSI analysis appears to be an accurate and facile procedure for polypeptide secondary structure assessment under a variety of solvent and temperature conditions. The ease of interpretation of chemical shift data for a completely assigned polypeptide makes CSI analysis ideal in situations where overlap or ambiguities in NOE data exist. CSI analysis was useful in the current study to confirm interpretation of short- and medium-range NOE data and CD data which exhibit a pattern of connectivities consistent with a completely helical conformation for pmh29.

Table 4 shows the CSI analysis of pmh29. The random coil values used for comparison were those of Wishart et al. (1995) because they most closely approximate the solution conditions under which pmh29 was investigated. The random coil values were obtained at pH 5.0 and 298 K, whereas pmh29 was studied at pH 3.45 and 300 K. According to the aforementioned studies, the small differences in pH and temperature and the presence of TFE should have negligible effect on the accuracy of the CSI analysis presented here. The continuum of "-1" indices from the N- to C-terminus of pmh29 presented in Table 4 suggests that pmh29 adopts a completely helical structure in 45% TFE at pH 3.45 and 300 K.

The chemical shift index has also been used as a quantitative measure of the relative amounts of helical structure (Rizo et al., 1993). An average conformational upfield shift of 0.35 ppm was assumed to represent 100% helicity. This value was derived as a "compromise" from several studies which assigned values of average upfield shift that ranged from 0.3 ppm to 0.4 ppm (Jiménez et al., 1987; Szilágyi & Jardetzky, 1989; Williamson, 1990; Wishart et al., 1991). Comparison of percent helicity from CSI to values obtained from CD spectroscopy showed a strikingly close correlation, and seemed to point to CSI analysis as an effective quantitative measure of helicity.

Quantitation of the pmh29 CSI analysis to derive an estimate of helical content using the procedure described in Rizo et al. (1993) provides some interesting results. Summing all $\Delta\delta$ (changes in chemical shift) values and dividing by the number of peptide bonds gives an average conformational shift of 0.53 ppm. To obtain the overall helicity content, the average conformational shift was divided by 0.35 (the 'compromise' value for average conformational shift (Rizo et al. (1995)) to obtain 151% helicity for pmh29. Even using the largest reported average upfield shift of 0.40 ppm gives a value of 134% helicity. Clearly, the percent helicity value is extremely inflated and/or erroneous.

Table 4: Chemical Shift Index analysis (Wishart et al., 1992) for pmh29 in 45% TFE/ 45% H_2O/ 10% D_2O at pH 3.45 and 300 K using random coil values of Wishart et al. (1995).

Residue	δ Coil	δ Expt.	δ Δ	CSI
Ala^{2}	4.32	3.85	- 0.47	- 1
Asp^{3}	4.64	4.27	- 0.37	- 1
Ala^{4}	4.32	3.76	- 0.56	- 1
Ile^{5}	4.17	3.46	- 0.71	- 1
Phe^{6}	4.62	4.08	- 0.54	- 1
Thr^{7}	4.35	4.04	- 0.31	- 1
Asn^{8}	4.74	4.23	- 0.51	- 1
Asn^{9}	4.74	4.26	- 0.48	- 1
Tyr^{10}	4.55	4.18	- 0.37	- 1
Arg^{11}	4.34	3.62	- 0.72	- 1
Arg^{12}	4.34	3.75	- 0.59	- 1
Val^{13}	4.12	3.38	- 0.74	- 1
Leu^{14}	4.34	3.76	- 0.58	- 1
Thr^{15}	4.35	4.11	- 0.24	- 1
Gln^{16}	4.34	3.80	- 0.54	- 1
Leu^{17}	4.34	3.85	- 0.49	- 1
Ser^{18}	4.47	3.91	- 0.56	- 1
Ala^{19}	4.32	3.88	- 0.44	- 1
Arg^{20}	4.34	3.76	- 0.58	- 1
Arg^{21}	4.34	3.83	- 0.51	- 1
Leu^{22}	4.34	3.94	- 0.40	- 1
Leu^{23}	4.34	3.83	- 0.51	- 1
Gln^{24}	4.34	3.69	- 0.65	- 1
Asp^{25}	4.64	3.95	- 0.69	- 1
Ile^{26}	4.17	3.46	- 0.71	- 1
Leu^{27}	4.34	3.90	- 0.44	- 1
Ser^{28}	4.47	4.08	- 0.39	- 1
Arg^{29}	4.34	4.02	- 0.32	- 1

Is the procedure of quantitation of helicity content using CSI analysis invalid, or are there factors contributing to an inflated percent helicity value? Several factors can contribute to an exaggeration of upfield proton chemical shifts (Williamson, 1990; Herranz et al., 1992; Williamson & Asakura, 1993). These factors include: ring-current effects from aromatic residues, electric-field effects from point charges and charge dipoles (e.g. C=O and C'—N bonds), and/or positioning of the proton proximal to a peptide group. The tertiary fold (see below) of pmh29 may allow some of these factors to exist. Examination of Table 4 reveals several residues that have $\Delta\delta$ values that are greater than 0.60 ppm. The residues are located either near the two aromatic residues, Phe^{6} and Tyr^{10}, or in a region near the C-terminus. The large upfield shift of residues 24-26 may be a result of their close proximity to Tyr^{10}. Similarly, α protons from neighboring residues of Phe^{6} and Tyr^{10} show large upfield chemical shifts. Also, the observed long-range NOEs indicate that the tertiary fold places several α protons in a close proximity to the peptide bond, which would make these resonances subject to electric-field effects. It is likely, therefore, that one or more of the above factors are functioning to skew the percent helicity content of pmh29 by CSI analysis. In addition, these results suggest that the percent helicity content calculated by CSI analysis data is not valid for all polypeptide molecules.

CONFORMATIONAL HETEROGENEITY. A closer examination TOCSY and NOESY spectra (Figures 3, 5, and 6) reveals a splitting or doubling of some of the crosspeaks. This phenomenon is particularly evident in some of the $C_{\alpha}H$ resonances (Figure 6) such as Ala^{2}, Ala^{4}, Ile^{5}, and Ala^{19}. Resonance splitting in NMR spectra can arise from dimeric interaction and/or conformational heterogeneity (Gooley et al., 1984, 1985; Folkers et al., 1993; Nilges, 1993). Light scattering microscopy experiments showed the peptide to exist as a monomer in aqueous TFE (45%) (G. F. Needham, Eli Lilly and

Company, personal communication). The peptide, therefore, must adopt more than one significantly populated conformation under the current solvent conditions.

Few cases of resonance splitting in NMR experiments have been reported (Gooley et al., 1984, 1985; Xu et al., 1991; Narula et al., 1993; Otting et al., 1993). In all of these cases the doubling was the result of conformational heterogeneity. In studies by Gooley et al. (1984, 1985) of cardiac stimulant peptides from sea anemones, the source of the resonance doubling was conformational heterogeneity due to a *cis-trans* proline isomerization process. A study of a zinc finger peptide ADR1a found that the peptide exists in two slowly interconverting folded conformations as evidenced by doubling of ^{1}H resonances (Xu et al., 1991). The heterogeneity observed was attributed to a difference in the geometry of the ligands in the Zn^{+2} clusters of residues in the two structures.

An investigation by Narula et al.(1993) of copper- and silver-substituted yeast metallothioneins concluded that an observed doubling of resonances in 2D ^{1}H NMR spectra was the result of an interaction either between two cysteine residues not involved in metal ligation or between these two cysteines and another portion of the protein. It was also suggested that the heterogeneity could be the result of these same two cysteines loosely ligating an additional metal ion. The ratios of the doubled peaks was temperature dependent in this case, which showed the two conformations to be in exchange. The presence of doubled peaks in the 2D ^{1}H NMR spectrum of BPTI and an analog BPTI(G36S) was ascribed to the existence of two conformationally isomeric forms of the peptides (Otting et al., 1993). The two conformers were in exchange and differed by the chirality of their Cys^{14}-Cys^{38} disulfide bond.

The GRF analog pmh29 contains no proline residues or disulfide bonds, nor does it contain any bound metal ligands. The observed doubling of resonances, therefore, must

be the result of a form of conformational heterogeneity that differs from the aforementioned studies. We propose that the conformational heterogeneity involves two slightly different global tertiary structures. In both conformers the peptide has the same type of fold, but differs by the region of interaction between the two ends of the chain.

TERTIARY STRUCTURE. Long-range NOE data indicates a close proximity (< 5.0 Å) between a wide span of residues in the N-terminal end (residues 4-13) and a wide span of residues in the C-terminal end (residues 22-29) of the peptide chain (Table 5). Tyr^{10} shows NOE connectivities to residues as far apart in the C-terminal region as Leu^{22} and Ser^{28}, while Asp^{25} shows NOEs to residues as separated as Phe^{6} and Val^{13} in the N-terminal region. These observations further suggest that the conformational heterogeneity may be the result of two similar folds with tertiary interactions at slightly different points along the peptide chain. The most distant long-range interaction, in terms of sequence separation, is $Ala^{4}\alpha H$-$Arg^{29}\beta H$, while the nearest long-range interaction is $Arg^{11}NH$-$Leu^{22}\alpha H$. It is clear that the interactions are between residues that are located in the N-terminal portion of the peptide (Ala^{4}, Phe^{6}, Thr^{7}, Asn^{9}, Tyr^{10}, Arg^{11}, and Val^{13}) and residues that are located in the C-terminal portion of the peptide (Leu^{22}, Gln^{24}, Asp^{25}, Ile^{26}, Ser^{28}, and Arg^{29}). This implies that the peptide forms a tertiary conformation by folding back onto itself. The turn, however, does not appear to be tight, i.e. a β- or γ-turn, because there is a lack of long-range NOEs in the 12-21 region of the peptide, and an NOE pattern that would suggest a β-turn is not observed.

CALCULATED STRUCTURES. A combination of distance geometry and simulated annealing has been used to calculate the three-dimensional structures of pmh29 from NOE data. A total of 302 NOEs were classified as strong, medium, and weak,

Table 5: Quantitative summary of the observed long-range NOEs for pmh29 in 45% TFE, pH 3.45 at 300 K. Symbols correspond to NOE connectivity with O= weak, ⊙= medium, and ●= strong intensity

Residue		L22	Q24		D25			I26		S28		R29
		αH	βH	NH	αH	βH	NH	βH	γH	NH	βH	αH
A4	αH									⊙		
	βH											O
F6	αH			O								
T7	βH			⊙		⊙						
	γH					O						
N9	αH			⊙				⊙				
	βH			⊙								
Y10	NH					⊙	⊙					
	αH									O	O	
	βH	⊙										
	δH		O	O	⊙	O			O			

corresponding to distance ranges of 1.8-2.5, 1.8-3.5, and 1.8-5.0 Å, respectively. As described above the long-range NOEs are suspected to arise from two different tertiary conformations. As a test to this hypothesis, structures have been calculated from three sets of NOEs. One set consists of all the long-range NOEs, while the other two NOE sets contain a subset of long-range NOEs (Table 6). The subsets of long-range NOEs have been created by dividing the NOEs according to the ability of the residue from which the NOE arose to satisfy all of the NOEs it exhibits. For example, NOEs between Asp^{25} and Phe^{6} were placed in one group, while NOEs between Asp^{25} and Val^{13} were placed into the other group. Likewise, the Ser^{28}-Ala^{4} and Ser^{28}-Tyr^{10} NOEs were placed into separate groups. The structure calculated by inclusion of all the long-range NOEs is a very high energy structure in comparison to the structures calculated from the subsets of long-range NOEs, further suggesting two tertiary conformations. This very high energy structure was examined to aid in the division of the NOEs into two subsets. Figure 8 (A and B) shows the lowest energy structure calculated from each of the two subsets of long-range NOEs. In both structures the peptide is nearly completely helical with a fold in the area of Gln^{16}. Distortions in the helical structure are due to the combination of an overestimation of peak integration caused by overlapping resonances in the NOESY spectra and the inherent conformational flexibility of this molecule in solution.

Two similar tertiary folds in pmh29 create two conformers that have an overall tertiary amphiphilicity, that is, one face of each of the structures is primarily hydrophobic while the other is primarily hydrophilic. Similar residues form the hydrophobic and hydrophilic faces in both conformers. In conformer A (Figure 8 A) residues Ala^{2}, Ala^{4}, Ile^{5}, Phe^{6}, the methyl group of Thr^{7}, Tyr^{10}, Leu^{14}, Leu^{22}, Leu^{23}, and Leu^{27} form the hydrophobic face (Figure 9A), and residues Asp^{3}, Asn^{8}, Arg^{11}, Arg^{12}, Glu^{16}, Arg^{20},

Table 6: The subsets of long-range NOEs that were used for the calculation of two three-dimensional structures by the combination of distance geometry and simulated annealing.

Subset A:	Subset B:
Ala^{4} βH -- Arg^{29} αH	Tyr^{10} NH -- Ile^{26} NH
Ala^{4} αH -- Ser^{28} NH	Tyr^{10} δH -- Asp^{25} NH
Phe^{6} αH -- Asp^{25} NH	Tyr^{10} δH -- Asp^{25} βH
Thr^{7} βH -- Asp^{25} NH	Tyr^{10} δH -- Asp^{25} αH
Thr^{7} βH -- Asp^{25} βH	Tyr^{10} NH -- Asp^{25} βH
Thr^{7} γH -- Asp^{25} βH	Tyr^{10} αH -- Ser^{28} βH
Asn^{9} αH -- Asp^{25} NH	Tyr^{10} αH -- Ser^{28} NH
Asn^{9} βH -- Asp^{25} NH	Tyr^{10} δH -- Ile^{26} γH
Asn^{9} αH -- Ile^{26} βH	Arg^{11} NH -- Asp^{25} NH
Tyr^{10} δH -- Gln^{24} βH	Val^{13} βH -- Asp^{25} αH
Tyr^{10} βH -- Leu^{22} αH	Val^{13} γH -- Asp^{25} αH
Arg^{11} NH -- Leu^{22} αH	

Figure 8: A) Ribbon drawing of the lowest energy distance geometry/simulated annealing structures for pmh29 calculated with subset A (see Table 6) of the long-range NOEs.

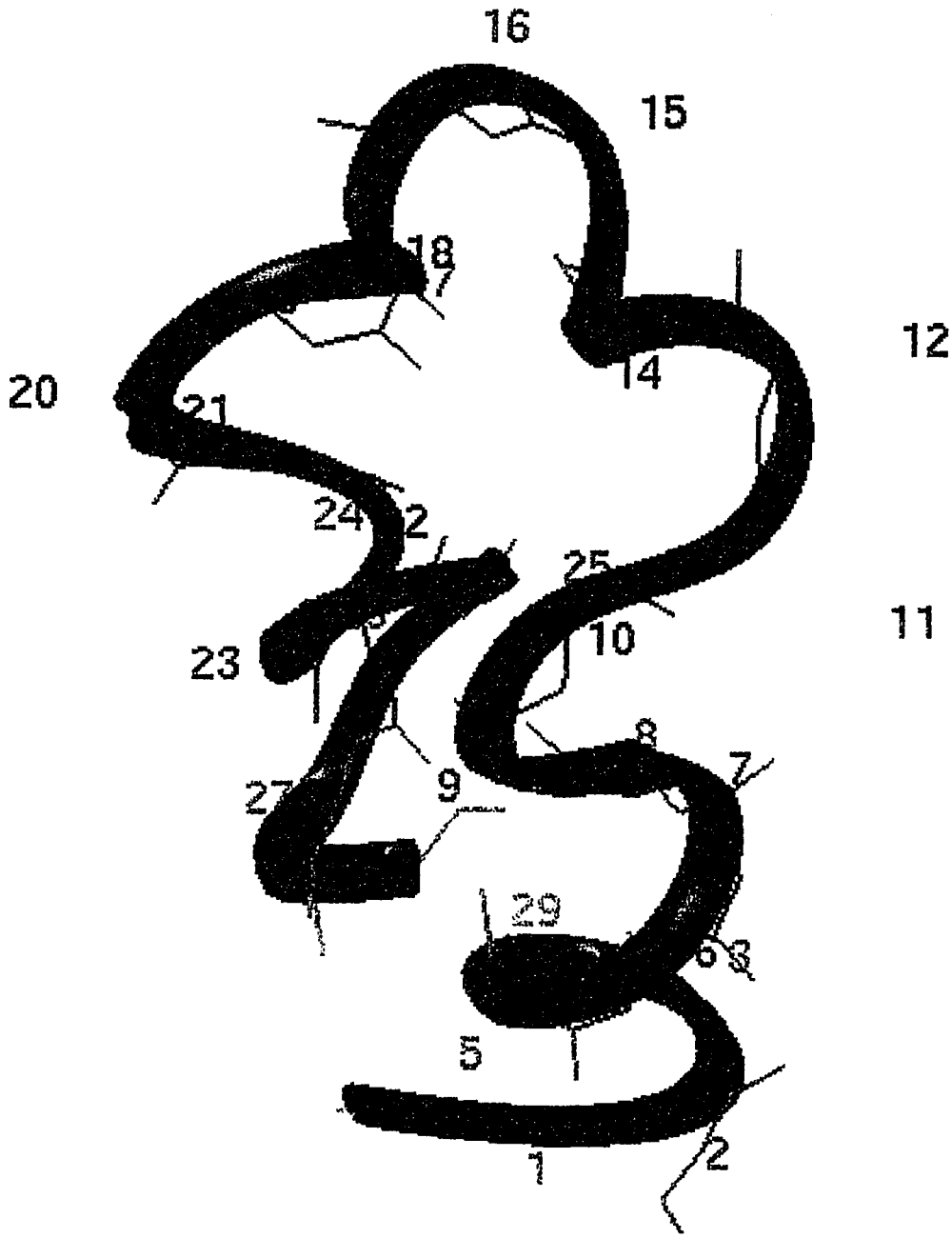

Figure 8: B) Ribbon drawing of the lowest energy distance geometry/simulated annealing structures for pmh29 calculated with subset B (see Table 6) of the long-range NOEs.

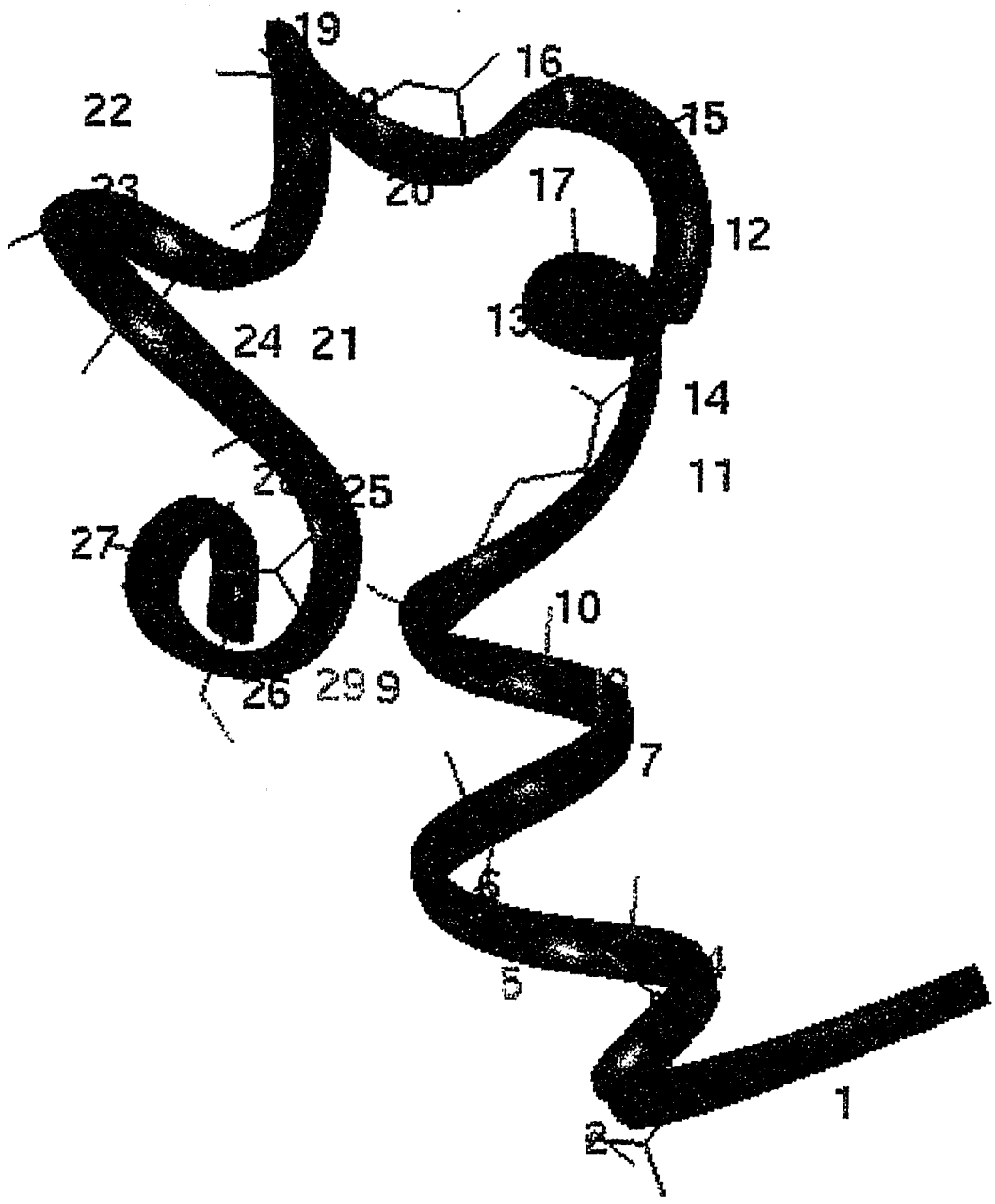

Figure 9: A) Backbone trace of structure A from Figure 8 with those residues that define the hydrophobic face of the tertiary structure labeled.

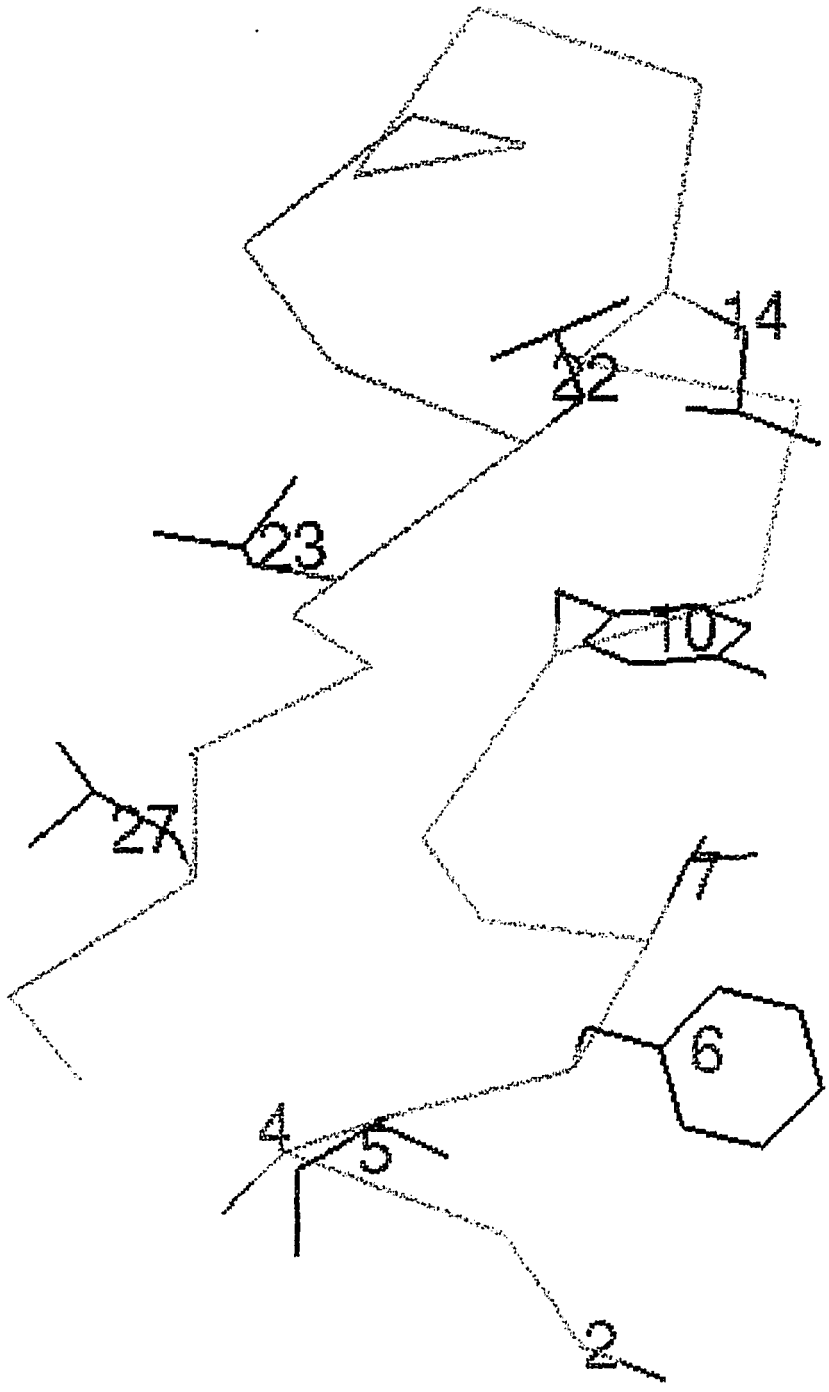

Figure 9: B) Backbone trace of structure A from Figure 8 with those residues that define the hydrophilic face of the tertiary structure labeled.

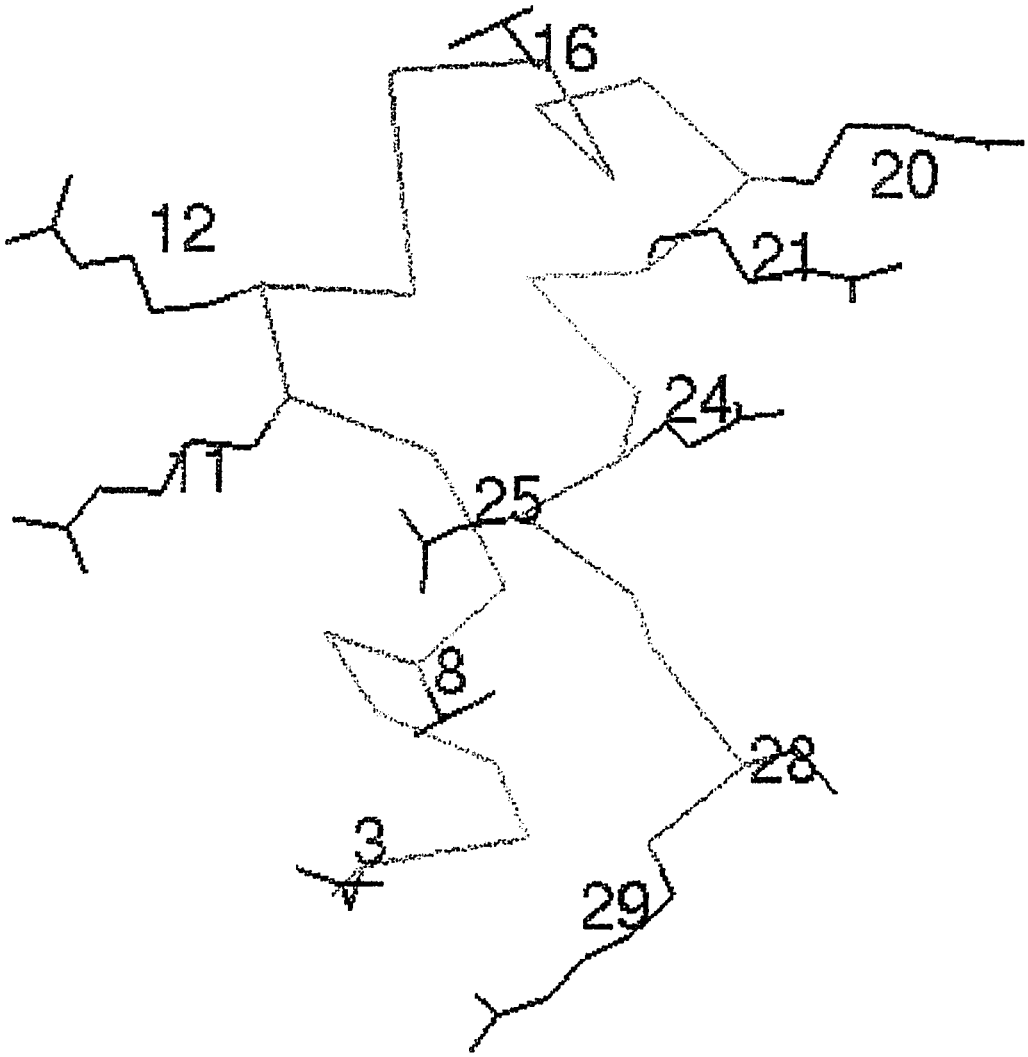

Figure 10: A) Backbone trace of structure B from Figure 8 with those residues that define the hydrophobic face of the tertiary structure labeled.

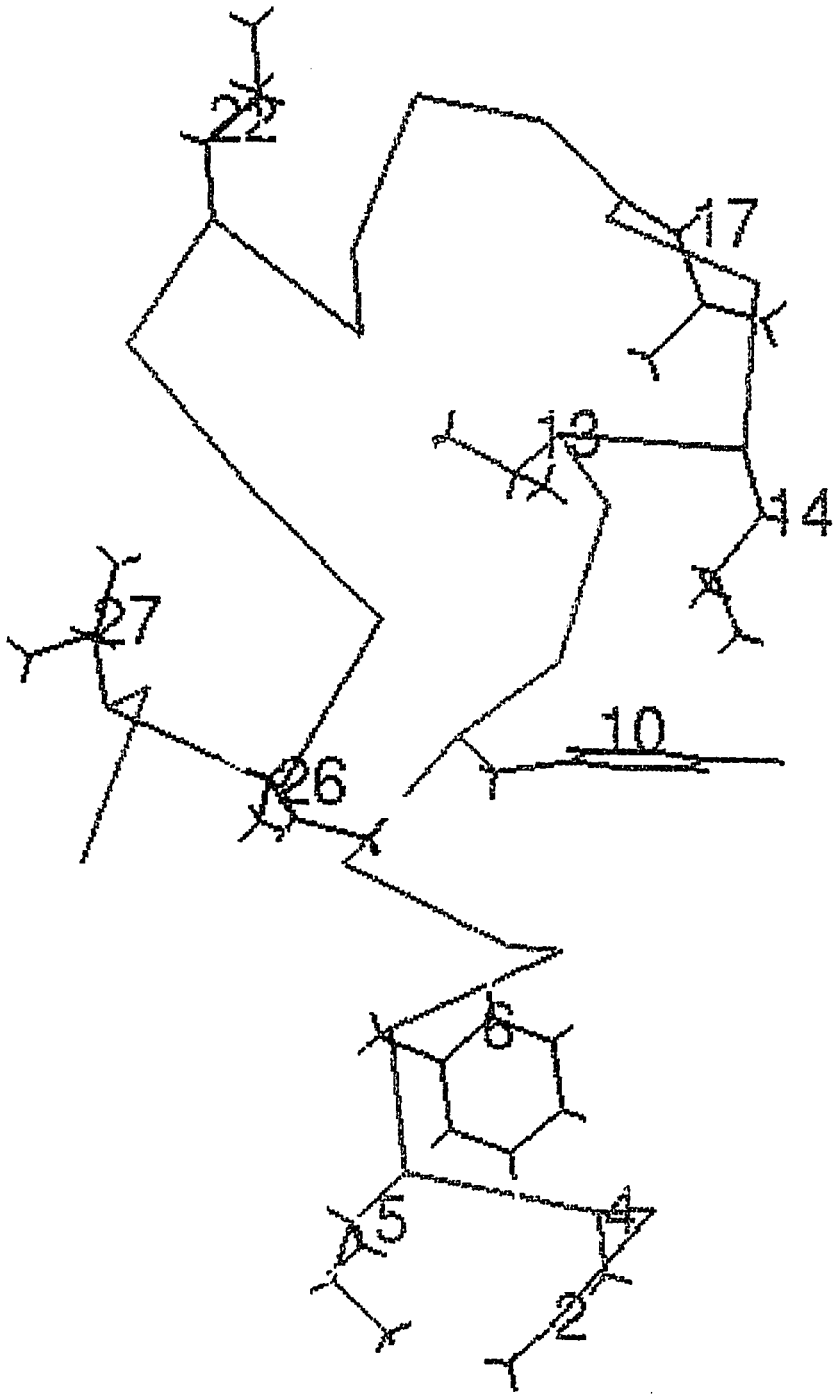

Figure 10: B) Backbone trace of structure B from Figure 8 with those residues that define the hydrophilic face of the tertiary structure labeled.

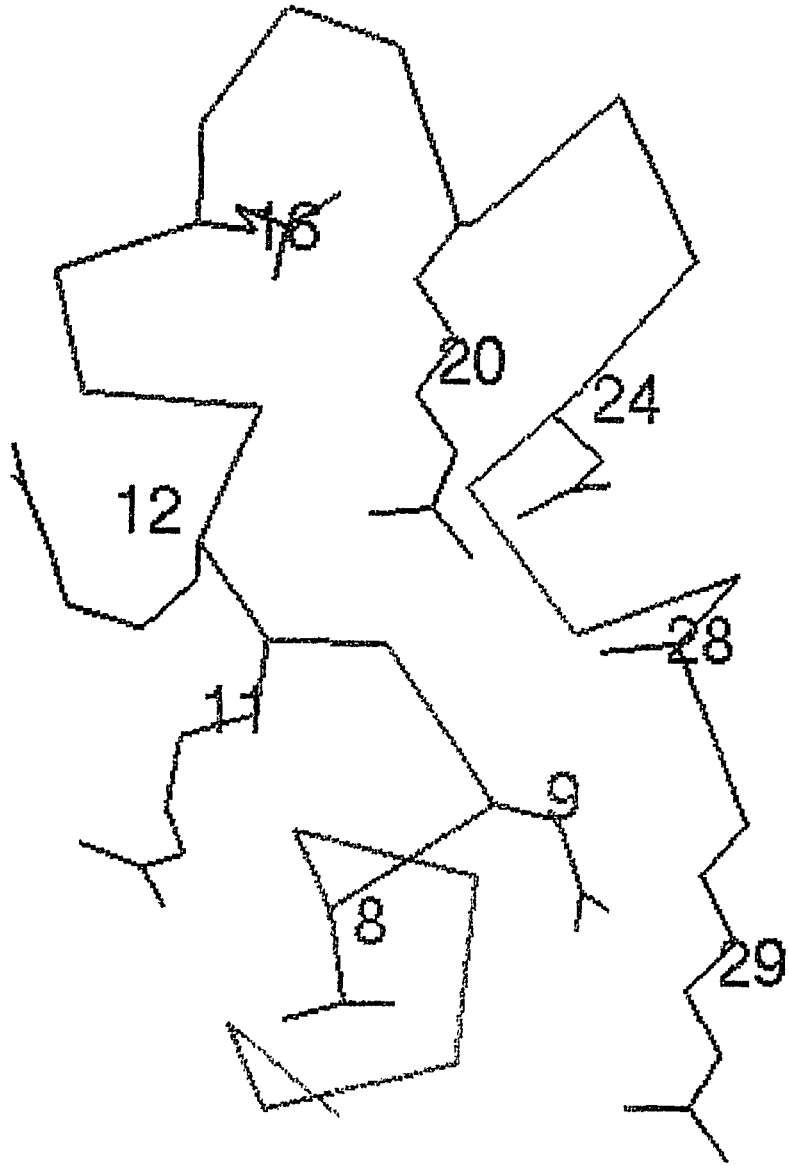

Arg^{21}, Glu^{24}, Asp^{25}, Ser^{28}, and Arg^{29} form the hydrophilic face (Figure 9B). Likewise, in conformer B (Figure 8B) residues Ala^{2}, Ala^{4}, Ile^{5}, Phe^{6}, Tyr^{10}, Val^{13}, Leu^{14}, Leu^{17}, Leu^{22}, Ile^{26}, and Leu^{27} form the hydrophobic face (Figure 10A), and residues Asn^{8}, Asn^{9}, Arg^{11}, Arg^{12}, Glu^{16}, Arg^{20}, Gln^{24}, Ser^{28}, and Arg^{29} form the hydrophilic face (Figure 10B).

VALIDITY OF CALCULATED STRUCTURES. The structures we have obtained from distance geometry calculations and simulated annealing refinement are subject to some inherent error caused by overlapping resonances. The doubling of peaks that is clearly observed in the TOCSY spectra is not as well defined in NOESY spectra, resulting in an overlapping of NOESY crosspeaks and a concomitant increase in the peak volumes of some, if not all, NOE crosspeaks. The structures, therefore, may more accurately be a pictorial representation of the tertiary folds that pmh29 assumes. The errors in NOE peak volume integration likely manifest themselves as distortions in the helical conformation that are observed in the calculated structures (Figure 8).

The pmh29 molecule, like most peptides of its size, is highly flexible, and as with any NMR solution structure, the structures shown in Figure 8 are time-averaged representations of an ensemble of molecular conformations (Cicero et al., 1995). The peptide visits numerous conformations within the ensemble, but populates the observed conformations proportionately more often than others. The stuctures observed are inherently unstable due not only to the flexibility of the molecule, but also to the denaturing effect of the TFE solvent system (see below). The structures are not in direct exchange with each other as indicated by the results of higher temperature TOCSY experiments (310 K and 320 K) which did not provide any evidence of coalescence of the doubled peaks or changes in the apparent peak volumes that would accompany conformations in direct exchange

PMH29: CONCLUSIONS

THE ROLE OF THE PARA-METHYLHIPPURYL GROUP. Several studies have been performed to investigate the roles of individual amino acids of the GRF sequence and to create potent and/or metabolically stable analogs using amino acid substitutions and/or deletions. It was determined that an aromatic residue with the potential to form hydrogen bonds was required at position 1 for bioactivity (Ling et al., 1984). An analog substituted at position 1 with histidine retained much of the *in vitro* activity measured for the parent GRF molecule. Substitutions of phenylalanine, tryptophan, and alanine for Tyr^1, however, showed greatly reduced activities. Aromaticity, therefore, must not have been the only factor contributing to the activity. Methylation of the phenolic hydroxy group of Tyr^1 and the imidazole amino group of His^1 also resulted in a decrease in bioactivity. These results suggested the participation of the amino terminal residue in an essential hydrogen bond either with the receptor or intramolecularly. Furthermore, substitution of Tyr^1 by its corresponding D-amino acid resulted in an analog with significantly decreased potency (Ling et al., 1984) and binding affinity (Lefrançois & Gaudreau, 1994), which indicated the existence of a structural requirement as well. Deletion of the amino terminal residue altogether also caused a severe reduction in activity (Guillemin et al., 1982) and binding affinity (Gaudreau et al., 1992), while acylation of the amino terminus (N-Ac-Tyr^1) resulted in a reduction in the activity and binding affinity of GRF (Ling et al., 1984; Gaudreau et al., 1992).

The amino-terminal position of GRF thus plays an important role in the binding affinity and potency of the molecule. In the pmh analogs Tyr^1 has been deleted and Ala^2 has been acylated with a para-methylhippuric acid group. Each of the resulting analogs is extremely potent versus the parent molecule, and removal of the hippuryl group results in analogs with significantly decreased activity (G. F. Needham, Eli Lilly and Company,

personal communication). Though the hippuryl group is not completely responsible for the increased activity versus the parent molecule (see discussion to follow), the part it plays can not be underestimated. The hippuryl group at least fulfills the aforementioned requirements for mere retention of native-like potency. The benzylic ring of the hippuryl group satisfies the requirement of aromaticity, and although there is no phenolic hydroxy group, the amide group can act in a hydrogen bonding capacity. The ability of the hippuryl group to meet the structural requirement demands a closer examination.

The hippuryl group resembles a glycine residue (with the methylene carbon approximating the α carbon) that is itself acylated with a 4-methyl-benzoyl group. A glycine residue can not only assume the dihedral angles adopted by a tyrosine residue at position-1, but also has a high propensity to be in the N-cap helix position (the interfacial residue that begins the helix and is half in and half out of the helix) in both proteins (Richardson & Richardson, 1988) and peptides (Chakrabartty et al., 1993). It appears that the hippuryl group indeed behaves like an acylated glycine residue in the pmh analogs. In each of the pmh analogs the helix begins at Ala^2 with the glycine-like portion of the hippuryl group acting as the N-cap residue.

Previous NMR studies of GRF analogs have shown the molecules to consist of one or two helices with the first or only helix starting as early as Asp^3 or Ala^4. An exception is the study of hGRF(1-29)NH_2 by Theriault et al. (1988) who found the helix to start at Ala^2. In the case of Theriault et al., however, the discrepancy appears to be the result of overzealous NOE interpretation. A single helical type (αH-NH) NOE between residues 2 and 6 was the justification for assignment of the helix initiation site as residue 2. This peak was observable in the 500 ms NOESY but not the 400 ms NOESY which makes it suspect as a spin-diffusion peak. The CSI analysis of the αH chemical shift assignments, alternatively, suggests the helix initiation site as Ile^5 or Ala^4 at best. The CSI analysis is

corroborated by a NH-NH NOE between residues 5 and 7 (present in the 400 ms NOESY) and residues 6 and 8, as well as an αH-NH NOE between residues 6 and 9.

The ability of the hippuryl group in the pmh analogs to promote helix formation at Ala^2 may contribute to the observed increased potency versus the natural product. It has been proposed that members of the secretin family require a disordered N-terminus of 6-8 residues for bioactivity (Gronenborn et al., 1987; Wray et al., 1993). Wray et al. (1993) went on to suggest that the N-terminal region must have flexibility to assume a specific structure at the peptide receptor. It appears that helicity is either a required or preferred conformation at the GRF receptor, as indicated by the results of studies of potent GRF analogs that form helical structure as early as residue 3 (Fry et al., 1992; Stevenson et al., 1992). The results reported here also lend credence to this hypothesis, as the pmh analogs are very potent and assume a helical conformation in the N-terminal region. Whether the results obtained for GRF analogs can be applied to the entire secretin family is uncertain. The N-terminal region may impart binding specificity to the individual members of the family. The role of the hippuryl group in extending the helical region to the N-terminus, however, contributes to the overall potency of the pmh analogs, likely by promoting a preferred binding conformation in the N-terminal region.

METABOLIC STABILITY. The hippuryl group also contributes to the potency of the pmh analogs by increasing metabolic stability. In contrast to the *in vitro* results of analogs substituted at position-1 (Ling et al., 1984), *in vivo* studies of $D\text{-}Tyr^1$ and $N\text{-}Ac\text{-}Tyr^1$ analogs showed a 10- and 12-fold increase in GH release, respectively (Lance et al., 1984). This increase in potency is most likely due to a decrease in enzymatic degradation and concomitant increase in bioavailability of these analogs at the receptor sites. The hippuryl acylation at Ala^2 in pmh29 may similarly act to decrease enzymatic degradation of the peptide molecule.

Other amino acid substitutions in the pmh analogs have been designed to increase metabolic stability. Several lysine residues have been replaced by arginine residues to prevent trypsin-like cleavage, and the two methionine residues have been replaced by leucines to prevent oxidative metabolic inactivation. These substitutions play a symbiotic role with the adoption of a preferred structure to confer a high potency to pmh29 via increased binding affinity and bioavailability.

EFFECT OF TFE ON PEPTIDE STRUCTURE. Trifluoroethanol (TFE) has increasingly been used as solvent for the study of peptides and protein fragments by NMR spectroscopy. The principal reason for the use of TFE has been to stabilize elements of structure in peptides that lack stable structures under purely aqueous conditions. TFE has been called a helix-inducing solvent, though stable β-strands (Goodman et al., 1971; Balcerski et al., 1976; Kelly et al., 1977; Narayanan et al., 1986; Wang et al., 1995) and β-turns (Cann et al., 1987; Siligardi et al., 1987; Sönnichsen et al., 1992; Blanco et al., 1994; Wang et al., 1995) have been observed in solutions of TFE. The *modus operandi* of TFE is not fully understood, however, there are several characteristics of TFE that may be responsible for its actions.

The dielectric constant of TFE is about one-third that of water (26.67 vs. 78.54, respectively), which may cause an increase in interactions between charged groups (Nelson & Kallenbach, 1986). This scenario would result in a stabilization of structure, however, Nelson and Kallenbach (1986) did not find any increase in the magnitude of the charge group effect (helix stability imparted by the interaction of charged side chains with the helix dipole (Shoemaker et al., 1985, 1987), upon addition of TFE, which would imply that this scenario is not significant. TFE is a stronger acid (pKa_2 12.4 for TFE vs. 15.3 for water) and a weaker base (pKa_1 ~ -8.2 for TFE vs. -1.8 for water) than water (Nelson & Kallenbach, 1986). Thus, TFE will more readily donate protons and will less

readily accept protons for hydrogen bonding than will water. This property may result in a decrease in hydrogen bonding to the solvent and an increase in intramolecular hydrogen bonding (Nelson & Kallenbach, 1986; Sönnichsen et al., 1992). Finally, TFE is less polar than water. This property may cause a stabilization of the hydrogen-bonding network while disrupting hydrophobic interactions (Sönnichsen et al., 1992; Albert & Hamilton, 1995). It was suggested by Sykes and co-workers (Sönnichsen et al., 1992) that this property may implicate TFE as a denaturant of tertiary and quaternary structure.

Indeed, TFE has been shown by this same group (Slupsky et al., 1995a,b) to denature quaternary structure in troponin C. The calcium-induced dimerization of troponin C was found to be a hydrophobic interaction between the N-terminal domains of the two monomers. Upon addition of 15%, v/v, TFE the quaternary structure was denatured, however, there were no substantial differences in the tertiary and secondary structures. Similar results were obtained by Buck et al. (1993) who found no significant change in the tertiary and secondary structure of hen egg white lysozyme in 15%, v/v, TFE. It would appear then that very low levels of TFE can stabilize secondary structure in proteins without denaturing tertiary structure.

At higher TFE concentrations, an alcohol-denatured or TFE state can be observed in some proteins. This TFE state is characterized by stabilization of native elements of secondary structure with a disrupted hydrophobic core. Dobson and co-workers have observed the TFE state of hen egg white lysozyme (Buck et al., 1993) and α-lactalbumin (Alexandrescu et al., 1994) at TFE concentrations greater than 15%. The TFE states of both proteins exhibited primarily native secondary structure, though there was an increase in total helical content, and exhibited tertiary structure that was similar to a partially folded protein intermediate of hen lysozyme and a molten globule state of α-lactalbumin. The primary difference between the TFE states and the partially folded and molten

globule states was the tightness of the hydrophobic core. The higher TFE concentrations appeared to have interfered with the hydrophobic interactions in the core resulting in a looser tertiary structure.

Studies of two predominantly β-sheet proteins showed a conversion of some β-structure to α-helical structure in TFE. Monellin is a polypeptide that consists of two chains, A and B, that have all β-structure and mixed α- and β-structure, respectively (Fan et al., 1993). In 50% aqueous TFE, one β-strand of the A chain forms a helix. Further characterization of the protein was not accomplished. The transition was attributed to a correlation between helical propensity and environment. Similar results were obtained for β-lactoglobulin (Shikari et al., 1995). CD spectra showed a cooperative conversion from β-sheet to α-helix at TFE concentrations between 10% and 20%. This concentration at which the transition occurs is coincident with the transitions observed for hen egg white lysozyme (Buck et al., 1993) and α-lactalbumin (Alexandrescu et al., 1994). Shikari et al. (1995) went on to measure the conformational behavior of 20 other proteins in TFE. They concluded, in agreement with Fan et al. (1993), that the observed structural transitions correlated with the helical propensities of the protein sequence as measured by secondary structure prediction methods.

Several studies of peptides and protein fragments have also shown that the helix-inducing ability of TFE may correspond to the inherent helix forming propensities of the peptide sequence (Nelson & Kallenbach, 1989; Segawa et al., 1991; Dyson et al., 1992a,b; Sönnichsen et al., 1992; Blanco et al., 1994). Dyson et al. (1992a,b) studied protein fragments from myohemerythrin and plastocyanin. In both cases addition of TFE merely stabilized helical structure in those regions that have elements of nascent helical structure in the corresponding protein. In fact, fragments of plastocyanin that had the highest helical propensity, but exhibited β-structure in the native protein, showed no

significant formation of helix in TFE concentrations of 50% and 90%. Nelson & Kallenbach (1989) studied the S-peptide of ribonuclease A, which forms helix in residues 3-12 in aqueous solution with residue 14 acting as a helix stop signal (Kim & Baldwin, 1984). Addition of TFE resulted in helix formation in residues 3 to 13 with the helix stop signal at residue 14 unchanged.

A study of the 28 amino-terminal residues of actin compared the structure of the fragment in 80% TFE to predicted structures and the crystal structure of the fragment in the intact protein (Sönnichsen et al., 1992). The peptide was found to be comprised of two helical regions (residues 4 to 13 and 16 to 20) connected by a β-turn region from 13-16 with the remaining residues unstructured. These results are consistent with secondary structure predictions using the algorithm of Eisenberg et al. (1984) which predicts helix in residues 5-10 and 16-20. Other prediction algorithms (Chou & Fasman, 1978; Garnier et al., 1978; Williams et al., 1987) differed primarily in the prediction of β-structure in residues 16 to 19. Residues 1-28 in the crystal structure of the actin protein form two β-sheet regions from residues 8 to 13 and 16 to 21 with a β-hairpin connecting them. The regions of β-sheet in the intact protein seemed to form α-helix in TFE. From these findings, Sönnichsen et al. (1992) concluded that TFE is a "helix-enhancing co-solvent" that stabilizes helix in those regions that have an inherent helical propensity.

The N-terminal fragment of streptococcal protein-G B_1 domain was studied in 30% TFE and found to form a β-hairpin in residues 8-11, while the regions preceding and following the turn formed flexible β-strands (Blanco et al., 1994). These results are in agreement with the structure of the fragment in the native protein (Gronenborn et al., 1991), although the β-strands are not as highly packed as in the native structure. The lack of induction of non-native helix and stabilization of a native turn in this peptide further supports the theory that TFE is not a non discriminate helix-promoting solvent.

An alternative hypothesis is proferred by (Zhong & Johnson, 1992), who suggest that solvent environment alone is responsible for observed peptide secondary structure and that TFE acts to promote helical structure whatever the secondary structure propensity of the peptide sequence. Two studies appear to support their hypothesis. In the first study, peptides with preferences for α-helical structure, but that were found to be β-strand in their respective proteins (Zhong & Johnson, 1992) were found to adopt α-helical structure in 100% TFE, yet to form mostly β-strand in non-micellar concentrations of SDS. In a subsequent study (Waterhous & Johnson, 1994), peptides predicted to be β-strand but found to be α-helical in their respective proteins were examined in 90% TFE and non-micellar SDS. Additionally, "well-behaved" peptides that have a strong propensity for only one type (α-helical or β-strand) of secondary structure were studied in the same solvents. Each of the peptides that was predicted to be β-strand, including those deemed "well-behaved", was found to be α-helical in 90% TFE. The authors concluded that the solvent conditions are solely responsible for observed peptide secondary structure, with TFE acting in a non discriminatory manner to induce helical structure.

Without a complete understanding of the relationship between peptide primary and secondary structure, it is difficult to understand the exact influence of TFE. At very high TFE concentrations (≥ 90%) the solvent appears to force a helical secondary structure. At lower concentrations, however, TFE appears to enhance the formation of secondary structures inherent to the specific polypeptide amino acid sequence. The enhancement of secondary structure comes at the expense of some elements of tertiary structure at TFE concentrations greater than 15%, while at very low concentrations TFE stabilizes secondary structure without disrupting the tertiary conformation. Aqueous TFE certainly provides an anisotropic solvent environment that likely resembles the environment at the membrane surface or at an extracellular receptor (Wray et al., 1993).

STABILITY OF PEPTIDE TERTIARY STRUCTURES. Tertiary structure has been observed in peptides of similar length to GRF. In some cases the peptides were designed to assume a specific conformation, while other studies observed stable tertiary structures in naturally occurring peptides. Fezoui et al. (1994) designed a peptide that would assume a helix-turn-helix tertiary conformation. It was intended that four interhelical hydrophobic pairs would stabilize the tertiary conformation Leu-Leu, Leu-Ile, Leu-Val, and Leu-Met. The 36-residue peptide was studied in aqueous solution by NMR and CD spectroscopies and found be helical in residues 1-17 and 22-38, while a type II turn was observed for residues 18-21. Long-range NOEs between residues Leu^{3}, Lys^{4}, Val^{7} and Leu^{11} in the N-terminal helix and residues Met^{28}, Glu^{29}, Leu^{32}, Ile^{36}, and Gln^{37} in the C-terminal helix confirmed the existence of a tertiary fold. Three of the four intended interhelical hydrophobic pairs exhibited a close proximity, and these hydrophobic interactions most likely contributed to the stability of the fold.

In a study by Butcher et al. (1995) a 20-residue model peptide was designed in an effort to achieve a helix-turn-extended strand tertiary conformation. In aqueous solution the peptide adopted a helix in residues 3-11, was disordered in residues 16-20, and showed evidence of a possible reverse turn in residues 13,14, and 15. The NMR spectra did not exhibit any long-range NOEs between the two segments, however, other indirect indications of tertiary structure were observed. Slowly exchanging protons in the disordered tail segment, a chemical shift index pattern characteristic of a reverse turn in residues 12-15, and differences in the behavior of the helical segment in the model peptide and a shortened (residues 1-14), helical region only analog in the presence of ammonium sulfate were purported to be indications of tertiary structure. Hydrophobic interactions were implicated as having a role in stabilizing the tertiary conformation.

Most recently, Struthers et al. (1996) effectively designed a 23 residue peptide that would mimic the ββα motif (two antiparallel β-strands followed by a helix) observed in zinc finger peptides, however, without the typical requirement of a metal cation. The tertiary structure was stable in aqueous solution and was characterized by CD and NMR spectroscopies. As in the previously designed structures, hydrophobic interactions proved the stabilizing force in the tertiary structure formation, and the II' β-turn connecting the two β-strands was implicated as a structural nucleation element which propagated the formation of the hydrophobic core.

An NMR study of the structure of the naturally occurring bovine pancreatic polypeptide (bPP) in aqueous solution (Li et al., 1992) revealed the presence of a tertiary fold similar to that previously characterized for avian pancreatic polypeptide (aPP) (Blundell et al., 1981). The 36-residue peptide forms a well-defined helix in the C-terminal region (residues 15-32), while only residues 4-8 are ordered in the N-terminal region. The ordering of residues 4-8 was attributed to tertiary interactions between the N- and C-terminal regions. A poorly defined turn facilitated the tertiary interaction.

Human parathyroid hormone (hPTH 1-37) also adopts a tertiary conformation in aqueous solution (Marx et al., 1995). Helices found in residues 5-10 and 17-28 are connected by a flexible link (12 and 13) and a well-defined turn region (14-17). The tertiary structure was proposed to be stabilized by a "small hydrophobic core" formed by Leu^{15} and Trp^{23}. The stability of the tertiary structure was confirmed by 200 ps of unrestrained molecular dynamics calculations.

These studies reveal the fundamental role that hydrophobic interactions play in the formation and stabilization of peptide tertiary structures. The importance of hydrophobic interactions in the stabilization of small protein folding subunits was previously identified by Alexander et al. (1992). They found two versions of the IgG binding domain (B1 and

B2, differing by six amino acids) of streptococcal protein G to have high denaturation temperatures (B1= 87.5 °C and B2= 79.4 °C). They attributed the high denaturation temperatures to the ability of the B-domains to efficiently bury hydrophobic surface. This conclusion concurred with the results of Livingstone et al. (1991) who found a direct correlation between the thermodynamics of the transfer of hydrocarbons from dilute aqueous solution to the pure liquid phase and the reduction in the water-accessible nonpolar surface area in protein folding. Livingstone et al. (1991) went on to conclude that large negative heat capacity changes observed in protein folding are dominated by the hydrophobic effect.

Each of the aforementioned stable peptide tertiary structures was studied in purely aqueous solution where hydrophobic interactions are likely to play a major role in the determination of peptide secondary and tertiary structure. In aqueous alcohol solvent systems the effects of hydrophobic stabilization is attenuated by the presence of the alcohol. In this study of pmh29 a solvent system involving 45% trifluoroethanol has been employed. TFE concentrations higher than 15% have been shown to partially denature protein tertiary structure resulting in a TFE state or alcohol denatured state (Buck et al., 1993; Alexandrescu et al., 1994) that has a loosened hydrophobic core yet retains secondary structural elements. The structure of pmh29 that we have described at 45% TFE, therefore, is subject to partial denaturation of the tertiary fold which leads to a conformationally heterogenous tertiary structure.

THE TERTIARY FOLD. Previous studies of GRF analogs have failed to identify any evidence of tertiary structure. The only deviations from the mostly linear helical conformation have been kinks or bends in the peptide chain. Brünger et al. (1987) performed restrained molecular dynamics using their NMR data (Clore et al., 1986) and described the resulting conformations as having an extended helical structure with a

"banana shape". They found no sharp kinks in the region lacking helical structure (13-16), although they did not rule out the existence of a kink in this region because molecular dynamics calculations of the length required for folding to occur had not been performed. Fry et al. (1992), on the other hand, discovered conformers calculated from molecular dynamics and energy minimization simulations that were kinked at residues 16 and/or 25. The presence of long-range NOEs in the present study between residues at opposite ends of the pmh29 chain are lucid evidence of the existence of tertiary structure.

In determining what enables pmh29 to assume a tertiary fold, the focus turns to the residues located in the turn region. The Gly^{15}-Thr substitution is the only residue in the all-important 13-21 portion of the peptide that significantly differs from the natural product. The Lys^{21}-Arg substitution is rather conservative, and since it occurs at the end of the turn region it should not have a profound effect on the initiation of the fold itself. Thr^{15} must be responsible, therefore, for enabling the fold to more easily form. In what capacity Thr^{15} acts is puzzling. Threonine does not have a high preference to participate in turns, rather it is predicted to participate in β-strand secondary structure (Chou & Fasman, 1978). According to the calculated structures (Figure 8), the threonine residue does not, however, significantly disrupt the helical structure. It appears that Thr^{15} changes the direction of the helix by assuming a more extended conformation. This extension or rise seems to facilitate a more effective kink or bend at Gln^{16}, the previously identified kink site (Fry et al., 1992), and/or to put Gln^{16} in a position where the bend or kink will naturally cause a reverse in the direction of the peptide chain.

One can envision pmh29 as a linear helix that could be formed simply by bending the C-terminal portion of the helix in line with the N-terminal portion. The turns that are formed in the two structures are not typical reverse turns, but are turns of the linear helix, that by virtue of the conformations of Thr^{15} and Gln^{16} are positioned to cause the peptide

to fold back onto itself. The CD and NMR data, therefore, should be expected to identify the peptide as almost completely helical, which it does. The data should not be expected to reveal an NOE pattern consistent with a tight reverse turn or β-turn, which it does not.

BIOACTIVE CONFORMATION. Numerous studies have been performed in an attempt to elucidate the bioactive conformation of GRF. The primarily helical secondary structure of other secretin family members, the predominantly helical conformation observed for GRF analogs, and the rather strict conservation of residues in the helical regions among variant GRF species led researchers to conclude that stabilizing and/or extending the helical structure could increase the potency of GRF analogs. To this end, an hGRF(1-29)NH_2 analog containing a Gly^{15}-Ala substitution, intended to promote helix formation and increase amphiphilicity in the central region of the peptide, and analog with a helix destabilizing substitution (Sar^{15}) were tested for binding affinity and GH-releasing activity (Felix et al., 1987; Campbell et al., 1991). The binding affinities and GH-releasing activities correlated with the helix forming tendencies of the substitutions. The Ala^{15} analog exhibited a 4-5 fold increase in binding affinity and potency versus hGRF(1-29)NH_2, while the Sar^{15} substitution resulted in an analog with significantly decreased binding affinity and GH-releasing activity. These results suggested that GRF binds to its receptor in a helical conformation, and stabilization of this preferred binding conformation will lead to potent analogs.

The results prompted studies of side-chain to side-chain cyclic lactam analogs that would induce a rigid, stable helical conformation. A lactam ring between residues *i* and *i*+4 was found to be the correct spacing for optimal stabilization of helical structure (Felix et al., 1988). An increase in the *in vitro* potency was observed for cyclo(Asp^8-Lys^{12})- and cyclo(Lys^{12}-Glu^{16})-[Ala^{15}]-hGRF(1-29)NH_2, whereas cyclo(Lys^4-Asp^8)- and cyclo(Lys^{21}-Asp^{25})-[Ala^{15}]-hGRF(1-29)NH_2 showed a slightly decreased potency versus

the linear parent hGRF(1-44)-NH_2 molecule (Campbell et al., 1995). A cyclo(Glu^{16}-Lys^{20})-[Ala^{15}]-hGRF(1-29)NH_2 analog exhibited a potency that was a third that of the two less active cyclic analogs. Dicyclic analogs involving combinations of the *i*-(*i*+4) lactam rings were less active than the parent hGRF(1-44)NH_2 molecule, with those molecules containing the cyclo(Glu^{16}-Lys^{20}) moiety showing a 10-fold decrease in potency versus the next most active dicyclo analog (Fry et al., 1992; Campbell et al., 1995). Finally, a tricyclic analog {tricyclo(Asp^{8}-Lys^{12})(Glu^{16}-Lys^{20})(Lys^{21}-Asp^{25})-[Ala^{15}]-hGRF(1-29)NH_2} contained a significant amount of helicity but lacked *in vitro* activity (Campbell et al., 1995).

The slight decrease in activity observed for those monocyclic and dicyclic analogs containing cyclo(Asp^{8}-Lys^{12}) and/or cyclo(Lys^{12}-Glu^{16}) lactam rings was attributed one or more of the following events: (1) an improper orientation of receptor-contact side chains; (2) a steric interaction inhibiting complete binding to the receptor; (3) the inability of these analogs to form a bend or kink that would be necessary for optimal binding (Fry et al., 1992). The bend or kink that Fry et al. (1992) observed at residue 16 in the linear analog [Ala^{15}]-hGRF(1-29)NH_2 would be unable to form in analogs containing the cyclo(Glu^{16}-Lys^{20}) moiety. Interestingly, cyclo(Glu^{16}-Lys^{20}) containing analogs have the lowest activity of the monocyclic and dicyclic analogs studied. Also, addition of the cyclo(Glu^{16}-Lys^{20}) lactam to form the tricyclic analog did not significantly alter helical content, yet caused a loss of *in vitro* activity. This led Campbell et al. (1995) to propose that helicity in the central region correlates with biological activity, however, rigidification of this region results in a decrease in potency.

A similar proposal was proffered by Gaudreau et al. (1992) who studied the effects on binding affinity of single and multiple amino acid deletions, acylation, and substitution of octanoyl groups in analogs of hGRF(1-29)NH_2. Their results confirmed the importance

of the 13-21 region of the GRF sequence. Replacement of residues 13-15, 16-18, or 19-21 with an octanoyl resulted in a dramatic loss in binding affinity, as did removal of one or more of the residues in the 13-21 region. Removal of single residues in the 24-29 region led to a decrease in binding affinity, although the loss was far less substantial. The authors of the study concluded that residues in the 13-21 segment of GRF play a more significant role in receptor binding than do those residues in the 24-29 region. Akin to Campbell et al. (1995), Gaudreau et al. went on to suggest that the 13-21 region may facilitate the formation of an optimal binding conformation.

Two other studies had also proposed a conformational change at the receptor and/or membrane surface. Honda et al. (1991) performed a CD spectroscopy study of hGRF(1-29)NH_2 in the presence and absence of 1,2-dimyristoyl-*sn*-glycero-3-phosphorylglycerol (DMPG) liposome and in aqueous TFE, and found differing amounts of helical structure in each of the three solvent conditions. In purely aqueous conditions the peptide was found to be 25% helical. Upon increasing the TFE concentration, the helical content of the peptide increased to that of 92% helical structure at 49.1% TFE (v/v). The helicity of the peptide also increased with increasing DMPG liposome concentration saturating at a value of 65-70% helix. Honda et al. point out that the amphiphilicity of the GRF molecule reverses in the middle of the peptide with the hydrophobic face becoming hydrophilic and vice versa following Leu^{17} (Figure 11).

The difference in helical content between TFE and DMPG liposomes were attributed to this reversal of amphiphilicity. It was suggested that to bind to the hydrophobic surface of the DMPG liposome the peptide would need to twist or fold to align the hydrophobic faces thus disrupting the helix rod in the middle portion. Honda et al. went on to purport that, according to the sequential step model of hormone-receptor interaction (Sargent & Schwyzer, 1986), *in vivo* GRF reaches the cell membrane and folds into its bioactive

conformation first, then diffuses laterally along the membrane surface, and finally binds to the receptor. The authors conclude, therefore, that the DMPG liposome conformation (the folded structure) is more representative of the bioactive conformation than is the TFE structure.

Figure 11: Helical wheel diagram of pmh29. Hydrophobic residues have been circled.

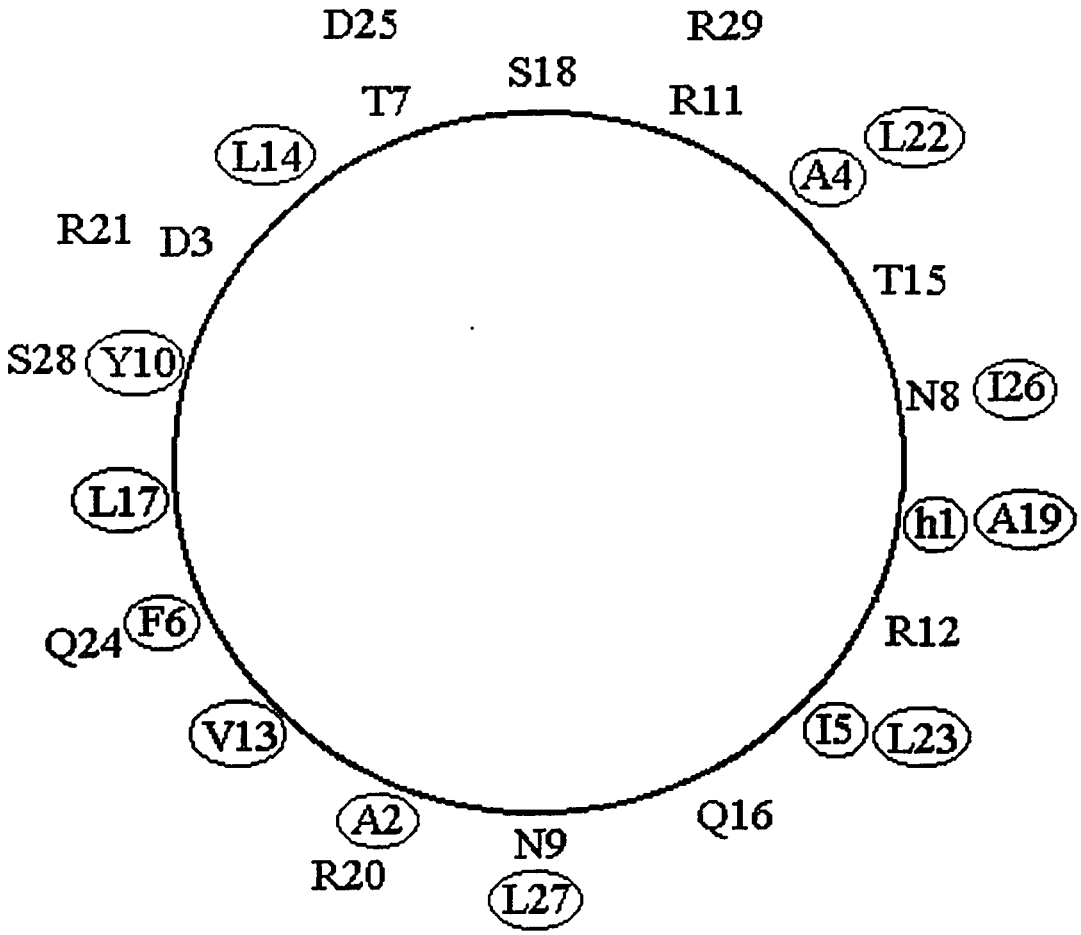

A study by Petersen et al. (1989) used the immune response to GRF to explore its conformation. Antibodies were produced in response to both hGRF(1-29)NH_2 and hGRF(1-44)OH. 85% of the antibodies to hGRF(1-44)OH recognized the 14 residue C-terminal portion of the molecule with high affinity. The other 15% had a low affinity for the 1-29 portion. Antibodies against hGRF(1-29)NH_2 had a low affinity for both the 44 and 29 residue molecules. These results led the authors to believe that the 1-29 portion of the molecule undergoes a conformational change in the anisotropic environment of the cell membrane (the conformation is predicted to be amphiphilic (Kaiser & Kézdy, 1984)), while the conformation of residues 30-44 remains constant. Furthermore, Petersen et al. (1989) suggested that their results support the idea that conformational flexibility may be the attribute that allows hormones to elude the binding of antibodies produced against them.

From these studies the bioactive conformation would appear to be primarily helical with a bend or fold in the 16-21 region, and may be conformationally flexible. The tertiary conformations observed for the pmh29 analog (Figure 8) adhere well to this proposed bioactive structure: they are nearly completely helical, contain a fold in the 16-21 region that increases its amphiphilicity, and are highly flexible.

Both calculated pmh29 structures contain a turn in the 15-21 region of the peptide. The turn, however, differs slightly in the two structures resulting in slightly different tertiary interactions. In structure A (Figure 8A) the N- and C-termini are closer, while in structure B (Figure 8B) the C-terminus is further up the chain. Common to both structures, however, is their high amphiphilicity. As predicted by Honda et al. (1991), pmh29 must fold to compensate for the reverse in amphiphilicity that occurs along the peptide helix. The resulting tertiary conformations have well-defined hydrophobic and hydrophilic faces creating an amphiphilic tertiary structure. Although Honda et al. (1991)

limit their interpretation for the necessity of increase amphiphilicity to the binding of the peptide to the membrane surface, an increase in amphiphilicity could also lead to more effective binding to a hydrophobic receptor in an extracellular milieu (see below).

The tertiary structures that we observe for pmh29 are in alcohol denatured states whereby a significant hydrophobic core consisting of hydrophobic side chain interactions is loosened by the actions of TFE. The TFE attenuates the hydrophobic interactions resulting in structures that are flexible and somewhat unstable. The resultant structures, however, may be more accurate representations of the conformations of the molecule in the anisotropic environment at the receptor binding site. Like other G-protein-coupled receptors, the GRF receptor has seven transmembrane helices connected by alternating intracellular and extracellular loops (Strader et al., 1994). The sequence of the GRF receptor has been characterized (Mayo, 1992) and the proposed extracellular binding site consists of 42% hydrophobic residues (Mayo, 1992; Mayo et al., 1995; Strader et al., 1995). Whether the peptide ligand binds first to the membrane and adopts a bioactive conformation as proposed by Sargent & Schwyzer (1986) or proceeds directly to the extracellular ligand binding site, it most likely encounters an environment that is similar to that of the anisotropic environment of the mixed TFE solvent system we have employed in this study.

PMH44: MATERIALS AND METHODS

SAMPLE PREPARATION. The pmh-GRF(2-44)OH was obtained from Eli Lilly and Company (Lot F35-2RT-51) and used without further purification. NMR samples were prepared by dissolving approximately 5.2 mg of lyophilized peptide in 0.5 ml of 45% 2,2,2,-Trifluoroethanol-d_3 (MSD Isotopes)/ 45% H_2O/ 10% D_2O (99.9% atom enrichment, Cambridge Isotope Laboratories) to give a final concentration of about 2.0 mM at pH 3.40. CD samples were prepared (G. F. Needham, Eli Lilly and Company) by appropriate dilution from stock solutions of TFE, water, and peptide in water (pH 3.9) following the method of Brems et al. (1985). All stock solutions were filtered through a 0.45 μm filter before mixing. Samples were made to constant volume and constant peptide concentration (0.15 mg/ml).

CD SPECTROSCOPY. Far UV Circular Dichroism (CD) spectra were collected (G. F. Needham, Eli Lilly and Company) at multiple TFE concentrations using an AVIV model 62 spectropolarimeter. Samples were collected at 0, 10, 20, 30, 40, and 50 percent TFE using a 1.0 nm bandwidth, a 0.25 nm stepsize, and an 8 second time constant in a 0.2 cm cell. All data were collected at room temperature. Results were reported as mean residue ellipticity ([Θ]) in degrees-cm^2-dmol^{-1} (MRE) and were calculated with a mean residue weight of 116.

NMR SPECTROSCOPY. ^{1}H NMR spectra were recorded on a Bruker AM 500 spectrometer at 300 K with a spectral width of 5000 Hz. Spectra were referenced to an external sample of dioxane at 3.751 ppm downfield from 4,4-dimethyl-4-silapentane-1-sulfonate. TOCSY experiments (Bax & Davis, 1985) were acquired with 32 transients, 900 complex points in the t_1 dimension, and 2048 points in the t_2 dimension. Phase-sensitive NOESY experiments (Jeener et al., 1979) were acquired with 64 transients, 900 complex points in t_1 dimension, and 2048 points in the t_2 dimension. All experiments

were performed with time proportional phase incrementation (Marion & Wüthrich, 1983), and were zero filled to 2K X 2K. A 60-degree shifted sine bell window function was applied to all experiments before transforming in both dimensions. NOESY experiments were recorded with mixing times of 200 and 300 ms. TOCSY experiments were recorded with mixing times of 46 and 100 ms.

PMH44: RESULTS AND DISCUSSION

CD SPECTROSCOPY. Figure 12 shows the CD spectrum of pmh44 at varying TFE concentrations. The spectrum shows little change at concentrations greater than 30%. In purely aqueous solution (0% TFE) the peptide exists largely in a random coil conformation. The minima that appear at 208 and 222 nm as the TFE concentration is increased are indicative of the formation of secondary structure. An increase in TFE concentration up to 50% results in an increase in helical content. At 50% the peptide exhibits nearly 100% helical content (G. F. Needham, Eli Lilly and Company, personal communication).

NMR SPECTROSCOPY. SPIN SYSTEM ASSIGNMENT. Standard assignment methodology (Wüthrich, 1986) was employed to assign the spin systems observed in TOCSY spectra to their respective residue types. Figure 13 shows the NH-aliphatic region of a 46 ms TOCSY spectrum. Four spin systems were observed that had only a lowfield αH peak and a single highfield peak and were assigned as alanines. The arginines were easily identified by their εH resonances which appear around 6.9 ppm and showed crosspeaks to the δ,γ,and β protons. The overlap of the arginine spin systems around 6.9 ppm was resolved in the aliphatic region where each of the 8 spin systems was observed. In the aliphatic region two spin systems showed αH-βH and γH peaks and βH-γH peaks and were ascribed to the two threonine residues. A single spin system in the amide-aliphatic region exhibited an α proton, a higher field β proton, and two highfield γ protons. This spin system was assigned to one of the valine residues. The other valine residue was visible in the aliphatic region of the spectrum where it showed a αH-βH and two αH-γH crosspeaks. One isoleucine residue was apparent in the NH-aliphatic region distinguished by its αH, strong γCH_3, and very highfield δH resonances. The second isoleucine showed only αH and γCH_3 resonances

Figure 12: Circular dichroism spectrum of pmh44 in varying concentrations of aqueous trifluoroethanol at pH 3.9 and 298 K. Mean residue ellipticity (MRE) is in units of cm^2-degrees-$dmol^{-1}$.

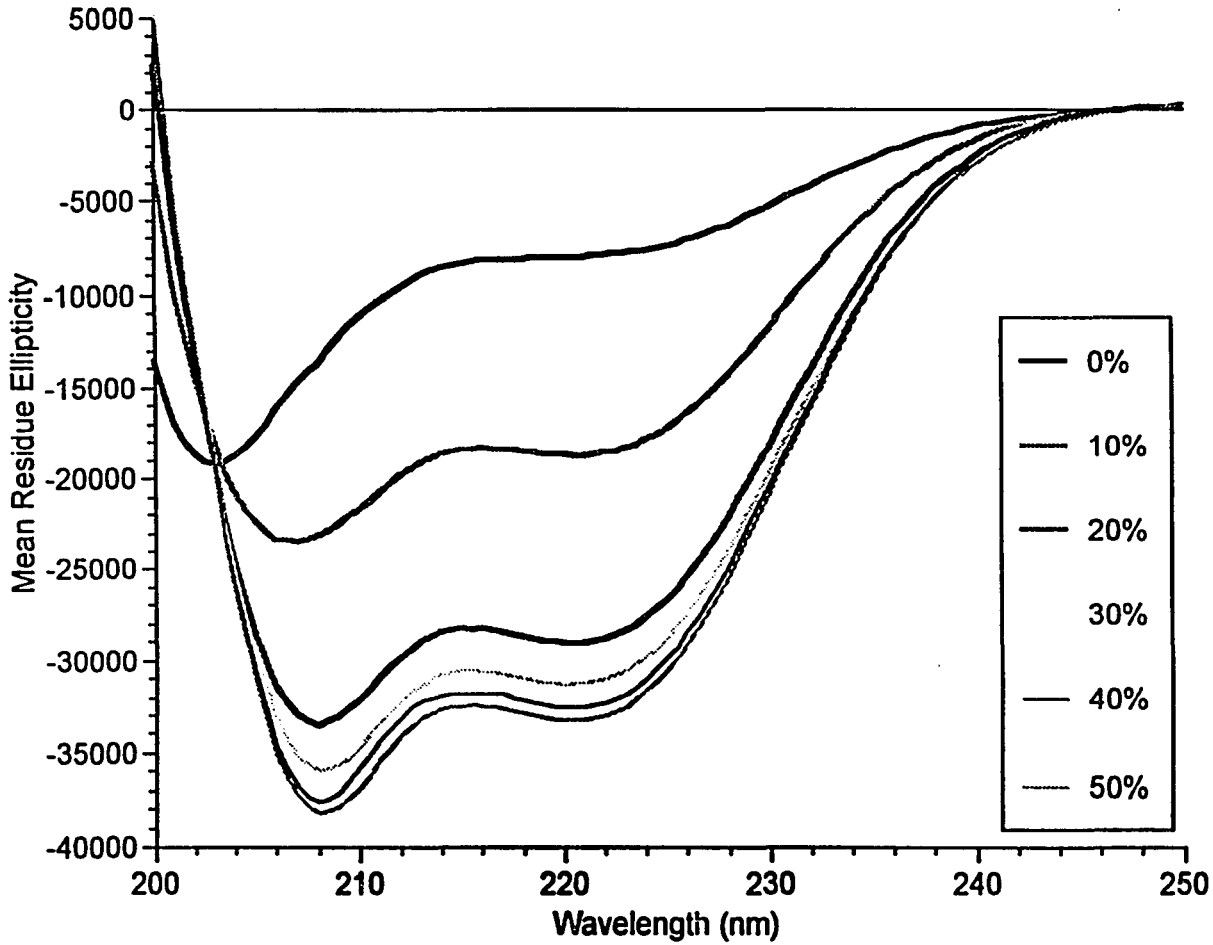

Figure 13: NH-aliphatic region of a 46 ms TOCSY spectrum for pmh44 in 45% d_3-trifluoroethanol, 45% H_2O, and 10% D_2O at pH 3.40 and 300 K, where the spin systems have been labeled at the αH resonance.

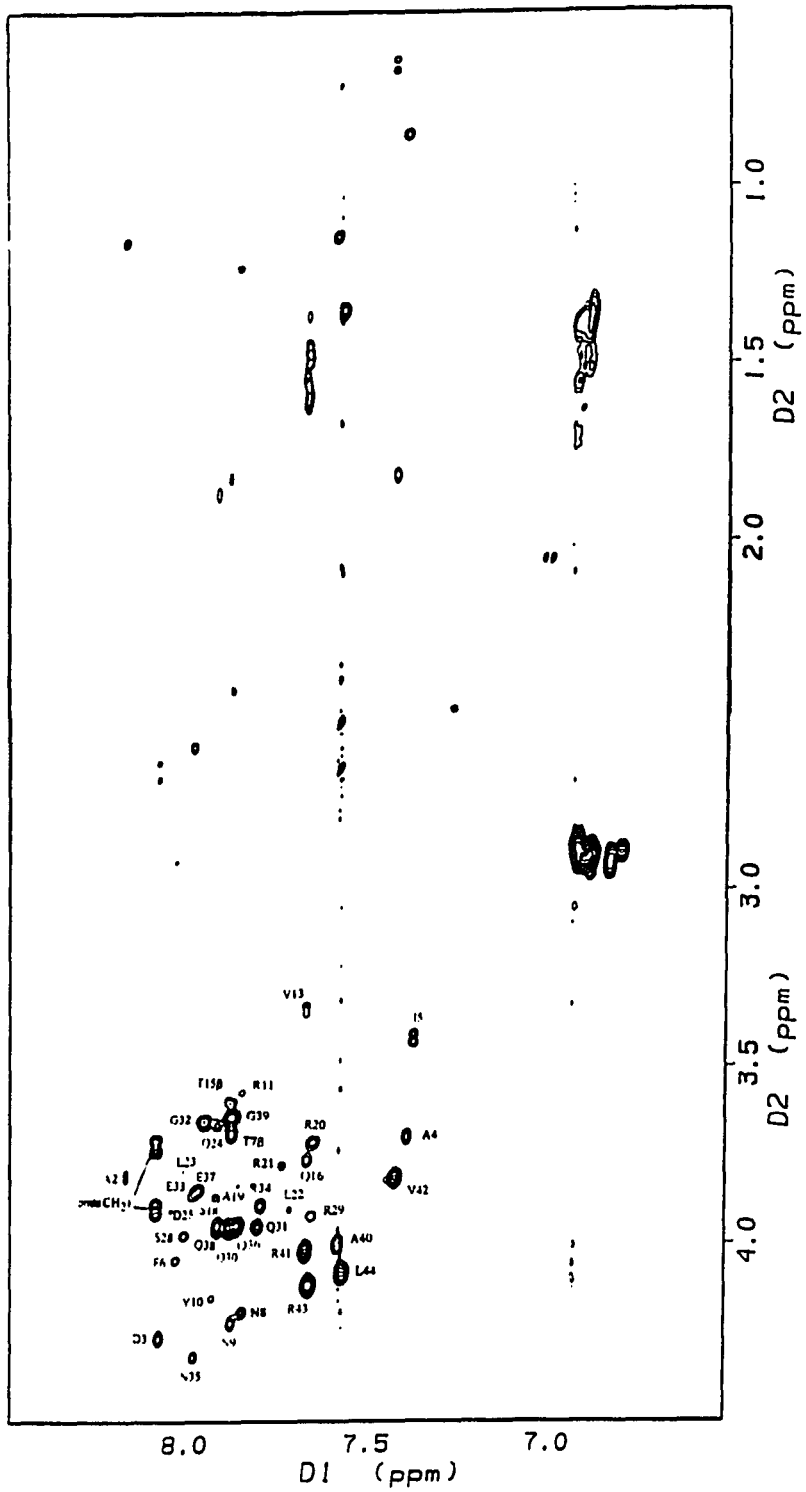

in the NH-aliphatic region, but showed αH-γCH_3 and δH crosspeaks in the amide region making it readily assignable. The remaining spin systems with resonances in the very highfield area of the spectrum were attributed to the 6 leucine residues. Two spin systems had an αH and a single higher field resonance around 2.0 ppm in the NH-aliphatic region of the spectrum and overlapping αH-βH and γH crosspeaks in the aliphatic region. These spin systems were deemed the two glutamate residues. Four residues with nearly degenerate αH chemical shifts and only slightly variant amide chemical shifts showed two β protons in the NH-aliphatic region and overlapping αH-βH and γH's in the aliphatic region and were determined to be four of the six glutamine residues. The other two glutamine residues were found in the aliphatic region exhibiting an α-β crosspeak and 2 γ-protons each. Two of the systems that had only an α-proton in the NH-aliphatic region did not show any other crosspeaks in the aliphatic region and were found to be the two glycine residues. The two serine residues had only an αH in the NH-aliphatic region, but they also had a low field αH-βH in the aliphatic region. The methylene protons of the hippuryl moiety were readily observable by the well-separated resonances that had been seen for the same spin system in pmh29. The balance of the spin systems were of the AMX type and were attributed to the 3 asparagines, 2 aspartates, 1 phenylalanine, and 1 tyrosine.

SEQUENCE-SPECIFIC ASSIGNMENTS. NOESY experiments were performed to facilitate the assignment of the spin systems observed in TOCSY spectra to specific amino acids in the peptide sequence using short-range NOEs between NH(i) and NH(i+1), αH(i+1), and/or βH(i+1). Figure 14 and 15 show the amide and fingerprint regions, respectively, from a 300 ms NOESY spectra. The small chemical shift dispersion of amide resonances resulted in significant overlap in the NOESY spectrum, which hindered the observation of any long stretches of NOE connectivities. Therefore, several of the assignments were

Figure 14: Expansion of the fingerprint region of a 300 ms NOESY spectrum for pmh44 in 45% d_3-trifluoroethanol, 45% H_2O, and 10% D_2O at pH 3.40 and 300 K, where the αH-NH and βH-NH NOEs have been labeled.

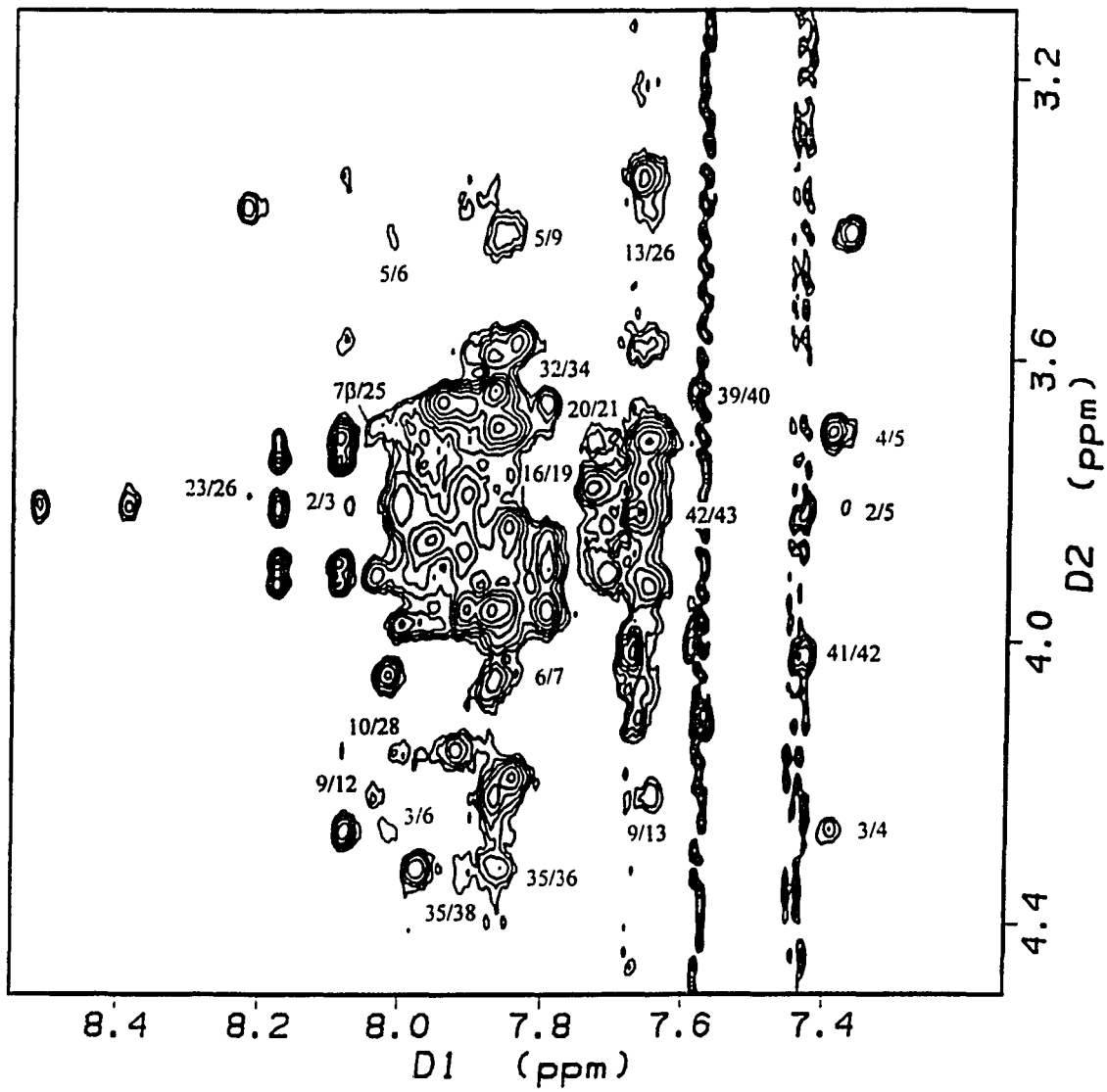

Figure 15: The amide region of a 300 ms NOESY spectrum for pmh44 in 45% d_3-trifluoroethanol, 45% H_2O, and 10% D_2O at pH 3.40 and 300 K, where the αH-NH and βH-NH NOEs have been labeled.

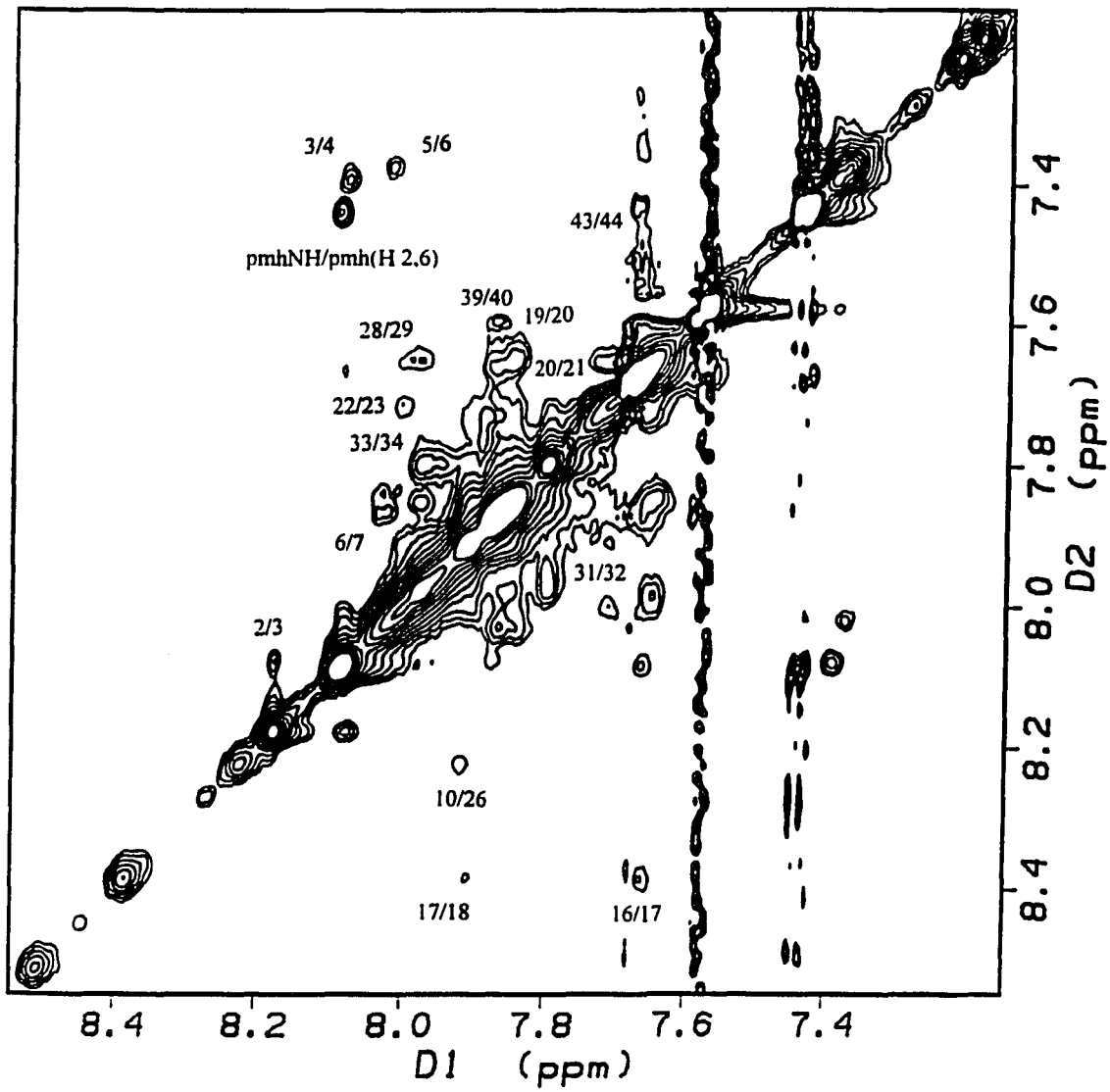

made by comparison of neighboring residues in the sequence to spin systems showing connectivities. Nearly identical chemical shifts for most assigned residues in pmh44 spectra and those in pmh29 spectra enabled transfer of assignments from pmh29 to corresponding residues in pmh44. Figure 16 shows an expansion of the fingerprint region of the 46 ms TOCSY spectrum in which sequence-specific assignments have been indicated for most of the residues of pmh44. The αH of Leu^{14} is hidden by the overlap of a methylene proton of the para-methylhippuric acid group. Table 7 details the chemical shifts of the assigned proton resonances for pmh44 in aqueous TFE.

SECONDARY AND TERTIARY STRUCTURE. A strictly qualitative representation of the observed short- and medium-range NOEs is shown in Table 8. Substantial overlap in the NH-αH and βH region of the NOESY spectra made quantitation of the observed crosspeaks futile. The overlap also concealed many of the short- and medium-range NOEs, although those that were visible were characteristic of helical secondary structure ($d_{NN}(i,i+1)$, $d_{\alpha N}(i,i+3)$, $d_{\alpha\beta}(i,i+3)$). Helical type NOEs were observed between residues contained throughout the peptide sequence, implying a completely helical secondary structure. The CSI analysis for pmh44 (Table 9) reveals a "-1" chemical shift index for all assigned α protons which supports the NOE results defining the molecule as completely helical under these solvent conditions. Long-range NOEs similar to those exhibited by pmh29 (although not as numerous) were present in NOESY spectra of pmh44 as shown in Table 10. The increase in 15 residues of pmh44 versus pmh29 created a more crowded NMR spectrum likely resulting in the obscuration of other long-range NOEs. Like those of pmh29, the long-range NOEs for pmh44 were between residues located at opposite ends of the sequence. This would suggest that the tertiary structure of pmh44 also involves the peptide chain folding back onto itself.

Figure 16: Expansion of the fingerprint region of a 40 ms TOCSY spectrum for pmh44 in 45% d_3-trifluoroethanol, 45% H_2O, and 10% D_2O at pH 3.40 and 300 K, where the sequence-specific assignments have been labeled.

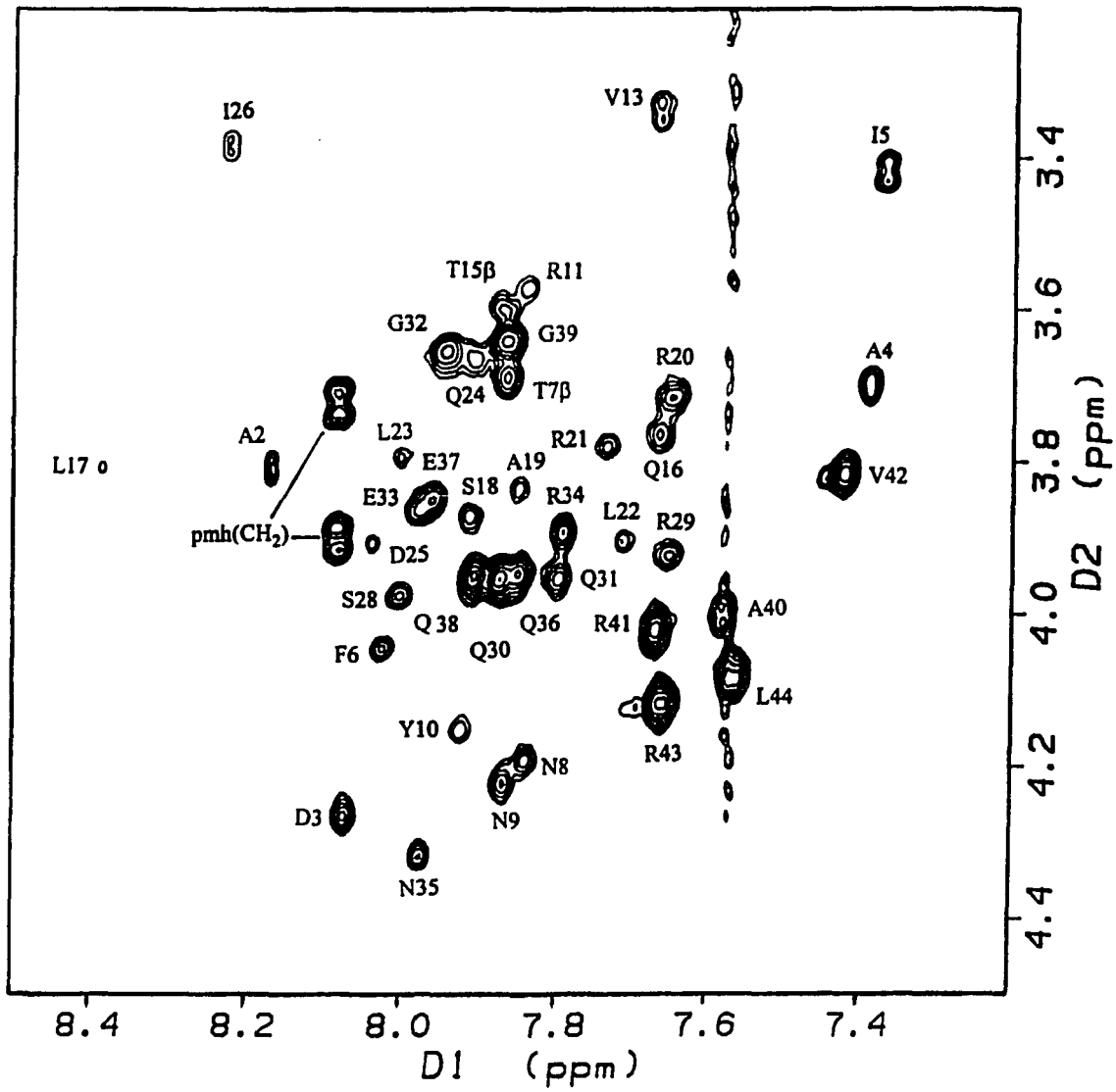

Table 7: ^{1}H Chemical Shifts for pmh44 in 45% TFE/ 45% H_2O/ 10% D_2O, pH 3.40 at 300 K.

residue	NH	αH	βH	γH	δH	others
pmh	8.08					CH_2 3.72, 3.90; H(2,6) 7.42;
Ala^2	8.17	3.81	1.15			
Asp^3	8.07	4.27	2.62, 2.69			
Ala^4	7.39	3.70				
Ile^5	7.37	3.42	1.58	0.80, 0.83		γCH_3 0.52
Phe^6	8.06	4.04	2.92			
Thr^7	7.87	3.99	3.69	1.02		
Asn^8	7.84	4.19	2.47, 2.61			
Asn^9	7.87	4.22	2.41, 2.56			
Tyr^{10}	7.93	4.15	2.65, 2.94			
Arg^{11}	7.84	3.57	1.53, 1.64	1.30		
Arg^{12}						
Val^{13}	7.67	3.34	1.88	0.63, 0.75		
Leu^{14}	8.08	3.70		1.17		
Thr^{15}	7.87	4.07	3.60	0.97		
Gln^{16}	7.67	3.76	1.89, 2.01	2.26		
Leu^{17}	8.39	3.81				
Ser^{18}	7.91	3.87	3.63			
Ala^{19}	7.85	3.83	1.23			
Arg^{20}	7.65	3.71	1.55, 1.71	1.38	2.88	
Arg^{21}	7.73	3.78	1.71			
Leu^{22}	7.71	3.90			0.62, 0.66	
Leu^{23}	8.00	3.79	1.46		0.60	
Gln^{24}	7.91	3.66	1.91, 2.08	2.27		
Asp^{25}	8.04	3.91	2.60, 2.68			
Ile^{26}	8.22	3.38	1.75	0.79, 0.83	0.55	γCH_3 0.62
Leu^{27}	8.52	3.82				
Ser^{28}	8.00	3.97	3.75, 3.83			
Arg^{29}	7.65	3.92	1.72		2.89	
Gln^{30}	7.88	3.95				
Gln^{31}	7.80	3.95				
Gly^{32}	7.95	3.65				
Glu^{33}	7.97	3.86	1.92	2.26		
Arg^{34}	7.79	3.89	1.62		2.92	
Asn^{35}	7.98	4.32	2.59			

Table 7 (*Continued*): ^{1}H Chemical Shifts for pmh44 in 45% TFE/ 45% H_2O/ 10% D_2O, pH 3.40 at 300 K.

Gln^{36}	7.85	3.95			
Glu^{37}	7.96	3.85	1.90	2.15	
Gln^{38}	7.91	3.95			
Gly^{39}	7.87	3.64			
Ala^{40}	7.58	4.00	1.14		
Arg^{41}	7.67	4.02	1.55, 1.61	1.40	
Val^{42}	7.42	3.82		0.64, 0.66	
Arg^{43}	7.66	4.12	1.47, 1.59	1.35	2.90
Leu^{44}	7.57	4.08		1.35	0.57, 0.61

Table 8: Qualitative summary of short- and medium-range NOEs for pmh44 in 45% TFE/ 45% H_2O/ 10% D_2O at pH 3.40 and 300 K.

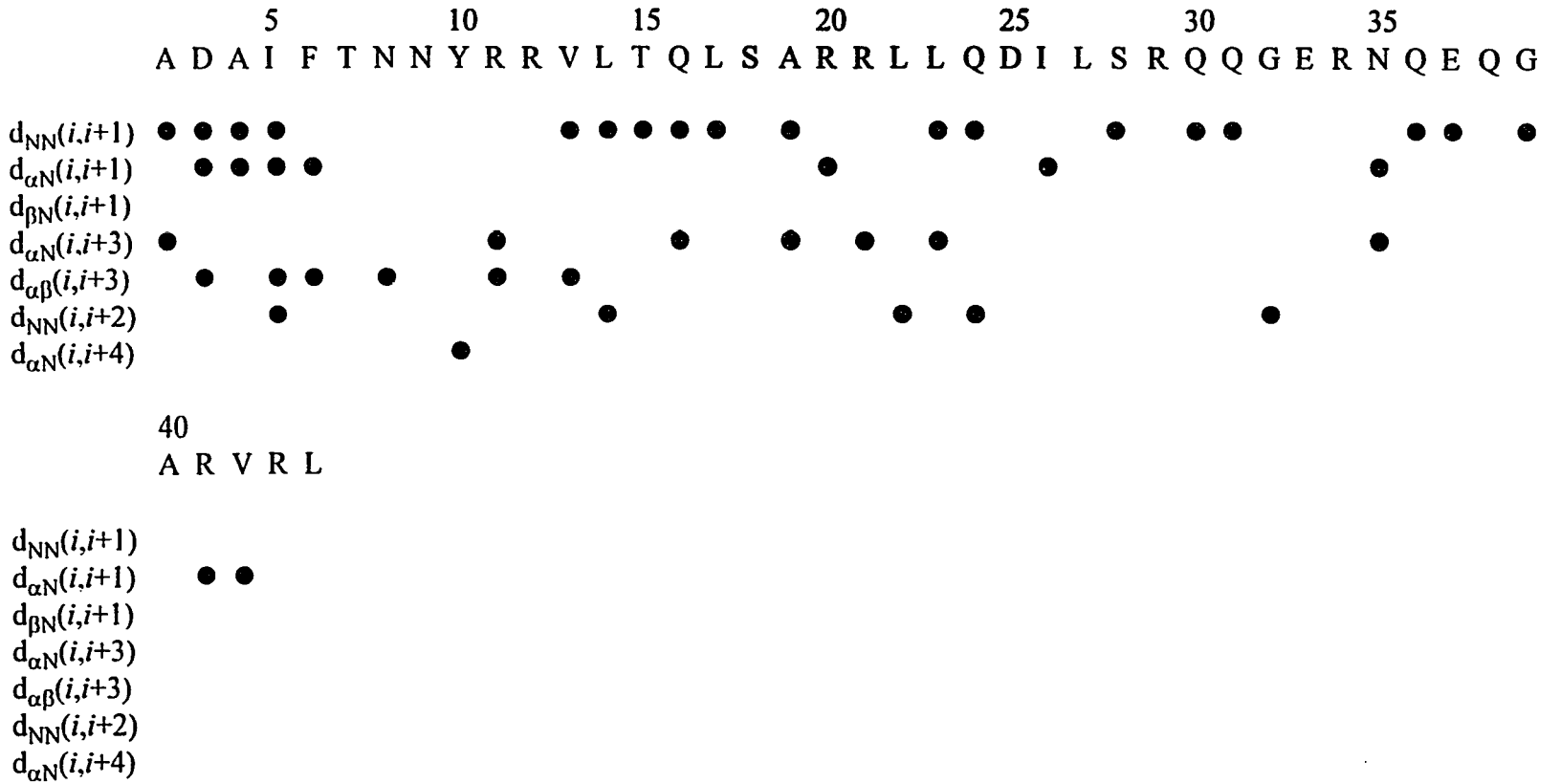

Table 9: Chemical Shift Index analysis (Wishart et al., 1992) for pmh44 in 45% TFE/ 45% H_2O/ 10% D_2O at pH 3.10 and 300 K using random coil values of Wishart et al. (1995).

Residue	δ Coil	δ Expt.	δ Δ	CSI
Ala^{2}	4.32	3.81	- 0.51	- 1
Asp^{3}	4.64	4.27	- 0.37	- 1
Ala^{4}	4.32	3.70	- 0.62	- 1
Ile^{5}	4.17	3.42	- 0.75	- 1
Phe^{6}	4.62	4.04	- 0.58	- 1
Thr^{7}	4.35	3.99	- 0.36	- 1
Asn^{8}	4.74	4.19	- 0.55	- 1
Asn^{9}	4.74	4.22	- 0.52	- 1
Tyr^{10}	4.55	4.15	- 0.40	- 1
Arg^{11}	4.34	3.57	- 0.77	- 1
Val^{13}	4.12	3.34	- 0.78	- 1
Leu^{14}	4.34	3.70	- 0.64	- 1
Thr^{15}	4.35	4.07	- 0.28	- 1
Gln^{16}	4.34	3.76	- 0.58	- 1
Leu^{17}	4.34	3.81	- 0.53	- 1
Ser^{18}	4.47	3.87	- 0.60	- 1
Ala^{19}	4.32	3.83	- 0.49	- 1
Arg^{20}	4.34	3.71	- 0.63	- 1
Arg^{21}	4.34	3.78	- 0.56	- 1
Leu^{22}	4.34	3.90	- 0.44	- 1
Leu^{23}	4.34	3.79	- 0.55	- 1
Gln^{24}	4.34	3.66	- 0.68	- 1
Asp^{25}	4.64	3.91	- 0.73	- 1
Ile^{26}	4.17	3.38	- 0.79	- 1
Leu^{27}	4.34	3.92	- 0.42	- 1
Ser^{28}	4.47	3.97	- 0.50	- 1
Arg^{29}	4.34	4.92	- 0.42	- 1
Gln^{30}	4.34	3.95	- 0.39	- 1
Gln^{31}	4.34	3.95	- 0.39	- 1
Gly^{32}	3.96	3.65	- 0.31	- 1
Glu^{33}	4.35	3.86	- 0.49	- 1
Arg^{34}	4.34	3.89	- 0.45	- 1
Asn^{35}	4.74	4.32	- 0.42	- 1
Gln^{36}	4.34	3.95	- 0.39	- 1
Glu^{37}	4.35	3.85	- 0.50	- 1
Gln^{38}	4.34	3.95	- 0.39	- 1

Table 9- *Continued*: Chemical Shift Index analysis (Wishart et al., 1992) for pmh44 in 45% TFE/ 45% H_2O/ 10% D_2O at pH 3.10 and 300 K using random coil values of Wishart et al. (1995).

Residue	δ Coil	δ Expt.	δ Δ	CSI
Gly^{39}	3.96	3.64	- 0.32	- 1
Ala^{40}	4.32	4.00	- 0.32	- 1
Arg^{41}	4.34	4.02	- 0.32	- 1
Val^{42}	4.12	3.82	- 0.30	- 1
Arg^{43}	4.34	4.12	- 0.32	- 1
Leu^{44}	4.34	4.08	- 0.26	- 1

Table 10: Long-range NOEs observed for pmh44 in 45% TFE. pH 3.40 at 300 K.

Thr^{7} NH -- Asp^{25} NH
Asn^{9} αH -- Arg^{20} NH
Asn^{9} αH -- Asp^{25} NH
Tyr^{10} αH -- Ile^{26} NH
Tyr^{10} NH -- Ile^{26} NH
Tyr^{10} αH -- Ser^{28} NH
Arg^{11} NH -- Asp^{25} NH

PMH44: CONCLUSIONS

The chemical shift values of the αH protons for the 28 amino-terminal residues of pmh44 are almost identical to those of the same resonances in pmh29. In addition long-range NOEs observed for pmh44 involve the same regions of the peptide and many of the same protons as the long-range NOEs for pmh29. The results as well as the fact that no long-range NOEs involving the 15 carboxy-terminal residues of pmh44 are observed suggest that the corresponding 28 residue amino-terminal portion (pmh-2-29) of pmh44 is conformationally similar to that of pmh29. CSI analysis data and the presence of some helical-type NOEs indicate that the 15 residue extension (residues 30-44) exists primarily in a linear helical conformation.

Examination of the αH region of the pmh44 TOCSY spectrum (Figure 16) reveals a splitting of peaks similar to that observed for pmh29. The splitting is not as well-resolved as in the pmh29 spectra, however, it does imply that pmh44 is subject to a conformational heterogeneity like that of pmh29. Severe overlap in the NOESY spectrum of pmh44 precluded accurate NOE peak integration and subsequent structure calculations. The long-range NOEs that are seen for pmh44 all occur between backbone protons. This suggests that pmh44, like pmh29, is in an TFE denatured conformation, whereby the hydrophobic core involving side-chain/side-chain interactions is disrupted by the presence of TFE.

PMH76: MATERIALS AND METHODS

SAMPLE PREPARATION. The pmh-GRF(2-76)OH was obtained from Eli Lilly and Company (Lot LY293404) and used without further purification. Three NMR samples were used to analyze pmh76. Two samples were in only an aqueous buffer (Glycine-HCl), while the third sample was in an aqueous organic (TFE/ Phosphate) solvent system. The first sample was prepared by dissolving approximately 10.0 mg of lyophilized peptide in a mixture of 1 ml of 0.2 M Glycine-HCl buffer and 0.1 ml D_2O (99.9% atom enrichment, Cambridge Isotope Laboratories) to give a final concentration of about 1.02 mM at pH 3.20. The second sample was prepared by dissolving 32.5 mg of lyophilized peptide in a mixture of 0.5 ml of 0.2 M Glycine-HCl buffer and 0.05 ml D_2O (99.9% atom enrichment, Cambridge Isotope Laboratories) to give a final concentration of about 7.20 mM at pH 3.46. The third sample was prepared by dissolving approximately 13.3 mg in 0.5 ml of a 30% d_3-TFE (MSD Isotopes)/ 60% 20 mM phosphate buffer/ 10% D_2O (99% atom enrichment, Cambridge Isotope Laboratories) mixture to give a final concentration of 3.01 mM at pH 3.05. CD samples were prepared (G. F. Needham, Eli Lilly and Company) by appropriate dilution from stock solutions of TFE, water, and peptide in water (pH 3.9) following the method of Brems et al. (1985). All stock solutions were filtered through a 0.45 μm filter before mixing. Samples were made to constant volume and constant peptide concentration (0.15 mg/ml).

CD SPECTROSCOPY. Far UV Circular Dichroism (CD) spectra were collected (G. F. Needham, Eli Lilly and Company) at multiple TFE concentrations using an AVIV model 62 spectropolarimeter. Samples were collected at 0, 10, 20, 30, 40, and 50 percent TFE using a 1.0 nm bandwidth, a 0.25 nm stepsize, and an 8 second time constant in a 0.2 cm cell. All data were collected at room temperature. Results were reported as mean residue

ellipticity ([Θ]) in degrees-cm^2-dmol^{-1} (MRE) and were calculated with a mean residue weight of 116.

NMR SPECTROSCOPY. ^{1}H NMR spectra were recorded on a Bruker AM 500 spectrometer at 300 K with a spectral width of 5813.95 Hz. Spectra were referenced to an external sample of dioxane at 3.751 ppm downfield from 4,4-dimethyl-4-silapentane-1-sulfonate. TOCSY experiments (Bax & Davis 1985) were acquired with 128 transients, 900 complex points in the t_1 dimension, and 2048 points in the t_2 dimension. Phase-sensitive NOESY experiments (Jeener et al., 1979) were acquired with 128 transients, 900 complex points in t_1 dimension, and 2048 points in the t_2 dimension. All experiments were performed with time proportional phase incrementation (Marion & Wüthrich, 1983), and were zero filled to 2K X 2K. A 60-degree shifted sine bell window function was applied to all experiments before transforming in both dimensions. TOCSY experiments of purely aqueous samples were recorded with mixing times of 40 and 60 ms. TOCSY experiments of organic samples were recorded with mixing times of 40 and 60 ms. NOESY experiments of purely aqueous samples were recorded with mixing times of 120 and 140 ms. NOESY experiments of organic samples were recorded with mixing times of 200 and 400 ms.

PMH76: RESULTS AND DISCUSSION

CD SPECTROSCOPY. Figure 17 shows the CD spectrum of pmh44 at varying TFE concentrations. The spectrum shows little change at concentrations greater than 30%. In purely aqueous solution (0% TFE) the peptide exists primarily in a random coil conformation. The minima that appear at 208 and 222 nm as the TFE concentration is increased are indicative of the formation of secondary structure. The peptide assumes a maximum helical content at approximately 30% TFE. Above 30% TFE the peptide exhibits nearly 100% helical content (G. F. Needham, Eli Lilly and Company, personal communication).

NMR SPECTROSCOPY (AQUEOUS). SPIN SYSTEM ASSIGNMENT. Figure 18 shows the NH-aliphatic region of a 40 ms TOCSY spectrum of pmh76 in aqueous buffer. Four spin systems were observed that had only an αH and highfield βH in the NH-aliphatic region and a single highfield αH-βH cross peak in the aliphatic region of the spectrum. These spin systems were attributed to four of the six alanine residues. The two spin systems that showed an αH and one or two highfield γH's in the NH-aliphatic and an αH-β and two γH's in the aliphatic region were determined to be valine spin systems. Five glutamines were identified by their midfield γH and two βH's. Three glycine spin systems were visible that had only a broad αH in the NH-aliphatic region. A single serine spin system exhibited its characteristic αH and two lowfield βH's. The hippuryl group showed a broad resonance stemming from its methylene protons. Four arginines spin systems were readily assigned by their εH that resonates near 6.9 ppm and shows crosspeaks to the δ,β,and γ protons. The aromatic region (Figure 19) gave rise to the aromatic resonances of four spin systems- histidine, tyrosine, phenylalanine, and tryptophan. The tryptophan spin system had the lowest field resonance at 9.83 ppm from its N1 proton which provided facile identification. The tyrosine, histidine, and

Figure 17: Circular dichroism spectrum of pmh76 in varying concentrations of aqueous trifluoroethanol at pH 3.9 and 298 K. Mean residue ellipticity (MRE) is in units of cm^2-degrees-$dmol^{-1}$.

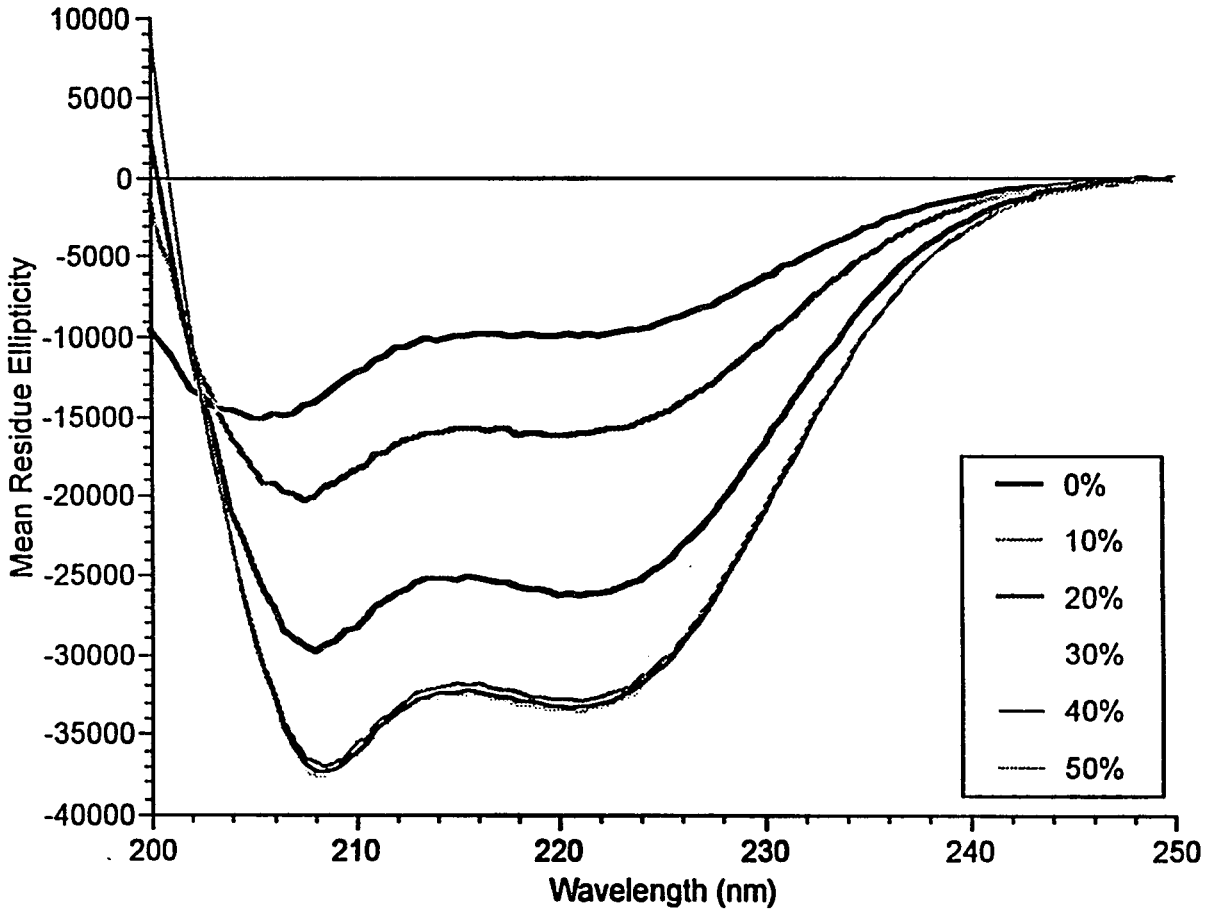

Figure 18: NH-aliphatic region of a 40 ms TOCSY spectrum for pmh76 in 90% Glycine-HCl buffer and 10% D_2O at pH 3.20 and 300 K, where spin systems have been labeled at the αH resonance.

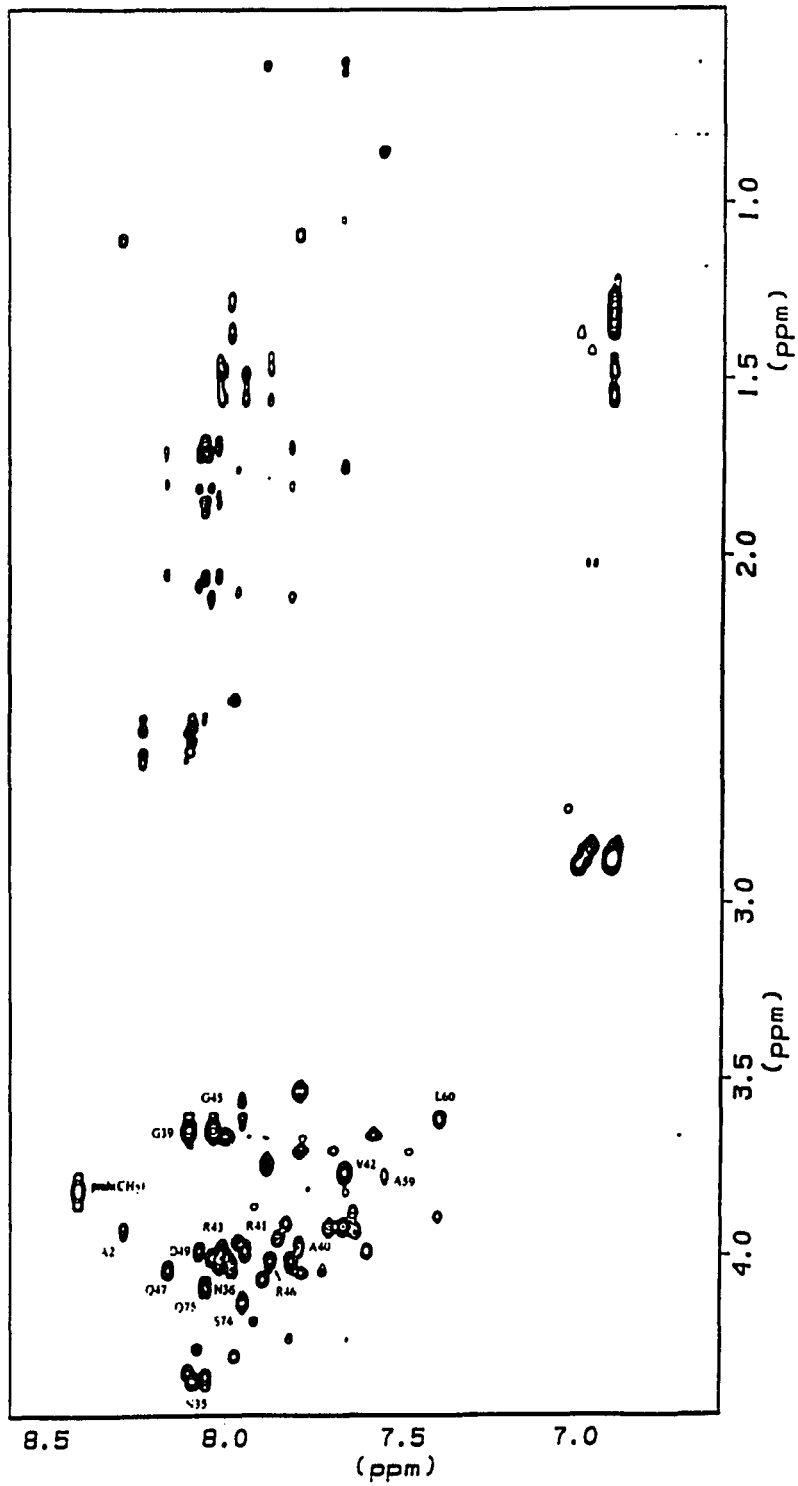

Figure 19: Amide and aromatic region of a 40 ms TOCSY spectrum for pmh76 in 90% Glycine-HCl buffer and 10% D_2O at pH 3.20 and 300 K, where the aromatic resonances have been labeled.

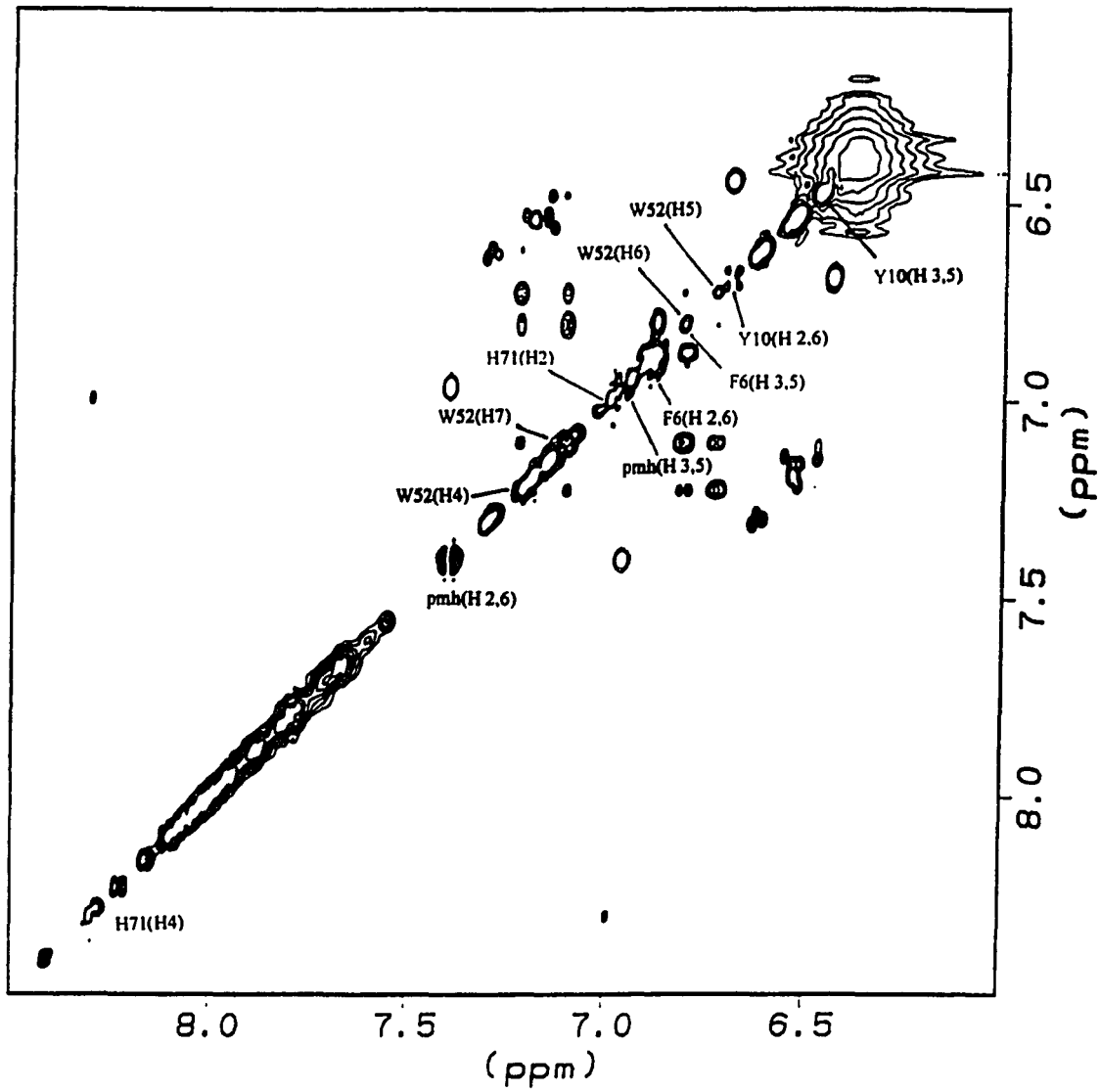

phenylalanine residues all had two aromatic resonances with a single crosspeak connectivity. These resonances were discerned by the chemical shift difference between their aromatic resonances. The largest shift difference was for the histidine, the next largest for tyrosine, and the smallest for phenylalanine. None of the aromatic residues exhibited visible resonances in other regions of the spectrum. Three of the remaining spin systems were of the AMX type while the fourth was either a leucine or isoleucine. These spin systems could not be identified until sequential assignment was made by analysis of NOESY spectra.

SEQUENCE-SPECIFIC ASSIGNMENTS. Sequential assignments were made by observation of NH(i)-NH(i+1), αH(i+1), and β(i+1) protons in the amide and fingerprint regions of a 160 ms NOESY spectrum (Figures 20 and 21). Table 11B lists the short-range NOEs that facilitated assignment of 25 of 75 residues for pmh76 in aqueous buffer. Figure 22 shows an expansion of the fingerprint region of a 40 ms TOCSY with the α protons of the assigned residues labeled. The portion of the sequence that had the most residue assignments was from Gly^{32} to Asp^{49}. The chemical shifts of the assigned proton resonances of pmh76 in aqueous buffer are shown in Table 12.

SECONDARY STRUCTURE. NOESY spectra did not provide any medium- or long-range NOEs. A chemical shift index analysis (Table 13) of pmh76 in purely aqueous solvent, however, shows that all residues that were assigned have an αH chemical shift index of -1 which correlates to a helical type index. Four consecutive -1 indices, however, are necessary to define a helical region. Regions 40-43 and 45-49 have at least four consecutive -1 indices thereby suggesting the presence of helical secondary structure in these regions. Significant overlap in the fingerprint region of the 40 ms NOESY spectrum inhibited confirmation of the CSI data by short- and medium-range NOE data.

Figure 20: Amide region of a 160 ms NOESY spectrum for pmh76 in 90% Glycine-HCl buffer and 10% D_2O at pH 3.20 and 300 K. where the NH-NH NOEs have been labeled.

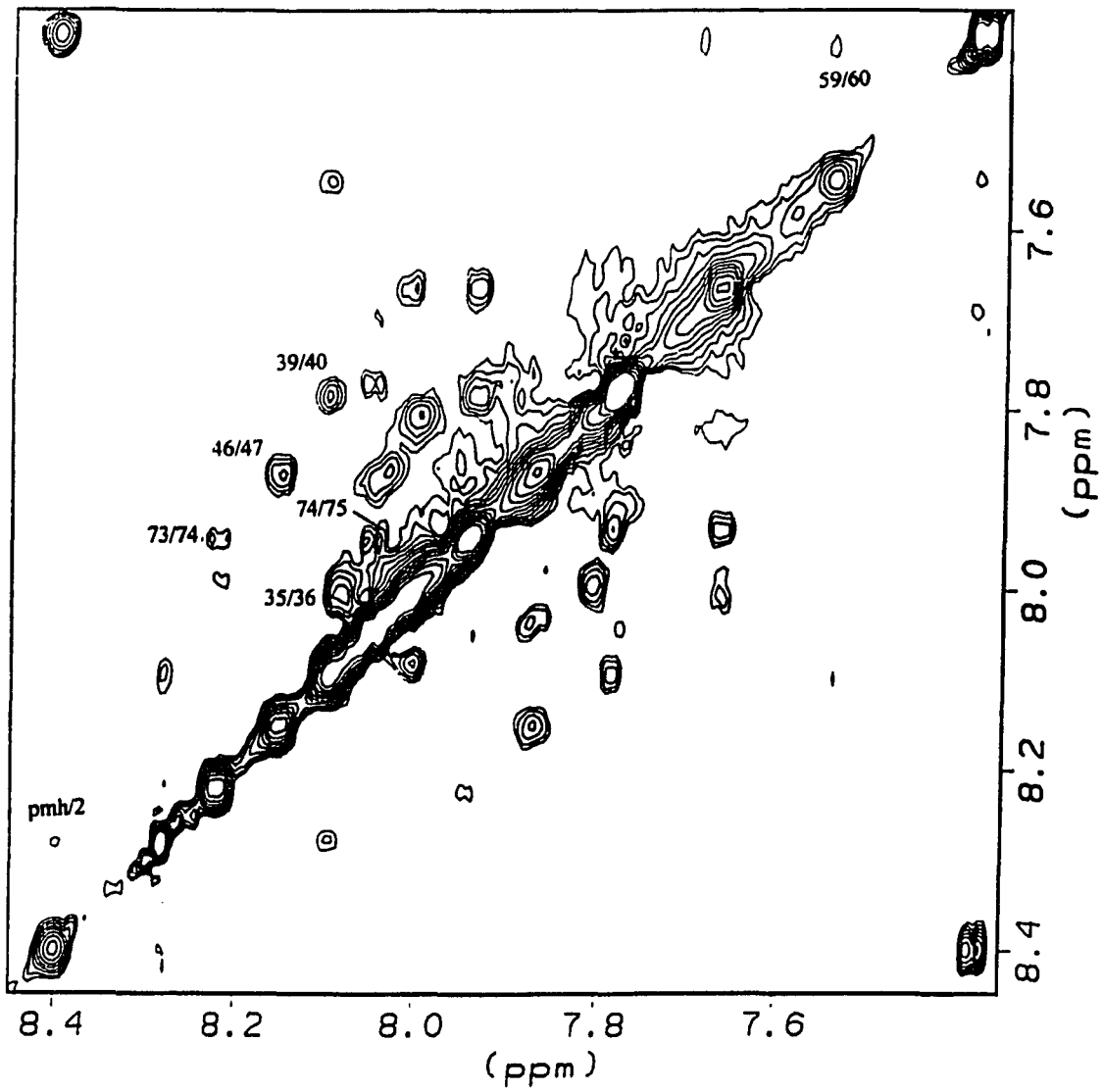

Figure 21: Expansion of the fingerprint region of a 160 ms NOESY spectrum for pmh76 in 90% Glycine-HCl buffer and 10% D_2O at pH 3.20 and 300 K, where the αH-NH NOEs have been labeled.

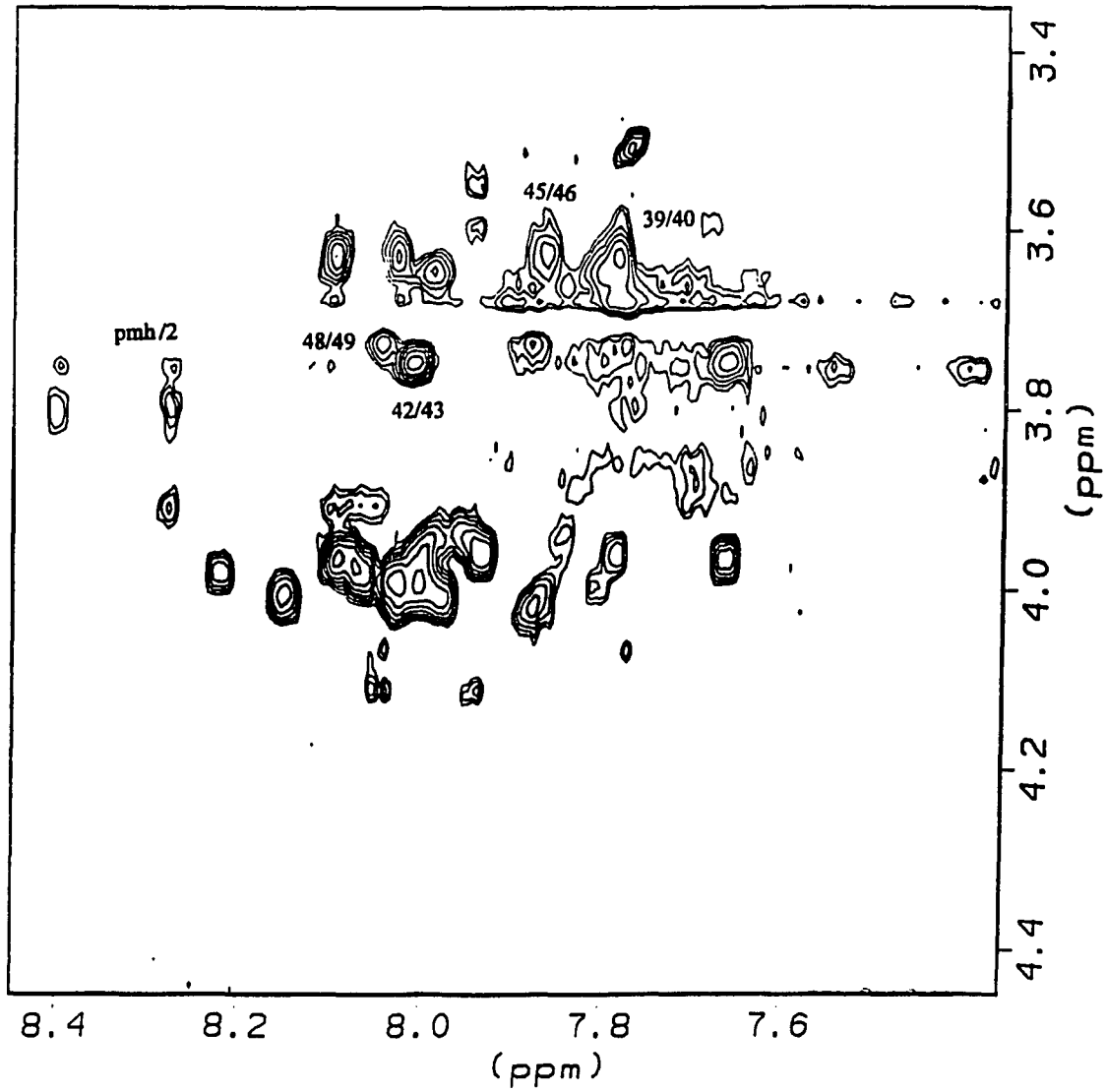

Figure 22: Expansion of the fingerprint region of a 40 ms TOCSY spectrum for pmh76 in 90% Glycine-HCl buffer and 10% D_2O at pH 3.20 and 300 K, where the sequence-specific assignments have been labeled.

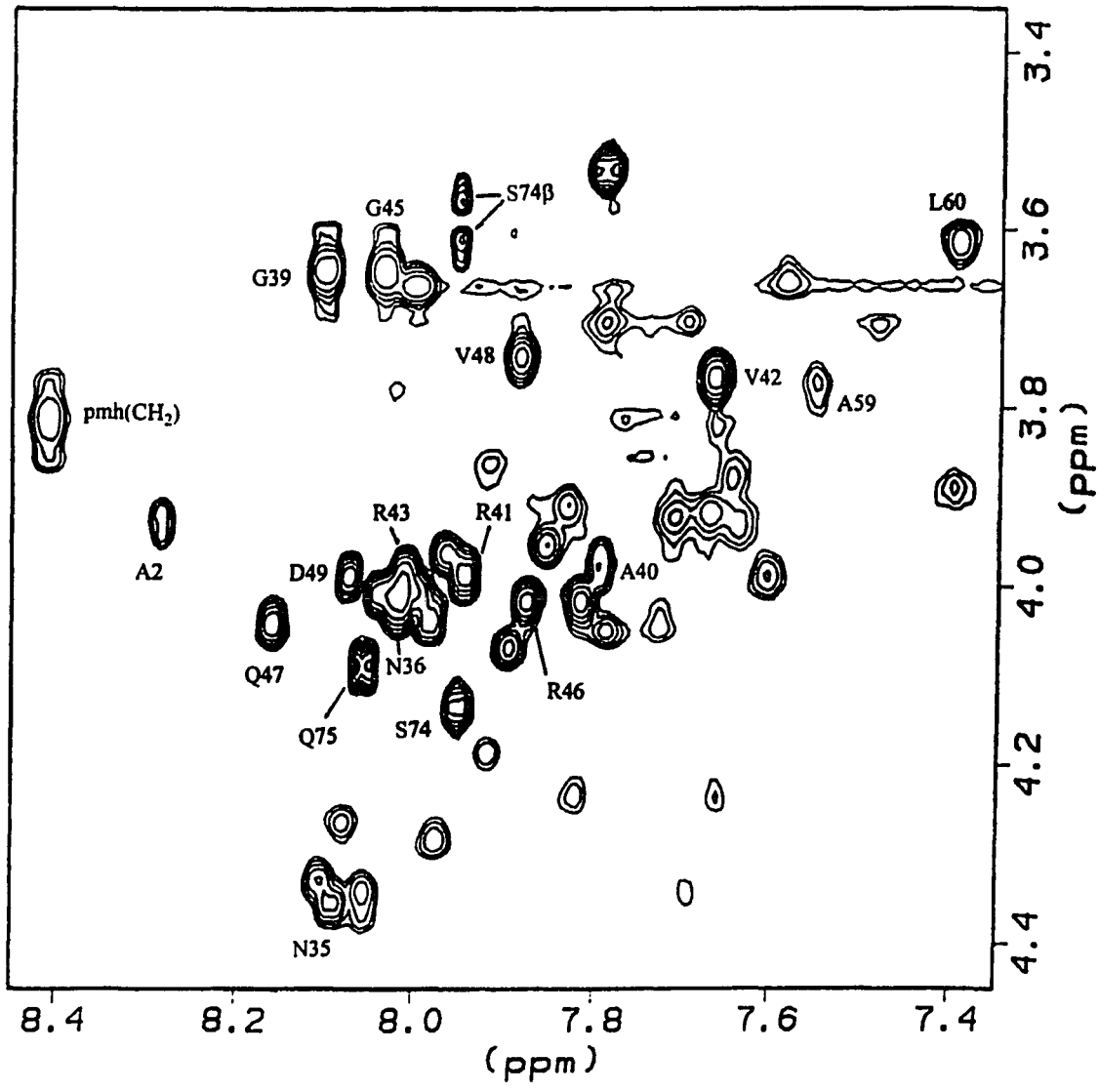

Table 11: Observed inter-residue NOEs for pmh76 (A) in 30% trifluoroethanol/ 60% H_2O/ 10% D_2O, pH 3.05 at 300 K and (B) in 90% 0.2 M Glycine-HCl buffer/ 10% D_2O, pH 3.20 at 300 K.

(A) NOE (30% TFE)	(B) NOE(aqueous)
pmh CH_2 -- Ala^2 NH	pmh NH -- Ala^2 NH
pmh NH -- Ala^4 βH	pmh CH_2 -- Ala^2 NH
pmh NH -- Ala^4 NH	Asn^{35} NH -- Gln^{36} NH
Ala^2 βH -- Asp^3 NH	Asn^{35} αH -- Gln^{36} NH
Ala^2 NH -- Asp^3 NH	Gly^{39} NH -- Ala^{40} NH
Asp^3 βH -- Ala^4 NH	Gly^{39} αH -- Ala^{40} NH
Asp^3 αH -- Ala^4 NH	Ala^{40} βH -- Arg^{41} NH
Asp^3 NH -- Ala^4 NH	Val^{42} αH -- Arg^{43} NH
Ala^4 αH -- Ile^5 NH	Gly^{45} αH -- Arg^{46} NH
Ala^4 βH -- Ile^5 NH	Arg^{46} NH -- Gln^{47} NH
Ile^5 δH -- Phe^6 NH	Val^{48} αH -- Asp^{49} NH
Ile^5 NH -- Phe^6 NH	Ala^{59} NH -- Leu^{60} NH
Ile^5 δH -- Asn^8 NH	Ala^{59} βH -- Leu^{60} NH
Phe^6 NH -- Thr^7 γH	Asn^{73} NH -- Ser^{74} NH
Thr^7 γH -- Tyr^{10} (2,6)H	Ser^{74} NH -- Gln^{75} NH
Tyr^{10} (2,6)H -- Val^{13} γH	Ser^{74} αH -- Gln^{75} NH
Tyr^{10} (2,6)H -- Leu^{14} δH	
Tyr^{10} (3,5)H -- Leu^{14} δH	
Val^{13} NH -- Thr^{15} γH	
Trp^{52} (4)H -- Ala^{53} αH	
Trp^{52} (4)H -- Ala^{53} βH	
Ala^{65} βH -- Thr^{66} NH	
Asn^{73} NH -- Ser^{74} NH	
Ser^{74} NH -- Gln^{75} NH	

Table 12: ^{1}H Chemical Shifts for pmh76 in 90% 0.2 M Glycine-HCl buffer/ 10% D_2O, pH 3.20 at 300 K.

residue	NH	αH	βH	γH	δH	others
pmh	8.40					CH_2 3.78, 3.84
						H(2,6) 7.39
						H(3,5) 6.95
Ala[2]	8.28	3.93	1.11			
Phe[6]						H(2,6) 6.80
						H(3,5) 6.88
Tyr[10]						H(2,6) 6.69
						H(3,5) 6.44
Asn[35]	8.09	4.35	2.50, 2.54			
Gln[36]	8.02	4.02	1.69, 1.84	2.06		
Gly[39]	8.10	3.61, 3.68				
Ala[40]	7.79	3.98	1.09			
Arg[41]	7.94	3.99	1.49, 1.56		2.80	
Val[42]	7.67	3.77	1.75	0.60, 0.63		
Arg[43]	8.01	3.98	1.48, 1.55		2.80	
Gly[45]	8.03	3.62, 3.67				
Arg[46]	7.90	4.07	1.46, 1.56		2.80	
Gln[47]	8.16	4.04	1.70, 1.80	2.06		
Val[48]	7.88	3.74	1.78	0.61		
Asp[49]	8.07	3.99	1.81, 2.09			
Trp[52]						N1 9.03 H2 6.94
						H4 7.22 H5 6.72
						H6 6.81 H7 7.10
Ala[59]	7.55	3.77	0.86			
Leu[60]	7.39	3.61	1.39		0.39	
His[71]						H2 8.30 H4 6.99
Ser[74]	7.95	4.13	3.56, 3.61			
Gln[75]	8.06	4.09	1.70, 1.87	2.06, 2.48		

Table 13: Chemical Shift Index analysis (Wishart et al., 1992) for pmh76 in 90% Glycine-HCl buffer/ 10% D_2O. pH 3.20 at 300 K using random coil values of Wishart et al. (1995).

Residue	δ Coil	δ Expt.	δ Δ	CSI
Ala^{2}	4.32	3.93	- 0.39	-1
Asn^{35}	4.74	4.35	- 0.39	-1
Gln^{36}	4.34	4.02	- 0.32	-1
Gly^{39}	3.96	3.65	- 0.31	-1
Ala^{40}	4.32	3.98	- 0.34	-1
Arg^{41}	4.34	3.99	- 0.35	-1
Val^{42}	4.12	3.77	- 0.35	-1
Arg^{43}	4.34	3.98	- 0.36	-1
Gly^{45}	3.96	3.65	- 0.31	-1
Arg^{46}	4.34	4.07	- 0.27	-1
Gln^{47}	4.34	4.04	- 0.32	-1
Val^{48}	4.12	3.74	- 0.38	-1
Asp^{49}	4.64	3.99	- 0.65	-1
Ala^{59}	4.32	3.77	- 0.55	-1
Leu^{60}	4.34	3.61	- 0.73	-1
Ser^{74}	4.47	4.13	- 0.34	-1
Gln^{75}	4.34	4.09	- 0.25	-1

NMR SPECTROSCOPY (TRIFLUOROETHANOL). SPIN SYSTEM ASSIGNMENT. Figure 23 shows the NH-aliphatic region of a 40 ms TOCSY of pmh76 in aqueous trifluoroethanol. The spin systems of all seven alanine residues were apparent in this region, and are distinguished by their αH and single highfield βH resonances. A serine residue, with an αH and two lowfield βH's, was also evident in this region. Several overlapping arginine spin systems could be identified by their εH protons that resonate near 6.9 ppm and show crosspeaks to the α, δ, γ, and β protons. The methylene protons of the hippuryl group appeared as two well-separated lowfield resonances. In the aliphatic region of the 40 ms TOCSY experiment three valine spin systems were identified by their αH-β and two highfield γH crosspeaks. Three threonine spin systems were assigned based upon their characteristic lowfield αH-βH and highfield αH-γH crosspeaks. An isoleucine spin system was seen in the aliphatic region that showed a strong γCH_3 and very highfield δCH_3 resonance. Four glutamine spin systems were discernible by the γH and two βH resonances. In the aromatic region of the TOCSY (Figure 24) the four aromatic spin systems were assigned. The imino resonance of a tryptophan residue (the lowest field resonance in the spectrum) was readily apparent and facilitated assignment of that spin system. The three other aromatic residues showed two aromatic resonances with a single off-diagonal crosspeak connectivity. The chemical shift difference between the aromatic resonances allowed assignment of the individual spin systems with histidine, tyrosine, and phenylalanine having the largest, smaller, and smallest chemical shift separations, respectively. The residual spin systems were of the AMX type and could be individuated only after sequential assignment was attempted.

SEQUENCE-SPECIFIC ASSIGNMENTS. Figures 25 and 26 show the fingerprint and the amide regions, respectively, of a 200 ms NOESY spectrum. These three regions were

Figure 23: NH-aliphatic region of a 40 ms TOCSY spectrum for pmh76 in 30% d_3-trifluoroethanol, 60% H_2O, 10% D_2O at pH 3.05 and 300 K, where the spin systems have been labeled at the αH resonance.

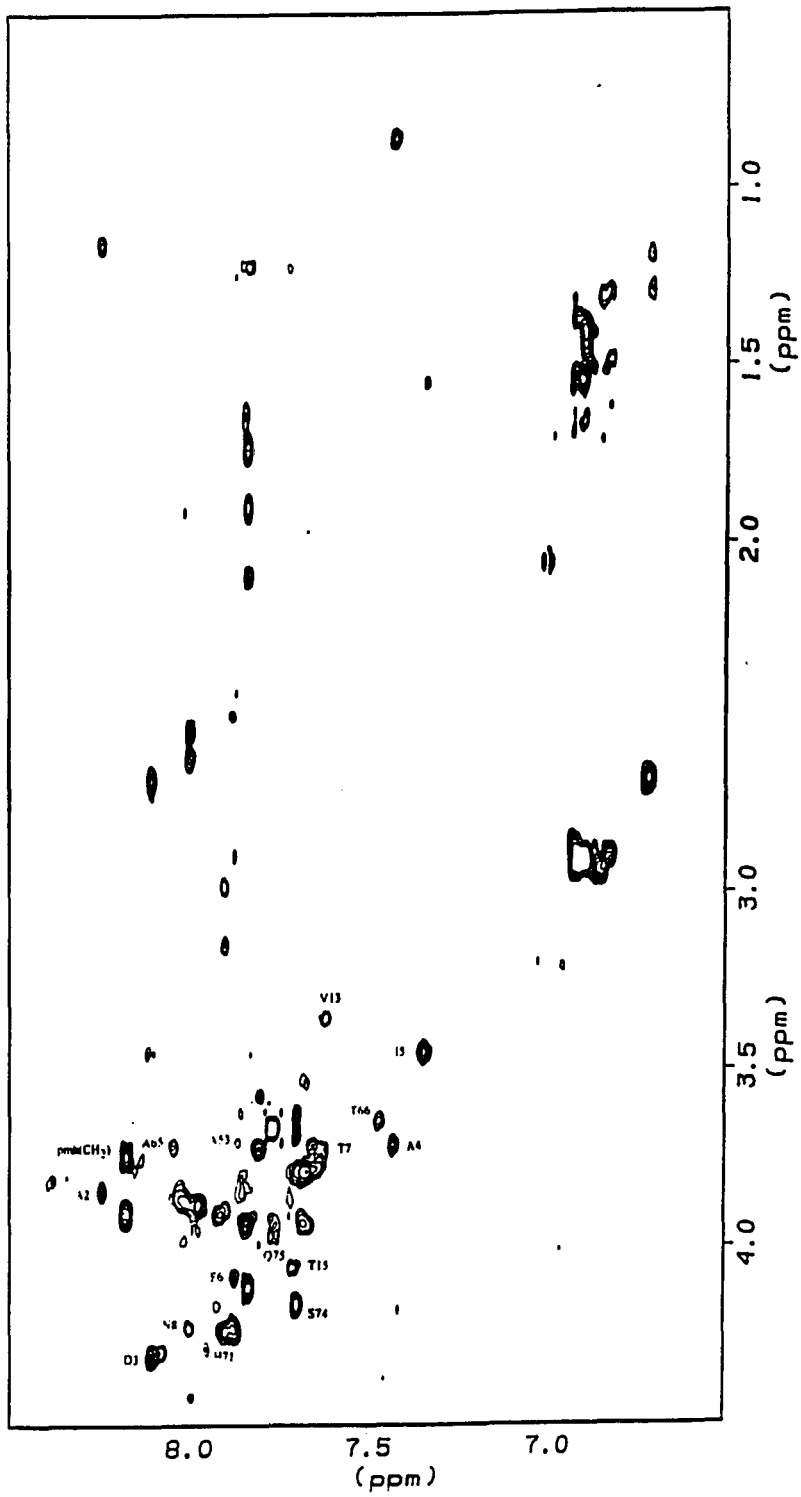

Figure 24: Amide and aromatic region of a 40 ms TOCSY spectrum for pmh76 in 30% d_3-trifluoroethanol, 60% H_2O, 10% D_2O at pH 3.05 and 300 K, where the aromatic resonances have been labeled.

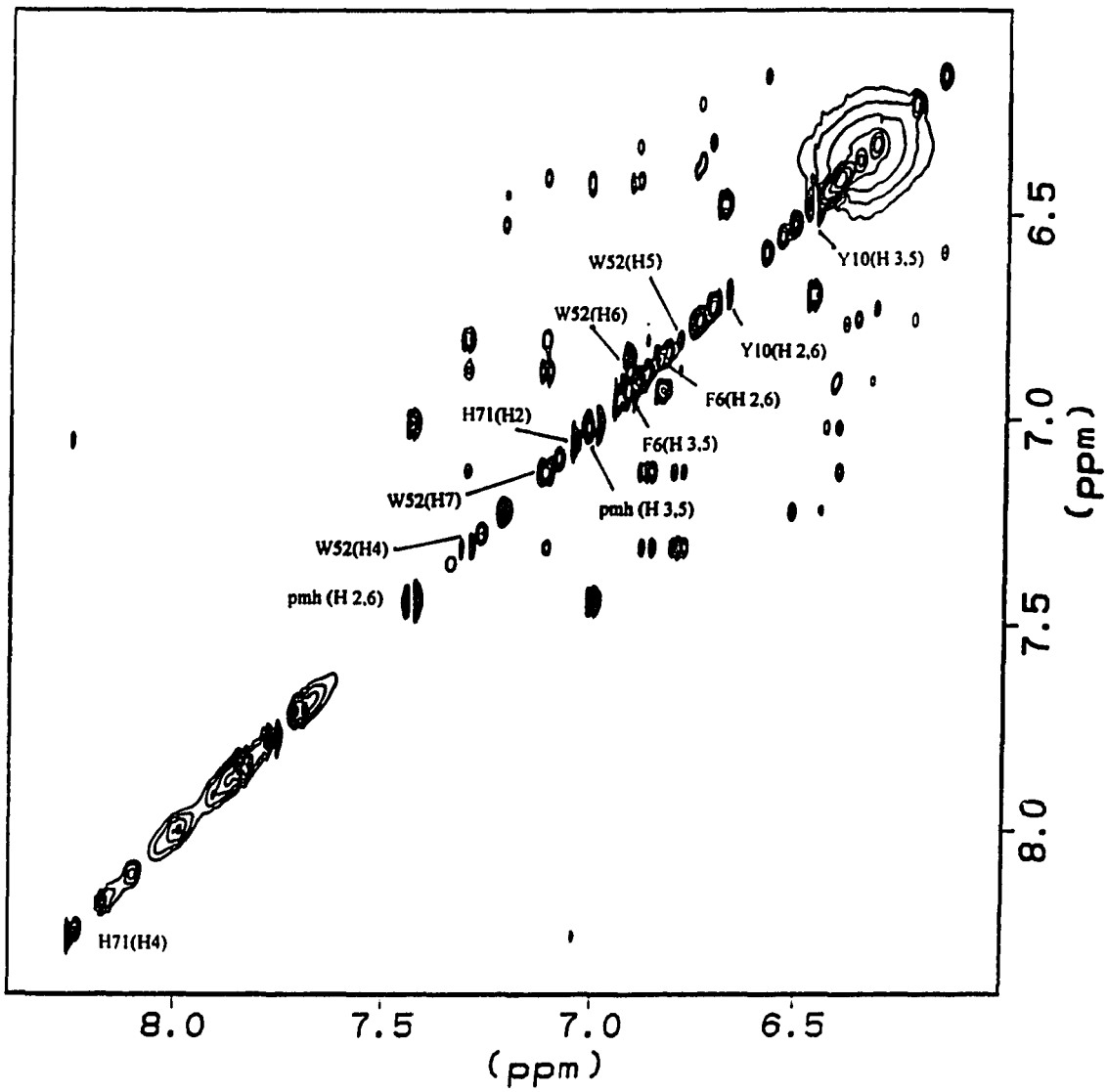

Figure 25: Expansion of the fingerprint region of a 200 ms NOESY spetrum for pmh76 in 30% d_3-trifluoroethanol, 60% H_2O, 10% D_2O at pH 3.05 and 300 K, where the αH-NH and βH-NH NOEs have been labeled.

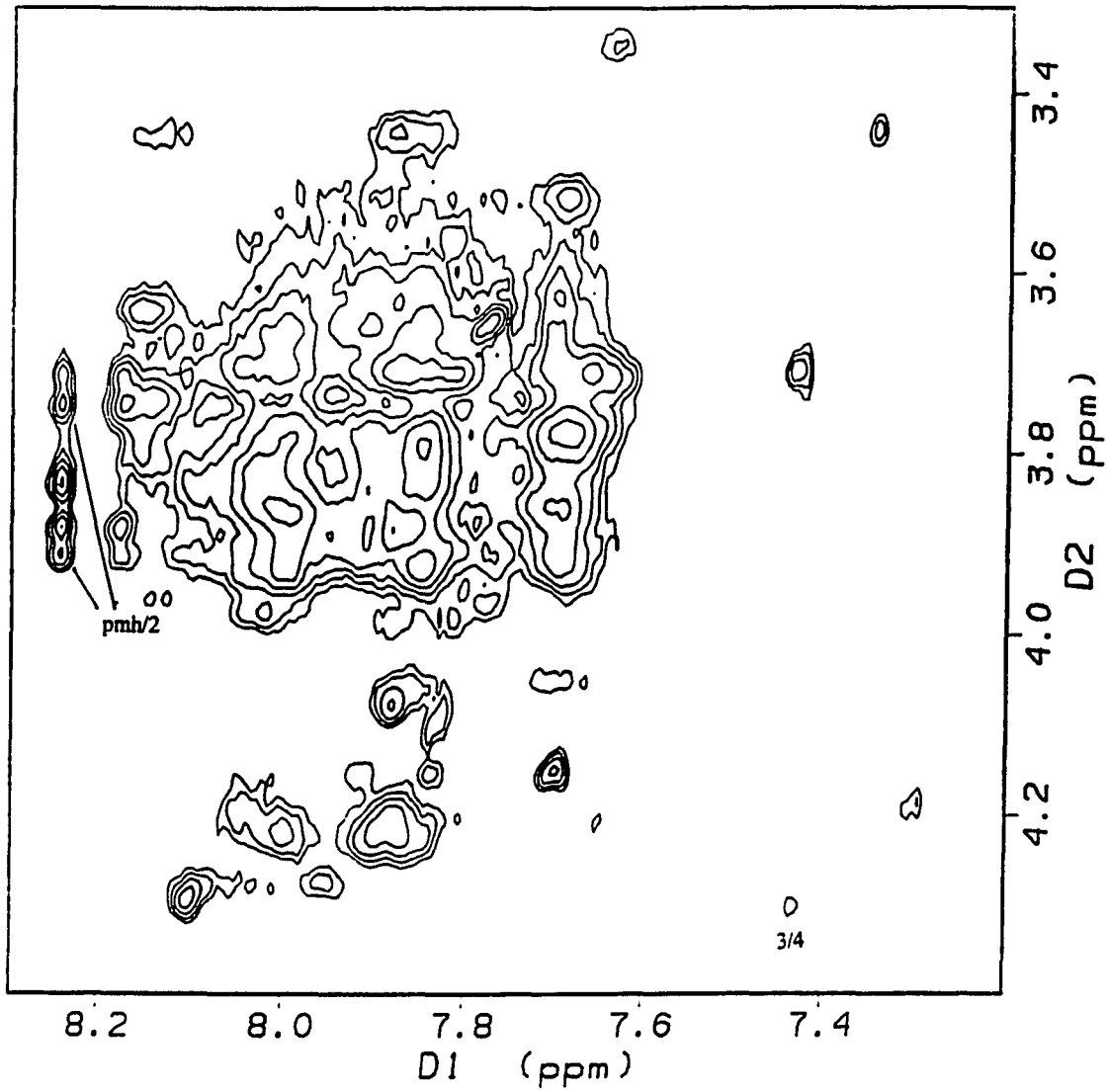

Figure 26: Amide region of a 200 ms NOESY spetrum for pmh76 in 30% d_3-trifluoroethanol, 60% H_2O, 10% D_2O at pH 3.05 and 300 K, where the NH-NH NOEs have been labeled.

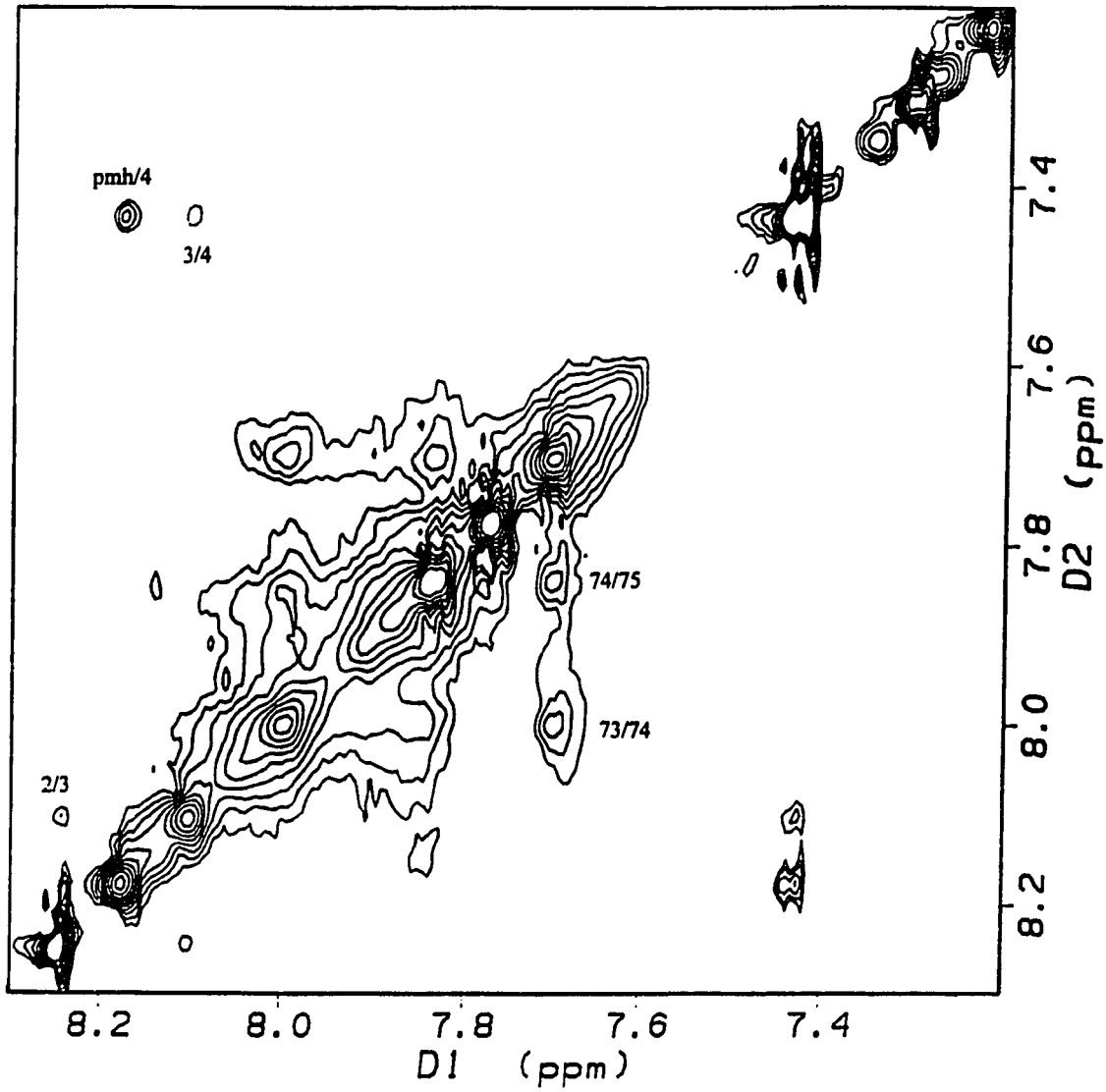

analyzed to obtain sequential assignments by identification of NH(*i*)-NH(*i*+1), αH(*i*)-NH(*i*+1), βH(*i*)-NH(*i*+1) according to standard assignment protocol (Wüthrich, 1986). Table 10A details the NOE connectivities observed for pmh76 in 30% TFE. Figure 27 shows the fingerprint region of the TOCSY of pmh76 in TFE with the assigned resonances labeled. Sequential assignments were made for 19 of the 75 residues. A stretch of residues from the hippuryl group to Asn^8 was the longest continuum identified. The chemical shifts of the assigned resonances of pmh76 in TFE are shown in Table 14.

Secondary Structure. The N-terminal region was the only portion of the polypeptide that exhibited an assignment of four or more continuous residues. The NOE pattern in this region [NH(*i*)-NH(*i*+1) and βH(*i*)-NH(*i*+1)] is characteristic of helical secondary structure. The CSI analysis of pmh76 in 30% TFE (Table 15) confirms the helical conformation identified by NOE data. A CSI value of -1 is observed for all assigned residues, with a helical region defined by the 10 continuous "-1's" beginning at the N-terminus and ending at Arg-11. Like the NOESY spectrum of pmh76 in Glycine-HCl buffer, the NOESY spectrum of pmh76 in 30% TFE is extremely crowded and substantially overlapped, making further confirmation of CSI analysis data and CD spectroscopy data impossible.

Figure 27: Expansion of the fingerprint region of a 40 ms TOCSY spectrum for pmh76 in 30% d_3-trifluoroethanol. 60% H_2O. 10% D_2O at pH 3.05 and 300 K. where the sequence-specific assignments have been labeled.

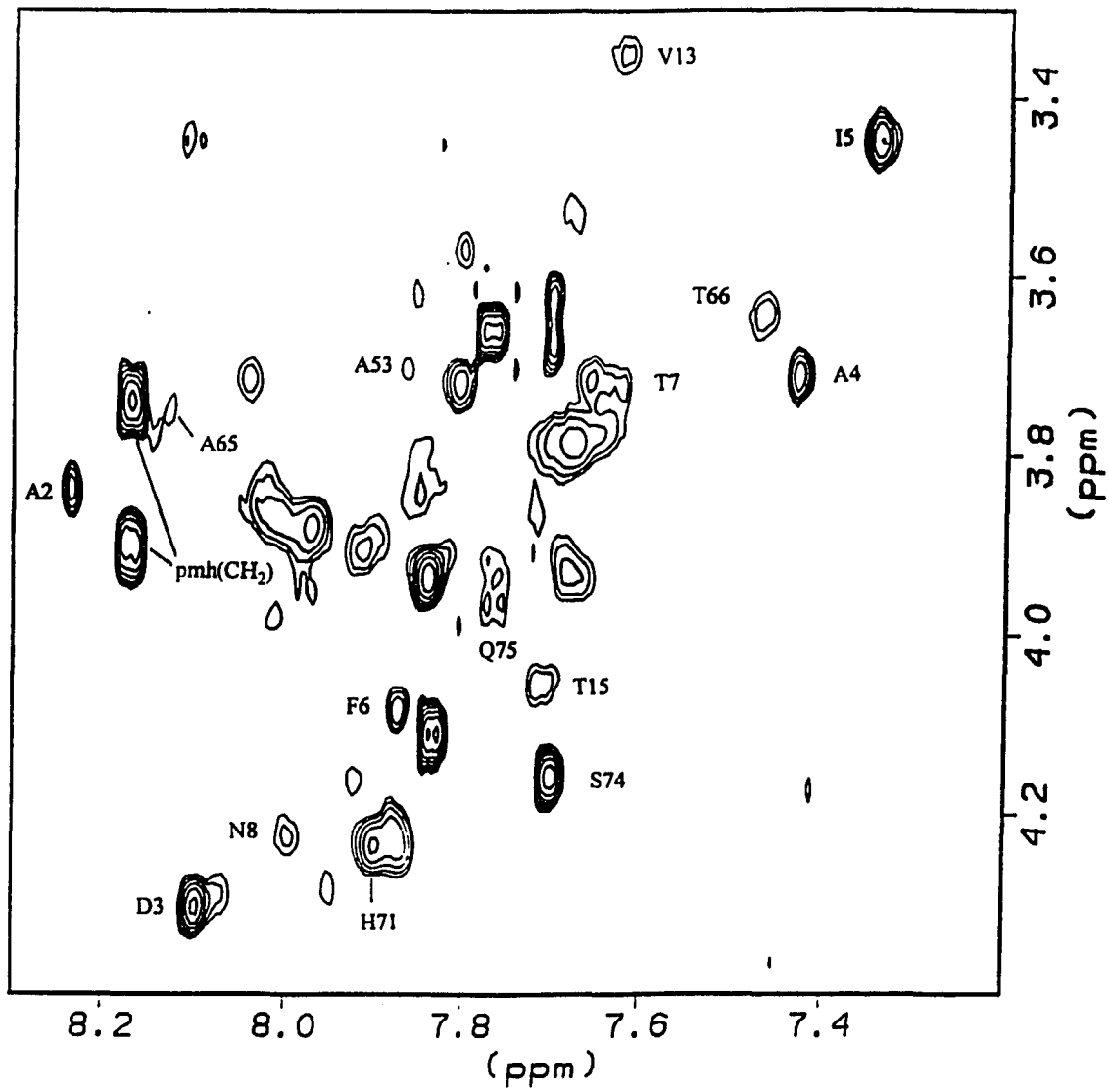

Table 14: ^{1}H Chemical Shifts for pmh76 in 30% TFE/ 60% H_2O/ 10% D_2O, pH 3.05 at 300 K.

residue type	NH	αH	βH	γH	others
pmh	8.17				CH_2 3.74, 3.90 H(3,5) 7.00 H(2,6) 7.44
Ala^2	8.24	3.84	1.15		
Asp^3	8.10	4.29	2.59		
Ala^4	7.43	3.71	0.85		
Ile^5	7.35	3.44	1.53		δH 0.48
Phe^6	7.88	4.08	2.09		H(2,6) 6.84 H(3,5) 6.92
Thr^7		3.99	3.71	0.99	
Asn^8	8.00	4.24	2.41, 2.53		
Tyr^{10}		3.90	2.58, 2.66		H(2,6) 6.69 H(3,5) 6.47
Val^{13}	7.62	3.35	1.86	0.62, 0.74	
Thr^{15}	7.71	4.06	3.60	0.96	
Trp^{52}		4.19	3.11		N1 9.48 H4 7.31 H7 7.12 H6 6.87 H5 6.80
Ala^{53}	7.87	3.70	1.24		
Ala^{65}	8.13	3.74	1.23		
Thr^{66}	7.47	4.19	3.64	0.94	
His^{71}	7.90	4.23	2.96, 3.14		H2 8.25 H4 7.04
Asn^{73}	8.01	4.22	2.54, 2.61		
Ser^{74}	7.70	4.16	3.67, 3.62		
Gln^{75}	7.84	4.11	1.73, 1.89	2.09	

Table 15: Chemical Shift Index analysis (Wishart et al., 1992) for pmh76 in 30% TFE/ 60% H_2O/ 10% D_2O, pH 3.05 at 300 K using random coil values of Wishart et al. (1995).

Residue	δ Coil	δ Expt.	δ Δ	CSI
Ala^{2}	4.32	3.84	- 0.48	- 1
Asp^{3}	4.64	4.29	- 0.35	- 1
Ala^{4}	4.32	3.71	- 0.61	- 1
Ile^{5}	4.17	3.44	- 0.73	- 1
Phe^{6}	4.62	4.08	- 0.54	- 1
Thr^{7}	4.35	3.99	- 0.36	- 1
Asn^{8}	4.74	4.24	- 0.50	- 1
Tyr^{10}	4.55	3.90	- 0.65	- 1
Val^{13}	4.12	3.35	- 0.77	- 1
Thr^{15}	4.35	4.06	- 0.29	- 1
Trp^{52}	4.66	4.19	- 0.47	- 1
Ala^{53}	4.32	3.70	- 0.62	- 1
Ala^{65}	4.32	3.74	- 0.58	- 1
Thr^{66}	4.35	4.19	- 0.16	- 1
His^{71}	4.73	4.23	- 0.50	- 1
Asn^{73}	4.74	4.22	- 0.52	- 1
Ser^{74}	4.47	4.16	- 0.31	- 1
Gln^{75}	4.34	4.11	- 0.33	- 1

PMH76: CONCLUSIONS

The sequence redundancy of pmh76 (11 glutamines, 11 arginines, and 12 leucines) creates substantial overlap in the TOCSY and NOESY spectra under both solvent conditions. This severe overlap precludes a complete sequential assignment and hinders the identification of NOEs which could identify the secondary and/or tertiary structure of the molecule.

The first 10 residues of pmh76 in TFE show a continuum of "-1" chemical shift indices which suggest that this region of pmh76 is in a helical conformation. Also, those residues that are assigned in TFE had αH chemical shifts that are nearly identical to corresponding residues in both pmh29 and pmh44. These results suggest that the N-terminal portion of pmh76 has a similar conformation to pmh29 and pmh44 in aqueous TFE. The remaining portion of the molecule likely adopts largely helical secondary structure as determined by CD spectroscopy. This secondary structure cannot be confirmed by NMR results, however, due to severely overlapped spectra.

Under purely aqueous conditions a stretch two stretches of helical type CSI indices are observed: residues 39-43 and residues 45-49. The αH chemical shifts for residues 39-42 of pmh76 in aqueous solution are within 0.05 ppm of the corresponding chemical shifts in the pmh44 molecule, while residue 43 differs by 0.14 ppm. Although the CD spectrum of pmh76 under purely aqueous conditions shows a largely unstructured peptide, these results imply the presence of a transient helical turn in the pmh76 molecule that is similar to a helical turn in the same region of the pmh44 molecule.

An *ab initio* molecular dynamics calculation of pmh76 showed the molecule to be stable in a helical fishhook structure (G. F. Needham, Eli Lilly and Company, personal communication). The structure was characterized by a primarily helical secondary structure with a tertiary folded conformation in the first 29 residues, while the 30-76

portion of the molecule formed a linear helical tail. The structure we deduce for pmh76 resembles a fishhook structure.

SUMMARY

The objective of these studies was to elucidate the structures of three potent GRF analogs and relate these findings to their increased potency. Complete sequential assignment was obtained for pmh29 and pmh44 (1 residue obscured). Limited assignment was achieved for pmh76 in both water and TFE due to the large number of residues and extensive sequence redundancy which resulted in severely overlapped spectra. In addition to the assignment of observable resonances, secondary and tertiary structures were identified for pmh44 and calculated for pmh29. This is the first evidence of a global tertiary structure for any member of the secretin family.

The structures calculated for the pmh29 analog adhere to a consensus of previously proposed conformational requirements for GRF bioactivity. They are helical, are conformationally flexible, are highly amphiphilic, and are able to form a turn in the 13-21 region. The structures are also similar to that proposed for the secretin family, in general, although the N-terminus is helical instead of disordered. The secondary structure adopted in the N-terminus, however, may supply a binding specificity versus other members of the family and/or be a generally preferred conformation. The TFE solvent system employed in this study prevents the formation of a hydrophobic core that has been seen in other stable tertiary folds for peptides of similar length. The solvent system, however, more effectively mimics the anisotropic environment of the 42% hydrophobic extracellular GRF receptor binding site than does a purely aqueous solvent. The results are two independent, flexible peptide structures that adopt two independent tertiary folds.

The tertiary fold appears to remain in the lengthened pmh44 and pmh76 analogs. In fact, it seems that the C-terminal extensions simply form a linear, primarily helical tail. These results are coincident with an *ab initio* study which characterized pmh76 as a fishhook structure (G. F. Needham, Eli Lilly and Company, personal communication).

These results are also in accordance with previous findings that the first 29 residues comprise the bioactive core of the GRF molecule (River et al., 1982; Grossman et al., 1984; Lance et al., 1984; Ling et al., 1984).

The very high potency of the pmh analogs is related to several factors. First, metabolic stability is imparted by the numerous amino acid substitutions, which results in an increase in bioavailability. Second, the para-methyl hippuryl group allows the extension of helical structure to the N-terminus. It appears that helical structure in this region is a preferred conformation at the GRF receptor. Third, the Thr^{15} substitution facilitates the formation of a tertiary fold without disrupting the required helical secondary structure. Fourth, the fold that is formed enables the molecule to increase its overall amphiphilicity by forming separate hydrophobic and hydrophilic faces. Finally, the tertiary structure agrees with proposed requisite bioactive characteristics and may represent a bioactive conformation.

This first-ever elucidation of a global tertiary fold in any member of the secretin family provides a starting point for further exploration into the bioactive conformation of GRF. Future studies of GRF analogs might include investigation of the structure of the ligand bound to the receptor or stabilization of a tertiary fold through chemical modification. Careful attention, however, must be paid to the inherent flexibility of the GRF molecule and the role that this flexibility plays in the facilitation of receptor binding. It is hoped that the information gained from the current study can provide insight into not only the preferred bioactive conformation of GRF analogs, but also its siblings in the secretin family and peptide hormones as a whole.

REFERENCES

Albert, J. S. & Hamilton, A. D. (1995) Stabilization of helical domains in short peptides using hydrophobic interactions. *Biochemistry 34*, 984-990.

Alexander, P., Fahnestock, S., Lee, T., Orban, J, & Bryan, P. (1992) Thermodynamic analysis of the folding of the streptococcal protein G IgG-binding domains B1 and B2: why small proteins tend to have high denaturation temperatures. *Biochemistry 31*, 3597-3603.

Alexandrescu, A. T., Ng, Y-L, Dobson, C. M. (1994) Characterization of a trifluoroethanol-induced partially folded state of α-lactalbumin. *J. Mol. Biol. 235*, 587-599.

Atkins, A. R., Martin, R. C., & Smith, R. (1995) ^{1}H NMR studies of sarafotoxin SRTb, a nonselective endothelin receptor agonist and IRL 1620, an ET_B receptor- specific agonist. *Biochemistry 34*, 2026-2033.

Balcerski, J. S., Pysh, E. S., Bonora, G. M., Toniolo, C. (1976) Vacuum ultraviolet circular dichroism of β-forming alkyl oligopeptides. *J. Am. Chem. Soc. 98*, 3470 3473.

Bax, A., & Davis, D. G. (1985) MLEV-17-based 2D homonuclear magnetization transfer spectroscopy. *J. Magn. Reson. 65*, 355-360.

Blanco, F. J., Jiménez, M. A., Pineda, A., Rico, M., Santoro, J., & Nieto, J. L. (1994) NMR solution structure of the isolated N-terminal fragment of protein-G B_1 domain. Evidence of trifluoroethanol induced native-like β-hairpin formation. *Biochemistry 33*, 6004-6014.

Blundell, T. L., Pitts, J. E., Tickle, I. J., Wood, S. P., & Wu, C.-W. (1981) X-ray analysis (1.4-Å resolution) of avian pancreatic polypeptide: small globular protein hormone. *Proc. Natl. Acad. Sci. USA 78*, 4175-4179.

Bodanszky, M., Ondetti, M. A., Levine, S. D., Narayanan, V. L., von Saltza, M., Sheehan, J. T., Williams, N. J., & Sabo, E. F. (1966) Synthesis of a heptacosapeptide amide with the hormonal activity of secretin. *Chem & Ind. 42*, 1757-1758.

Braun, W., Wider, G., Lee, K. H., & Wüthrich, K. (1983) Conformation of glucagon in a lipid-water interphase by ^{1}H nuclear magnetic resonance. *J. Mol. Biol. 169*, 921-948.

Brems, D. N., Plaisted, S. M., Havel, H. A., Kauffman, E. W., Stodola, J. D., Eaton, L. C., & White, R. D. (1985) *Biochemistry 24*, 7662-7668.

Bromer, W. W., Sinn, L. G., & Behrens, O. K. (1957) The amino acid sequence of glucagon. V. Location of amide groups, acid degradation studies and summary of sequential evidence. *J. Am. Chem. Soc. 79*, 2807-2810.

Brünger, A. T., Clore, G. M., Gronenborn, A. M., & Karplus, M. (1987) Solution conformation of human growth hormone releasing factor: comparison of the restrained molecular dynamics and distance geometry methods for a system without long-range distance data. *Protein Engineering 1*, 399-406.

Buck, M., Radford, S. E., & Dobson, C. M. (1993) A partially folded state of hen egg white lysozyme in trifluoroethanol: structural characterization and implications for protein folding. *Biochemistry 32*, 669-678.

Butcher, D. J., Bruch, M. D., Moe, G. R. (1995) Design and characterization of a model αβ peptide. *Biopolymers 35*, 109-120.

Campbell, R. M., Lee, Y., Rivier, J., Heimer, E. P., Felix, A. M., & Mowles, T. F. (1991) GRF analogs and fragments: correlation between receptor binding, activity, and structure. *Peptides 12*, 569-574.

Campbell, R. M., Bongers, J. & Felix, A. M. (1995) Rational design, synthesis, and biological evaluation of novel growth hormone releasing factor analogues. *Biopolymers (Peptide Science) 37*, 67-88.

Cann, J. R., London, R. E., Unkefer, C. J., Vavrek, R. J., & Stewart, J. M. (1987) CD-n.m.r. study of the solution conformation of bradykinin analogs containing alpha-aminoisobutyric acid. *Int. J. Peptide Protein Res. 29*, 486-496.

Chakrabartty, A., Doig, A. J., & Baldwin, R. L. (1993) Helix capping propensities in peptides parallel those in proteins. *Proc. Natl. Acad. Sci. USA 90*, 11332-11336.

Chou, P. Y. & Fasman, G. D. (1978) Prediction of the secondary structure of proteins from their amino acid sequence. *Advan. Enzymol. 47*, 45-147.

Cicero, D. O., Barbato, G., & Bazzo, R. (1995) NMR analysis of molecular flexibility in solution: a new method for the study of complex distributions of rapidly exchanging conformations. Application to a 13-residue peptide with an 8-residue loop. *J. Am. Chem. Soc. 117*, 1027-1033.

Clore, G. M., Martin, S. R., & Gronenborn, A. M. (1986) Solution structure of human growth hormone releasing factor. *J. Mol. Biol. 191*, 553-561.

Clore, G. M., Nilges, M., Brünger, A., & Gronenborn, A. M. (1988) Determination of the backbone conformation of secretin by restrained molecular dynamics on the basis of interproton distance data. *Eur. J. Biochem. 171*, 479-484.

Craescu, C. T., Bouhss, A., Mispelter, J., Diesis, E., Popescu, A., Chiriac, M., & Bârzu, O. (1995) Calmodulin binding of a peptide derived from the regulatory domain of *Bordatella pertussis* adenylate cyclase. *J. Biol. Chem. 270*, 7088-7096.

Dyson, H. J., Merutka, G., Waltho, J. P., Lerner, R. A., & Wright, P. E. (1992a) Folding of peptide fragments comprising the complete sequence of proteins: models for initiation of protein folding. I. Myohemerythrin. *J. Mol. Biol. 226*, 795-817.

Dyson, H. J., Merutka, G., Waltho, J. P., Lerner, R. A., & Wright, P. E. (1992b) Folding of peptide fragments comprising the complete sequence of proteins: models for initiation of protein folding. II. Plastocyanin. *J. Mol. Biol. 226*, 819- 835.

Eisenberg, D., Weiss, R. M., & Terwilliger, R. C. (1984) The hydrophobic moment detects periodicity in protein hydrophobicity. *Proc. Natl. Acad. Sci. U.S.A. 81*, 140-144.

Fan, P., Bracken, C., & Baum, J. (1993) Structural characterization of monellin in the alcohol-denatured state by NMR: evidence for β-sheet to α-helix conversion. *Biochemistry 32*, 1573-1582.

Felix, A. M., Heimer, E. P., Mowles, T. F., Eisenbeis, H., Leung, P., Lambros, T. J., Ahmad, M., Wang, C. T., & Brazeau, P. (1987) in *Peptides 1986* (Theodoropoulus, D.,Ed.) pp. 481-484, Walter de Gruyter, New York.

Felix, A. M., Heimer, E. P., Wang, C.-T., Lambros, T. J., Fournier, A., Mowles, T. F., Maines, S., Campbell, R. M., Wegrzynski, B. B., Toome, V., Fry, D., & Madison, V. S. (1988) Synthesis, biological activity and conformational analysis of cyclic GRF analogs. *Int. J. Peptide Protein Res. 32*, 441-454.

Fezoui, Y, Weaver, D. L., & Osterhout, J. J. (1994) *De novo* design and structural characterization of an α-helical hairpin peptide: a model system for the study of protein folding intermediates. *Proc. Natl. Acad. Sci. USA 91*, 3675-3679.

Folkers, P. J. M., Folmer, R. H. A., Konings, R. N. H., & Hilbers, C. W. (1993) Overcoming the ambiguity problem encountered in the analysis of nuclear magnetic resonance spectra of symmetric dimer proteins. *J. Am. Chem. Soc. 115*, 3798-3799.

Friedman, A. R., Ichpurani, A. K., Brown, D. M., Hillman, R. M., Krabill, L. F., Martin, R. A., Zurcher-Neely, H. A., & Guido, D. M. (1991) Degradation of growth hormone releasing factor analogs in neutral aqueous solution is related to deamidation of asparagine residues. *Int. J. Peptide Protein Res. 37*, 14-20.

Frohman, L.A., Downs, T. R., Williams, T. C., Heimer, E. P., Pan, Y.-C., & Felix, A. M. (1986) Rapid enzymatic degradation of growth hormone releasing hormone by plasma *in vitro* and *in vivo* to a biologically inactive N-terminally cleaved product. *J. Clin. Invest. 78*, 906-913.

Frohman, L. A., Downs, T. R., Heimer, E. P., & Felix, A. M. (1989) Dipeptidylpeptidase IV and trypsin-like enzymatic degradation of human growth hormone-releasing hormone in plasma. *J. Clin. Invest. 83*, 1533-1540.

Fry, D. C., Madison, V. S., Bolin, D. R., Greeley, D. N., Toome, V., & Wegrzynski, B. B. (1989) Solution structure of an analogue of vasoactive intestinal peptide as determined by two-dimensional NMR and circular dichroism spectroscopies and constrained molecular dynamics. *Biochemistry 28*, 2399-2409.

Fry, D. C., Madison, V. S., Greeley, D. N., Felix, A. M., Heimer, E. P., Frohman, L., Campbell, R. M., Mowles, T. F., Toome, V., & Wegrzynski, B. B. (1992) Solution structures of cyclic and dicyclic analogues of growth hormone releasing factor as determined by two-dimensional NMR and CD spectroscopies and constrained molecular dynamics. *Biopolymers 32*, 649-666.

Garnier, J. Ogusthorpe, D. J., & Robson, B. (1978) Analysis of the accuracy and implications of simple methods for predicting the secondary structure of globular proteins. *J. Mol. Biol. 120*, 97-120.

Gaudreau, P., Boulanger, L., & Abribat, T. (1992) Affinity of human growth hormone-releasing factor (1-29)NH_2 analogues for GRF binding sites in rat adenopituitary. *J. Med. Chem. 35*, 1864-1869.

Goodman, M., Naider, F., & Toniolo, C. (1971) Circular dichroism studies of isoleucine oligopeptides in solution. *Biopolymers 10*, 1719-1730.

Gooley, P. R., Blunt, J. W., & Norton, R. S. (1984) Conformational heterogeneity in polypeptide cardiac stimulants from sea anemones. *Febs Lett. 174*, 15-19.

Gooley, P. R. & Norton, R. S. (1985) Specific assignment of resonances in the ^1H nuclear magnetic resonance spectrum of the polypeptide cardiac stimulant anthopleurin-A. *Eur. J. Biochem. 153*, 529-539.

Gronenborn, A. M., Bovermann, G., & Clore, G. M. (1987) A ^1H-NMR study of the solution conformation of secretin. *FEBS Lett. 215*, 88-94.

Gronenborn, A. M., Filpula, D. R., Essig, N. Z., Achari, A., Whitlow, M., Wingfield, P. T., & Clore, G. M. (1991) A novel, highly stable fold of the immunoglobulin binding domain of streptococcal protein G. *Science 253*, 657-661.

Grossman, A., Savage, M. O., Lytras, N., Preece, M. A., Sueiras-Diaz, J., Coy, D. H., Rees, L.H., & Besser, G. M. (1984) Responses to analogues of growth hormone-releasing hormone in normal subjects, and in growth-hormone deficient children and young adults. *Clin. Endocrinol. 21*, 321-330

Guillemin, R., Brazeau, P., Bohlen, P., Esch, F., Ling, N., & Wehrenberg, W. B. (1982) Growth hormone-releasing factor from a human pancreatic tumor that caused acromegaly. *Science 218*, 585-587.

Hawkins, B. L., Cross, K. J., & Craik, D. J. (1994) A ^1H-NMR determination of the solution structure of the A-chain of insulin: comparison with the crystal structure and an examination of the role of solvent. *Biochim. Biophys. Acta 1209*, 177-182.

Herranz, J., González, C., Rico, M., Nieto, J. L., Santoro, J., Jiménez, M. A., Bruix, M., Neira, J. L., Blanco, F. J. (1992) Peptide group chemical shift computation. *Magn. Reson. Chem. 30*, 1012-1018.

Honda, S., Ohashi, S., Morii, H., & Uedaira, H. (1991) Solution structure of human growth hormone-releasing factor fragment (1-29) by CD: characteristic conformational change on phospholipid membrane. *Biopolymers 31*, 869-876.

Huang, G. S. & Oas, T. G. (1995) Structure and stability of monomeric λ repressor: NMR evidence for two-state folding. *Biochemistry 34*, 3884-3892.

Huq, N. L., Cross, K. J., & Reynolds, E. C. (1995) A ^{1}H-NMR study of the casein phosphopeptide α_{s1}-casein(59-79). *Biochim. Biophys. Acta 1247*, 201-208.

Inooka, H., Endo, S., Chieko, K., Mizuta, E., Fujino, M. (1992) Pituitary adenylate cyclase activating polypeptide (PACAP) with 27 residues. *Int. J. Peptide Protein Res. 40*, 456-464.

Jarvis, J. A., Munro, S. L. A., & Craik, D. J. (1994) Structural analysis of peptide fragment 71-93 of transthyretin by NMR spectroscopy and electron microscopy: insight into amyloid fibril formation. *Biochemistry 33*, 33-41.

Jeener, J., Meier, B. H., Bachmann, P., & Ernst, R. R. (1979) Investigation of exchange processes by two-dimensional NMR spectroscopy. *J. Chem. Phys. 71*, 4546-4553.

Jiménez, M. A., Nieto, J. L., Herranz, J., Rico, M, & Santoro, J. (1987) ^{1}H NMR and CD evidence of the folding of the isolated ribonuclease 50-61 fragment. *FEBS Lett. 221*, 320-324.

Kaiser, E. T. & Kézdy, F. J. (1984) Amphiphilic secondary structure: design of peptide hormones. *Science 223*, 249-255.

Kelly, M. M., Pysh, E. S., Bonora, G. M., & Toniolo, C. (1977) Vacuum ultraviolet circular dichroism of potential homooligomers derived from L-leucine. *J. Am. Chem. Soc. 99*, 3264-3266.

Kim, P. S. & Baldwin, R. L. (1984) A helix stop signal in the isolated S-peptide of ribonuclease A. *Nature 307*, 329-334.

Kloosterman, D. A., Scahill, T. A., Friedman, A. R. (1993) Secondary structure of a human growth hormone-releasing factor fragment (Leu^{27}-hGRF(15-32)NH_2) in aqueous/SDS micelle environments. *Peptide Res. 6, 211-218.*

Lance, V. A., Murphy, W. A., Sueiras-Diaz, J., & Coy, D. H. (1984) Super-active analogs of growth hormone-releasing factor(1-29)-amide. *Biochem. Biophys. Res. Commun. 119 (1)*, 265-272.

Lee, G. M., Chen, C., Marschner, T. M., & Andersen, N. H. (1994) Does the solid-state structure of endothelin-1 provide insights concerning the solution-state conformational equilibrium. *FEBS Lett 355*, 140-146.

Lefrançois, L. & Gaudreau, P. (1994) Identification of receptor-binding pharmacophores of growth-hormone-releasing factor in rat adenopituitary. *Neuroendocrinology 59*, 363-370.

Li, X., Sutcliffe, M. J., Schwartz, T.W., & Dobson, C. M. (1992) Sequence-specific ^1H NMR assignments and solution structure of bovine pancreatic polypeptide. *Biochemistry 31*,1245-1253.

Ling, N., Baird, A., Wehrenberg, W. B., Ueno, N., Munegumi, T., & Brazeau, P. (1984) Synthesis and *in vitro* bioactivity of c-terminal deleted analogs of human growth hormone-releasing factor. *Biochem. Biophys. Res. Commun. 123*, 854-861.

Ling, N., Zeytin, F., Böhlen, P., Esch, F., Brazeau, P., Wehrenberg, W. B., Baird, A., & Guillemin, R. (1985) Growth hormone releasing factors. *Ann. Rev. Biochem 54*, 403-423.

Livingstone, J. R., Spolar, R. S., & Record, Jr., M. T. (1991) Contribution to the thermodynamics of protein folding from the reduction in water-accessible nonpolar surface area. *Biochemistry 30*, 4237-4244.

Lu, J. & Hall, K. B. (1995) An RBD that does not bind RNA: NMR secondary structure determination and biochemical properties of the C-terminal RNA binding domain from the human U1A protein. *J. Mol. Biol. 247*, 739-752.

Madison, V., Berkovitch-Yellin, Z., Fry, D., Greeley, D., & Toome, V. (1989) in *Synthetic Peptides: Approaches to biological problems. vol 86.* (Tam, J. & Kaiser, E. T., Eds.) pp. 109-123, Alan R. Liss Inc., New York.

Maciejewski, M. W. & Zehfus, M. H. (1995) Structure of a compact peptide from staphylococcal nuclease determined by circular dichroism and NMR spectroscopy. *Biochemistry 34*, 5795-5800.

Marion, D., & Wüthrich, K. (1983) Application of phase-sensitive two-dimensional correlated spectroscopy (COSY) for measurement of ^{1}H-^{1}H spin-spin coupling constants in proteins. *Biochem. Biophys. Res. Commun. 117*, 967-974.

Marx, U. C., Austermann, S., Bayer, P., Adermann, K., Ejchart, A., Sticht, H., Walter, S., Schmid, F.-X., Jaenicke, R., Forssmann, W.-G., & Rösch, P. (1995) Structure of human parathyroid hormone 1-37 in solution. *J. Biol. Chem. 270*, 15194-15202.

Mayo, K. E., Vale, W., Rivier, J., Rosenfeld, M. G., & Evans, R. M. (1983) Expression, cloning and sequence analysis of cDNA encoding human growth hormone-releasing factor, somatocrinin. *Nature 306*, 86-88

Mayo, K. E. (1992) Molecular cloning and expression of a pituitary-specific receptor for growth hormone-releasing hormone. *Mol. Endocrinol. 6*, 1734-1744.

Mayo, K. E., Godfrey, P. A., Suhr, S. T., Kulik, D. J., & Rahal, J. O. (1995) Growth hormone-releasing hormone: synthesis and signaling. *Recent Prog. Horm. Res. 50*, 35-73.

Mehigh, C. S., Elias, V. D., Mehigh, R. J., Helferich, W. G. & Tucker, H. A. (1993) Development of a recombinant bovine leukemia virus vector for delivery of a synthetic bovine growth hormone-releasing factor gene into bovine cells. *J. Animal Sci. 71*, 687-693

Merutka, G., Dyson, H. J., & Wright, P. E. (1995) 'Random coil' ^{1}H chemical shifts obtained as a function of temperature and trifluoroethanol concentration for the peptide series GGXGG. *J. Biomol. NMR 5*, 14-24.

Miyata, A., Arimura, A., Dahl, R. R., Minamino, N., Uehara, A., Jiang, L., Culler, M. D., & Coy, D. H. (1989) Isolation of a novel 38-residue hypothalamic polypeptide which stimulates adenylate cyclase in pituitary cells. *Biochem. Biophys. Res. Comm. 164*, 567-574.

Mulhern, T. D., Howlett, G. J., Reid, G. E., Simpson, R. J., McColl, D. J., Anders, R. F., & Norton, R. S. (1995) Solution structure of a polypeptide containing four heptad repeat units from a merozoite surface antigen of *Plasmodium falciparum Biochemistry 34*, 3479-3491.

Mullen, G. P., Vaughn, Jr., J. B., & Mildvan, A. S. (1993) Sequential proton NMR resonance assignments, circular dichroism, and structural properties of a 50-residue substrate-binding peptide from DNA polymerase I. *Arch. Biochem. Biophys. 301,* 174-183.

Narula, S. S., Winge, D. R., & Armitage, I. M. (1993) Copper- and silver-substituted yeast metallothioneins: sequential ^{1}H NMR assignments reflecting conformational heterogeneity at the C terminus. *Biochemistry 32*, 6773-6787.

Narayanan, U., Keiderling, T. A., Bonora, G. M., & Toniolo, C. (1986) Vibrational circular dichroism of polypeptides. 7. Film and solution studies of β-sheet-forming homooligopeptides. *J. Am. Chem. Soc. 108*, 2431-2437.

Nelson, J. W. & Kallenbach, N. R. (1986) Stabilization of the ribonuclease S-peptide α-helix by trifluoroethanol. *Proteins 1*, 211-217.

Nelson, J. W. & Kallenbach, N. R. (1989) Persistence of the α-helix stop signal in the S-peptide in trifluoroethanol solutions. *Biochemistry 28*, 5256-5261.

Nilges, M. (1993) A calculation strategy for the structure determination of symmetric dimers by ^{1}H NMR. *Proteins 17*, 297-309.

Otting, G., Liepinsh, E., Wüthrich, K. (1993) Disulfide bond isomerization in BPTI and BPTI (G36S): an NMR study of correlated mobility in proteins. *Biochemstry 32*, 3571-3581.

Pardi, A., Wagner, G., & Wüthrich, K. (1983) Protein conformation and proton nuclear-magnetic-resonance chemical shifts. *Eur. J. Biochem. 137*, 445-454.

Pastore, A. & Saudek, V. (1990) The relationship between chemical shift and secondary structure in proteins. *J. Magn. Reson. 90*, 165-176.

Petersen, K. -G., Zeisel, H. -J., Kerp, L. (1989) The immune response to GHRH, relationship to conformation. *Horm. Metabol. Res. 21*, 427-430.

Richardson, J. S. & Richardson, D. C. (1988) Amino acid preferences for specific locations at the ends of α helices. *Science 240*, 1648-1652.

Rivier, J., Spiess, J., Thorner, M., & Vale, W. (1982) Characterization of growth hormone-releasing factor from a human pancreatic islet tumor. *Nature 300*, 276- 278.

Rivier, J., Speiss, J., & Vale, W. (1984) in *Peptide Chemistry 1983* (Munekata, E., Ed.) pp. 11-17, Protein Research Foundation, Osaka.

Rizo, J., Blanco, F. J., Kobe, B., Bruch, M. D., & Gierasch, L. M. (1993) Conformational behavior of *Escherichia coli* OmpA signal peptides in membrane mimetic environments. *Biochemistry 32*, 4881-4894.

Rochiccioli, P. E., Tauber, M. T., Coude, F. X., Arnone, M., Morre, M., Uboldi, F., & Barbeau, C. (1987) Results of 1-year growth hormone (GH)-releasing hormone-(1-44) treatment on growth, somatomedin-C, and 24-hour GH secretion in six children with partial GH deficiency. *J. Clin. Endocrinol. Metab. 65*, 268-274.

Said, S. I. & Mutt, V. (1970) Polypeptide with broad biological activity: isolation from small intestine. *Science 169*, 1217-1218.

Said, S. I. & Mutt, V. (1972) Isolation from porcine-intestinal wall of a vasoactive octacosapeptide related to secretin and to glucagon. *Eur. J. Biochem. 28*, 199-204.

Sargent, D. F., & Schwyzer, R. (1986) Membrane lipid phase as catalyst for peptide-receptor interactions. *Proc. Natl. Acad. Sci. USA 83*, 5774-5778.

Segawa, S., Fukuno, T., Fujiwara, K., & Noda, Y. (1991) Local structures in unfolded lysozyme and correlation with secondary structures in the native conformation: helix-forming or -breaking propensity of peptide segments. *Biopolymers 31*, 497-509.

Shiraki, K., Nishikawa, K., Goto, Y. (1995) Trifluoroethanol-induced stabilization of the α-helical structure of β-lactoglobulin: implication for non-hierarchical protein folding. *J. Mol. Biol. 245*, 180-194.

Shoemaker, K. R., Kim, P. S., Brems, D. N., Marqusee, S., York, E. J., Chaiken, I. M., Stewart, J. M., & Baldwin, R. L. (1985) Nature of the charge-group effect on the stability of the C-peptide helix. *Proc. Natl. Acad. Sci. U.S.A. 82*, 2349-2353.

Shoemaker, K. R., Kim, P. S., York, E. J., Stewart, J. M., & Baldwin, R. L. (1987) Tests of the helix dipole model for stabilization of alpha-helices. *Nature 326*, 563-567.

Siligardi, G., Drake, A. F., Mascagni, P., Neri, P., Lozzi, L., Niccolai, N., & Gibbons, W. A. (1987) Resolution of conformational equilibria in linear peptides by circular dichroism in cryogenic solvents. *Biochem. Biophys. Res. Commun. 143*, 1005-1011.

Sipos, D., Andersson, M., & Ehrenberg, A. (1992) Two-dimensional proton-NMR studies on a hybrid peptide between cecropin A and melittin: resonance assignments and secondary structure. *Eur. J. Biochem. 209*, 163-169.

Slupsky, C. M., Reinach, F. C., Smillie, L. B., & Sykes, B. D. (1995a) Solution secondary structure of calcium-saturated troponin C monomer determined by multidimensional heteronuclear NMR spectroscopy. *Protein Sci. 4*, 1279-1290.

Slupsky, C. M., Kay, C. M., Reinach, F. C., Smillie, L. B., & Sykes, B. D. (1995b) Calcium-induced dimerization of troponin C: mode of interaction and use of trifluoroethanol as a denaturant of quaternary structure. *Biochemistry 34*, 7365-7375.

Sönnichsen, F. D., Van Eyk, J. E., Hodges, R. S., & Sykes, B. D. (1992) Effect of trifluoroethanol on protein secondary structure: an NMR and CD study using a synthetic actin peptide. *Biochemistry 31*, 8790-8798.

Stevenson, C. L., Donlan, M. E., Friedman, A. R., & Borchardt, R. T. (1993) Solution conformation of Leu^{27} hGRF(1-32)NH_2 and its deamidation products by 2D NMR. *Int. J. Peptide Protein Res. 42*, 24-32.

Strader, C. D., Fong, T. M., Tota, M. R., Underwood, D., & Dixon, R. A. F. (1994) Structure and function of G protein-coupled receptors. *Annu. Rev. Biochem. 101-32.*

Strader, C. D., Fong, T. M., Graziano, M. P. & Tota, M. R. (1995) The family of G-protein-coupled receptors. *Faseb J. 9*, 745-754.

Strickland, L. A., Bozzato, R. P., & Kronis, K. A. (1993) Structure of human parathyroid hormone (1-34) in the presence of solvents and micelles. *Biochemistry 32*, 6050-6057.

Struthers, M. D., Cheng, R. P., & Imperiali, B. (1996) Design of a monomeric 23-residue polypeptide with defined tertiary structure. *Science 271*, 342-345.

Szilágyi, L. & Jardetzky, O. (1989) α–Proton chemical shifts and secondary structure in proteins. *J. Magn. Reson. 83*, 441-449.

Tatemoto, K. & Mutt, V. (1981) Isolation and characterization of the intestinal peptide porcine PHI (PHI-27), a new member of the glucagon-secretin family. *Proc. Natl. Acad. Sci. USA 78*, 6603-6607.

Theriault, Y., Boulanger, Y., & St-Pierre, S. (1991) Structural determination of the vasoactive intestinal peptide by two-dimensional ^{1}H-NMR spectroscopy. *Biopolymers 31*, 459-464.

Theriault, Y., Boulanger, Y., & Saunders, J. K. (1988) Secondary structure of the human growth hormone releasing factor (GRF 1-29) by two-dimensional ^{1}H-NMR spectroscopy. *Biopolymers 27*, 1897-1904.

Thornton, K. & Gorenstein, D. G. (1994) Structure of glucagon-like peptide (7-36) amide in a dodecylphosphocholine micelle as determined by 2D NMR. *Biochemistry 33*, 3532-3539.

Vance, M. L. (1990) Growth hormone-releasing hormone. *Clin. Chem. 36*, 415-420.

Vandermeers, A., Gourlet, P., Vandermeers-Piret, M. C., Cauvin, A., De Neef, P., Rathe, J., Svoboda, M., Robberecht, P., & Christophe, J. (1987) Chemical, immunological and biological properties of peptides like vasoactive intestinal peptide and peptide isoleucinamide extracted from the venom of two lizards (*Heloderma horridum* and *Heloderma suspectum*). *Eur. J. Biochem. 164*, 321-327.

Wang, J., Hodges, R. S., & Sykes, B. D. (1995) Effect of trifluoroethanol on the solution structure and flexibility of desmopressin: a two-dimensional NMR study. *Int. J. Peptide Protein Res. 45*, 471-481.

Waterhous, D. V. & Johnson, W. C., Jr. (1994) Importance of environment in determining secondary structure in proteins. *Biochemistry 33*, 2121-2128.

Williams, R. W., Chang, A., Juretic, D., & Loughrams, S. (1987) Secondary structure predictions and medium range interactions. *Biochem. Biophys. Acta 916*, 200-204.

Williamson, M. P. (1990) Secondary-structure dependent chemical shifts in proteins. *Biopolymers 29*, 1423-1431.

Williamson, M. P. & Asakura, T. (1993) Empirical comparisons of models for chemical-shift calculation in proteins. *J. Magn. Reson. 101*, 63-71.

Wishart, D. S., Sykes, B. D., & Richards, F. M. (1991) Relationship between nuclear magnetic resonance chemical shift and protein secondary structure. *J. Mol. Biol. 222*, 311-333.

Wishart, D. S., Sykes, B. D., & Richards, F. M. (1992) The chemical shift index: a fast and simple method for the assignment of protein secondary structure through NMR spectroscopy. *Biochemistry 31*, 1647-1651.

Wishart, D. S., Bigam, C. G., Holm, A., Hodges, R. S., & Sykes, B. D. (1995) ^{1}H, ^{13}C, and ^{15}N random coil NMR chemical shifts of the common amino acids. I. Investigations of nearest-neighbor effects. *J. Biomol. NMR 5*, 67-81.

Wray, V., Kakoschke, C., Nokihara, K., & Naruse, S. (1993) Solution structure of pituitary adenylate cyclase activating polypeptide by nuclear magnetic resonance spectroscopy. *Biochemistry 32*, 5832-5841.

Wray, V., Federau, T., Gronwald, W., Mayer, H., Schomburg, D., Tegge, W., & Wingender, E. (1994) The structure of human parathyroid hormone from a study of fragments in solution using ^{1}H NMR spectroscopy and its biological implications. *Biochemistry 33*, 1684-1693.

Wüthrich, K. (1986) *NMR of Proteins and Nucleic Acids*, Wiley and Sons, New York.

Xu, R. X., Horvath, S. J., & Klevit, R. E. (1991) ADR1a, a zinc finger peptide, exists in two folded conformations. *Biochemistry 30*, 3365-3371.

Zhong, L. & Johnson, W. C., Jr. (1992) Environment affects amino acid preference for secondary structure. *Proc. Natl. Acad. Sci U.S.A. 89*, 4462-4465.